TRACE FOSSILS, SEDIMENTARY FACIES AND PARASEQUENCE ARCHITECTURE FROM THE LOWER CRETACEOUS MULICHINCO FORMATION OF ARGENTINA: THE ROLE OF FAIR-WEATHER WAVES IN SHOREFACE DEPOSITS

A Thesis Submitted to the College of

Graduate and Postdoctoral Studies

In Partial Fulfillment of the Requirements

For the Degree of Master of Science

In the Department of Geological Sciences

University of Saskatchewan

Saskatoon

By

LINDSEY JOHN-NICHOLAS WESOLOWSKI

PERMISSION TO USE

In presenting this thesis in partial fulfillment of the requirements for a Postgraduate degree from the University of Saskatchewan, I agree that the Libraries of this University may make it freely available for inspection. I further agree that permission for copying this thesis in any manner, in whole or in part, for scholarly purposes may be granted by the professor or professors who supervised my thesis work or, in their absence, by the Head of the Department or the Dean of the college in which my thesis work was done. It is understood that any copying or publication or use of this thesis or parts thereof for financial gain shall not be allowed without my written permission. It is also understood that due recognition shall be given to me and to the University of Saskatchewan in any scholarly use which may be made of any material in my thesis. Requests for permission to copy or to make other use of material in this thesis in whole or part should be addressed to:

Head of the Department of Geological Sciences

University of Saskatchewan

114 Science Place

Saskatoon, Saskatchewan, Canada

S7N 5E2

ABSTRACT

Shorefaces can display strong facies variability and integration of sedimentology and ichnology provides a high-resolution model to identify variations among strongly storm-dominated (high energy), moderately storm-affected (intermediate energy), and weakly storm-affected (low energy) shoreface deposits. In addition, ichnology has proved to be of help to delineate parasequences as trace-fossil associations are excellent indicators of environmental conditions which typically change along the depositional profile. Shallow-marine deposits and associated ichnofaunas from the Mulichinco Formation (Valanginian, Lower Cretaceous) in Puerta Curaco, Neuquén Basin, western Argentina, were analyzed to evaluate stress factors on shoreface benthos and parasequence architecture.

During storm-dominated conditions, the *Skolithos* Ichnofacies prevails within the offshore transition and lower shoreface represented by assemblages dominated by *Thalassinoides* isp. and *Ophiomorpha irregulaire*. Under weakly storm-affected conditions, the *Cruziana* Ichnofacies is recognized, characterized by assemblages dominated by *Thalassinoides* isp. and *Gyrochorte comosa* in the offshore transition, and by *Gyrochorte comosa* within the lower shoreface. Storm-influenced conditions yield wider ichnologic variability, showing elements of both ichnofacies.

Storm influence on sedimentation is affected by both allogenic (e.g. tectonic subsidence, sea-level, and sediment influx) and autogenic (e.g. hydrodynamic) controls at both parasequence and intra-parasequence scales. Four distinct types of parasequences were recognized, strongly storm-dominated, moderately storm-affected, moderately storm-affected – strongly fair-weather reworked, and weakly storm-affected, categorized based on parasequence architectural variability derived from varying degrees of storm and fair-weather wave influence. The new type of shoreface described here, the moderately storm-affected – strongly fair-weather reworked

shoreface, features storm deposits reworked thoroughly by fair-weather waves. During fair-weather wave reworking, elements of the *Cruziana* Ichnofacies are overprinted upon relict elements of the *Skolithos* Ichnofacies from previous storm induced deposition. This type of shoreface, commonly overlooked in past literature, expands our understanding of the sedimentary dynamics and stratigraphic architecture in a shoreface susceptible to various parasequence and intra-parasequence scale degrees of storm and fair-weather wave influence.

ACKNOWLEDGEMENTS

First and foremost, I would like to extend my gratitude to those on the graduate student selection committee for the College of Graduate and Postdoctoral Studies as it has been both a privilege and an honour to be accepted to participate in the Geological Sciences Master of Science Thesis Program at the University of Saskatchewan. I would also like to thank the graduate student funding committee for providing me half a graduate teaching fellowship during winter term 2017, as well as the Department of Geological Sciences masters student scholarship granted May 2017.

Luis and Gabriela, I would like to thank you for your exceptional patience, guidance, and time throughout this journey as demonstrated by your ability to cope with my countless, long winded emails and regular meetings over the years pouring over photographs, sedimentary logs, and providing insightful discussion. In the outcrops, your refined perception, knowledge, and teaching ability, provided me an unequaled opportunity to learn. Over the course of knowing you for many years, I have developed a profound level of respect and admiration for you both.

I would like to thank Juan Jose Ponce, and Noelia Carmona for their discussion and wealth of knowledge of the study area as well as Debora Campetella who aided in field work. I would like to extend my gratitude to my committee member Robin Renaut, as well as my external reviewer Chris Hawke for his interest to learn about my work in the Neuquén Basin their thoughtful feedback.

To my mom and dad, Christine and Fred Wesolowski. From a young age you instilled the values of education in me, and guided me to relentlessly pursue my passions. Without your

support, this degree would not have been possible. To Alyssa, you have been a pillar of strength throughout this journey, motivating me not only to do the best I can, but to also be my best self.

TABLE OF CONTENTS

page

LIST OF TABLES

LIST OF FIGURES

CHAPTER 1.0: INTRODUCTION

Shorefaces display a wide range of both sedimentologic and ichnologic variability controlled by the type of wave influence (storm-wave vs. fair-weather) in conjunction with various degrees of storm-wave activity on the substrate resulting in strongly storm-dominated (high energy), moderately storm-affected (intermediate energy), and weakly storm-affected (low energy) shoreface deposit (MacEachern and Pemberton, 1992). In this study, however, detailed analysis of parasequence architecture of the Mulichinco Formation near the area of Yesera del Tromen yields a previously undescribed shoreface presented here, i.e., the moderately storm-affected – strongly fair-weather reworked shoreface. The moderately storm-affected – strongly fair-weather reworked shoreface encompasses unique storm deposits reworked thoroughly by fair-weather waves, slotting between storm wave and fair-weather wave dominance on previous conceptual shoreface model ternary diagrams designed to illustrate the three main influences on deposition at the sediment substrate interface, including tides in addition to the aforementioned storm and fair-weather waves (Dashtgard et al., 2012). Discovery of new shoreface deposits have the potential to further alter and evolve our understanding of sedimentary processes and classification schemes in these types of open marine, unrestricted environments.

1.1 Research Objective

Primary research hypothesis: Detailed integration of sedimentologic, ichnologic and sequence-stratigraphic datasets will allow differentiation of various types of wave-dominated, shallowing upward parasequences.

Primary research objective: To expand our understanding of the sedimentary dynamics and parasequence architecture in shoreface complexes. Previous schemes have emphasized the

importance of storm waves in shaping facies characteristics and sedimentary architecture of shoreface deposits. This study highlights the importance of fair-weather waves through the recognition of a type of shoreface parasequence, commonly overlooked in past literature.

Steps necessary for completion of the primary research objective:

1) Logging of three sections of the Mulichinco Formation near the area of Yesera del Tromen (70 km E-NE of the locality of Chos Malal);

2) Description and interpretation of facies associations of the Mulichinco Formation within the research area;

3) Integration of sedimentologic, ichnologic and sequence-stratigraphic datasets to delineate parasequences; and

4) Identification and analysis of important sequence stratigraphic surfaces.

CHAPTER 2.0: METHODOLOGY

The methodology for this research consisted of systematic mapping and standard sedimentary facies analysis based on bed-by-bed measuring of three stratigraphic sections; PCS1 (S 37º 22.577' W 069º 56.846'), PCS2 (S 37º 23.764' W 069º 56.195'), and PCS3 (37º 24.388' W 069º 56.888'), with a Jacob's staff and an abney level. These three outcrops were selected based on exposure quality, accessibility, and distance from PCS1 and PCS3 from PCS2 being roughly equidistant (Fig. 1) as well as covering the entire unit.

Sedimentologic analysis of outcrops involved detailed facies characterization on the basis of lithology, sedimentary structures, mean grain size, bioturbation, macrofossils, composition and sorting. Outcrops were photographed at different scales to exhibit important sedimentary features and stratigraphic surfaces.

Ichnologic analysis involved trace-fossil sampling, preliminary recognition and identification of the ichnofossils present; study of density, abundance and distribution of individual ichnotaxa; degree of bioturbation quantified based on Taylor and Goldring (1993); estimation of ichnodiversity; identification of trophic types and ethologic groups; reconstruction of tiering structure, and relationships among trace fossils, physical sedimentary structures, and bedding types in each sedimentary facies. Both sedimentologic and ichnologic features are depicted in the legend (Fig. 2). Detailed maps and photographic panels of the ichnofossil-bearing strata were prepared similarly to photographs of sedimentary features and photo-mosaics of stratigraphic surfaces using CorelDraw X8. Bed-by-bed stratigraphic columns of PCS1 (Appendix I, and condensed section as seen in Fig. 3), PCS2 (Appendix II), and PCS3 (Appendix III) have been drawn with CorelDraw X8, depicting all important sedimentologic and ichnologic features. In addition, a summary column is provided for PCS1 (Fig. 3). Sedimentologic and

ichnologic information was integrated in a sequence stratigraphic framework as outlined by Catuneanu (2006) and incorporated into a regional depositional model for the Mulichinco Formation within the Neuquén Basin (Schwarz and Howell, 2005; Schwarz et al. 2006; Schwarz, 2012; Schwarz et al. 2016, Veiga and Schwarz, 2016) in order to provide an accurate delineation of parasequences. Field work has allowed for in situ characterization of trace fossil content and sedimentary facies of the units studied. Additionally, ichnologic analysis allows careful evaluation of ichnofabrics, tiering structure and ichnoguilds. Integration of ichnologic data with sedimentologic and sequence stratigraphic data is essential to evaluate the paleoenvironmental distribution of trace fossils and their paleoecologic significance. Trace and body fossil specimens were stored at the University of Rio Negro (UNRN).

The Neuquén Basin is unique in that it provides a nearly continuous record of up to 6000 m of stratigraphy from the Late Triassic to early Cenozoic (Schwarz, 2012) facilitating past sequence stratigraphic studies of the Mulichinco Formation (Schwarz and Howell, 2005). Within the Mulichinco Formation near the Puerta Curaco vicinity, there is both a high abundance and wide diversity of trace fossils within the shallowing upward, shoreface successions that are in close proximity (PCS1) to a gravel road (Fig. 1) allowing for an integrated sedimentological and iconological study of the parasequence architecture. On the other hand, the two outcrops to the south, PCS2 and PCS3, were only reached by long hikes of several hours to and from as the terrain was steep filled with mountains and valley, and traversed under highly fluctuating weather conditions including rain, sleet, and snow. A total of 11 days was spent in the field, arriving on April 17th, 2016 and leaving on April 27th, 2016, with mapping of outcrops and conducting sedimentary facies analysis based on bed-by-bed measurements from April 18th to

April 26th, 2016. Fieldwork outlined here was assisted by Juan Jose Ponce, a professor at UNRN, co-supervisor M. Gabriela Mángano, and Debora Campetella, a PhD. student.

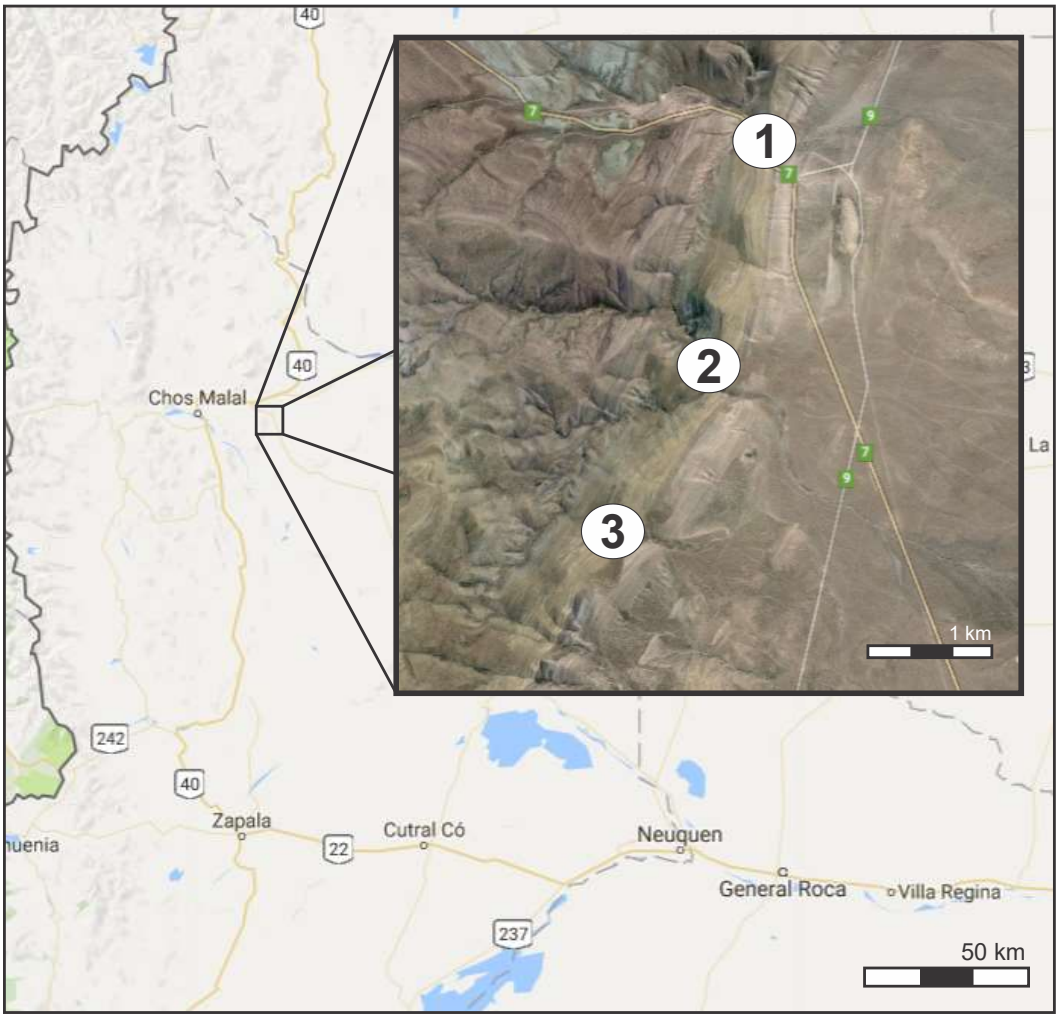

Fig. 1. Location of study area and outcrops; PCS1 (**1**), PCS2 (**2**), and PCS3 (**3**) within the Neuquén Basin.

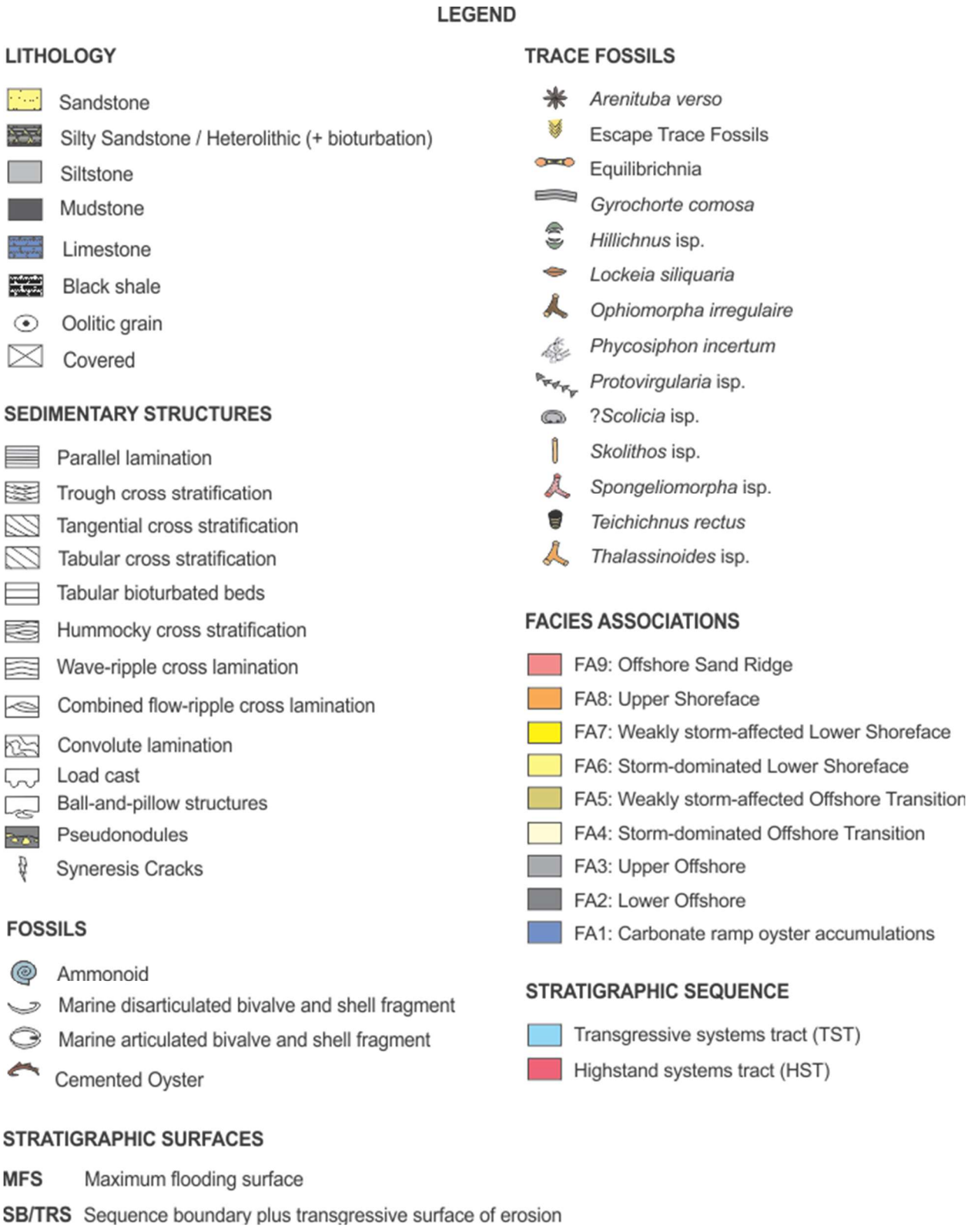

Fig. 2. Sedimentary log legend.

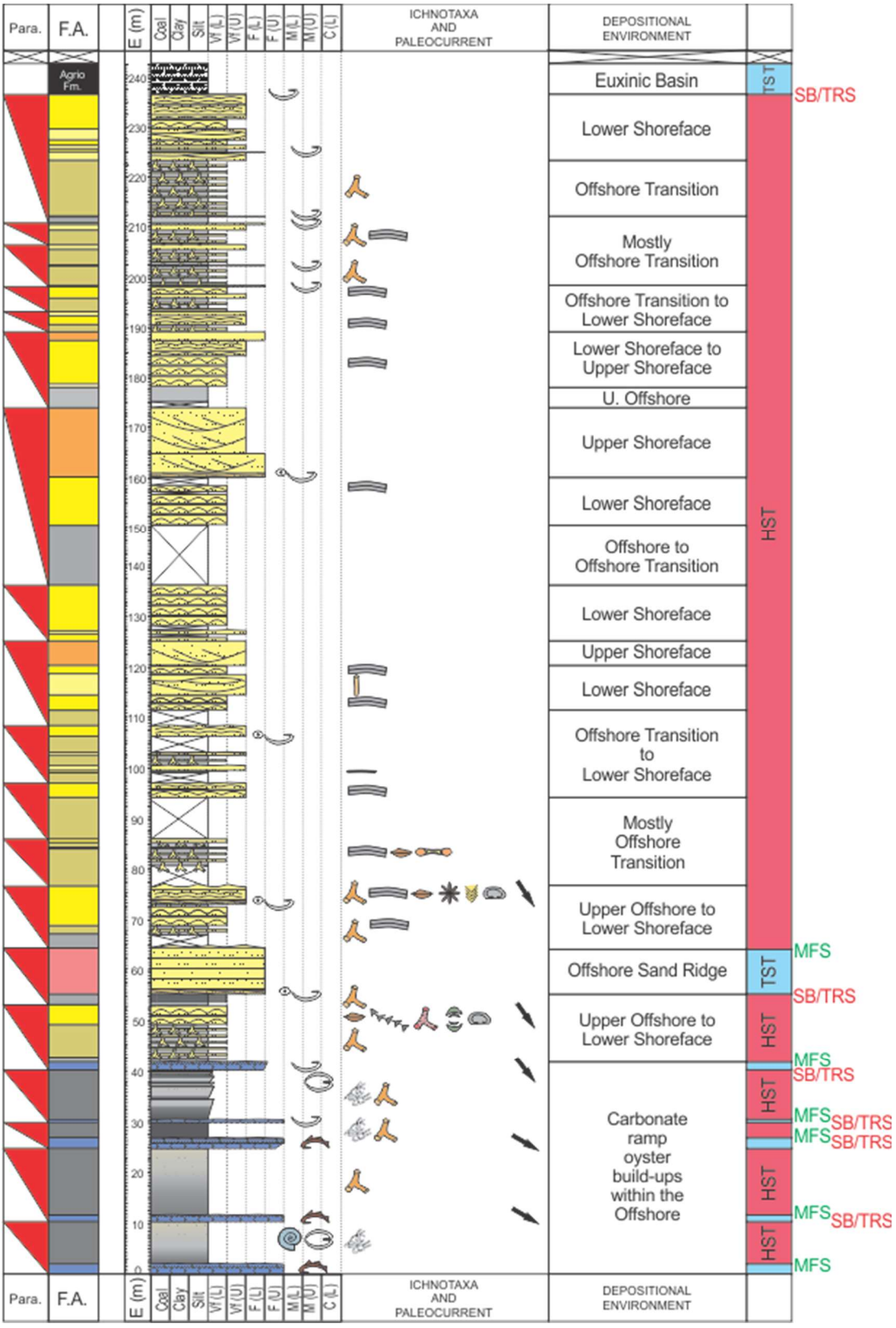

Fig. 3. Sedimentary Log for PCS1. Measured interval corresponds to the upper member, with the exception of the lowermost carbonate interval, which belongs to the middle member.

CHAPTER 3.0: BACKGROUND RESEARCH

3.1 Parasequences

A parasequence is defined as a shallowing-upward succession bounded by marine flooding or drowning surfaces (Van Wagoner et al., 1990), which is useful in shallow-marine successions as it can categorize both wave-dominated, tide-dominated, and deltaic progradation.

3.1.1 Parasequence Characterization

Wave-dominated parasequences are characterized by 1) sandstone bedsets and beds that thicken upward, 2) the sandstone/mudstone ratio increasing upward, 3) grain-size increasing upward, 4) laminae geometry becoming steeper upwards [in general], 5) bioturbation decreasing upward to the parasequence boundary, and 6) facies within each parasequence shoaling upwards (Van Wagoner et al., 1990) (Fig. 4).

3.1.2 Parasequence Boundaries

Parasequence boundaries are marked by 1) an abrupt change in lithology from sandstone below the boundary to mudstone or siltstone above the boundary; 2) an abrupt decrease in bed thickness; 3) possible minor truncation of underlying laminae; 4) a horizon of bioturbation with intensity diminishing downwards; 5) glauconite, phosphorite, shell hash, organic-rich shale, shale pebbles; and 6) evidence of an abrupt deepening in depositional environment across the boundary (Van Wagoner et al., 1990) (Fig. 4). This boundary represents a marine-flooding surface with deeper, distal rocks overlying shallower, proximal rocks that formed nearer a contemporary shoreline. Flooding surfaces may contain a transgressive lag, although most have only minor erosion representing a non-depositional hiatus. These characteristics suggest

parasequence boundaries formed in response to a rapid increase in water depth that outpaced the rate of deposition (Van Wagoner et al., 1990).

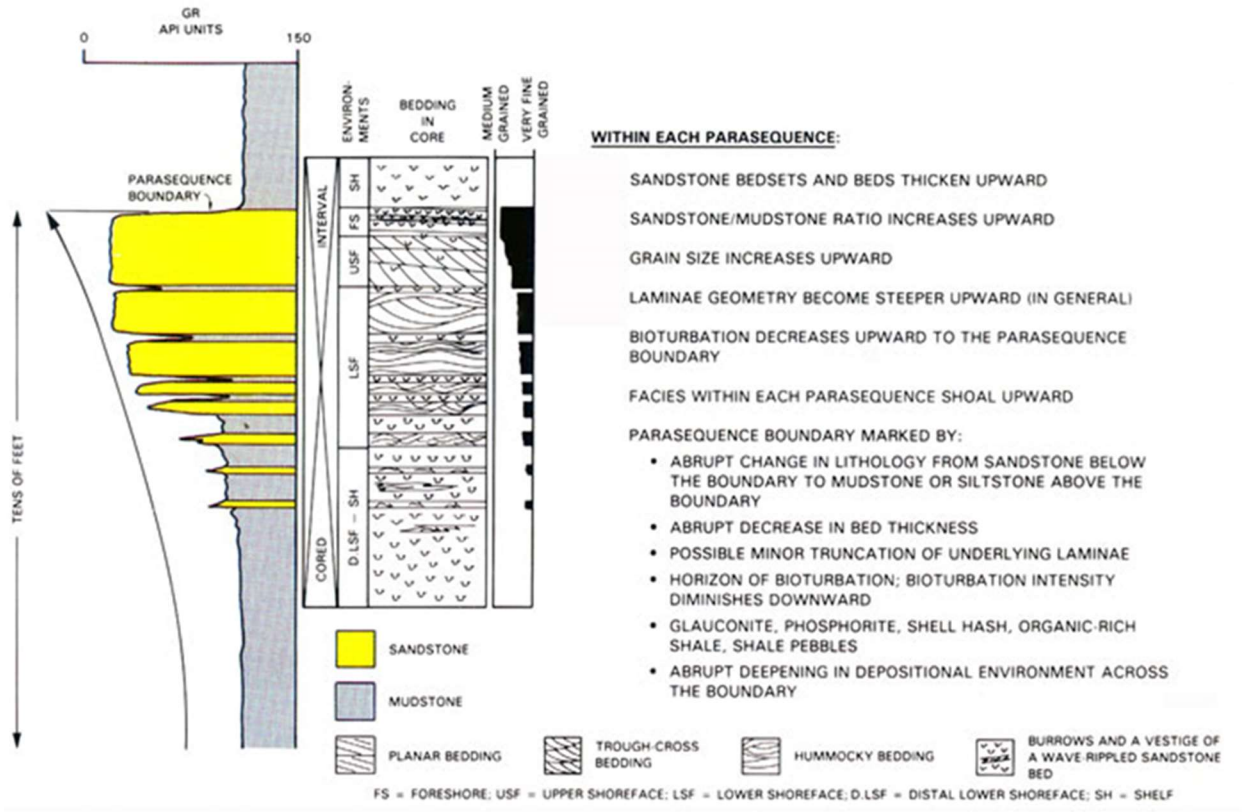

Fig. 4. Stratal characteristics of an upward-coarsening parasequence. This type of parasequence is interpreted to form in a beach environment on a sandy, wave- or fluvial-dominated shoreline. From Van Wagoner et al. (1990).

3.2 Ichnology of wave-dominated parasequences

Integrating both ichnology and sedimentology within a sequence-stratigraphic framework has been instrumental for refining facies models (e.g. Pemberton et al., 2001; Buatois and Mángano, 2011). The use of ichnology to delineate parasequences is based on the fact that trace-fossil associations are excellent indicators of environmental conditions that typically change along the depositional profile (Buatois and Mángano, 2011).

A wave-dominated parasequence coarsens and thickens upwards in succession indicating shoreline progradation bounded by a marine-flooding surface (MacEachern et al., 2010),

representing an increase in hydrodynamic energy, degree of oxygenation, sand content, amount of organic particles in suspension, and mobility of the substrate that control the vertical distribution of trace fossils (Pemberton et al., 1992; Mángano et al., 2002, 2005; Buatois and Mángano, 2011). Still, very few studies have been published documenting in detail the vertical changes in ichnofabrics as a response to parasequence architecture (e.g. Carmona et al., 2008, 2012).

3.3 Ichnofacies of wave-dominated parasequences

Ichnofacies in wave-dominated parasequences include distal *Cruziana*, archetypal *Cruziana*, proximal *Cruziana*, *Skolithos*, *Macaronichnus* assemblage of *Skolithos*, and *Psilonichnus*. The shelf (Facies A) is represented by the *Zoophycos* ichnofacies. With decreasing proximity to the shoreline, the lower offshore (Facies B) is represented by the distal *Cruziana* ichnofacies, while both the upper offshore (Facies C) and offshore transition (Facies D) are represented by the archetypal *Cruziana* ichnofacies. The lower shoreface (Facies E) includes a combined proximal *Cruziana* and *Skolithos* ichnofacies. With decreasing proximity to the shoreline the *Cruziana* ichnofacies is replaced by the *Skolithos* ichnofacies in the middle shoreface (Facies F). *Skolithos* ichnofacies continues to the upper shoreface (Facies G), with more proximal deposits of the foreshore (Facies H) being represented by a *Macaronichnus* dominated assemblage of the *Skolithos* ichnofacies. Lastly, the backshore (Facies I) is represented by the *Psilonichnus* ichnofacies (MacEachern and Pemberton, 1992; MacEachern et al., 1999; Mángano et al., 2002, 2005; Buatois and Mángano, 2011).

3.4 Facies of wave-dominated parasequences

3.4.1 Shelf

The shelf is the most distal facies in the wave-dominated shallow marine deposits, located below the storm wave base to the continental slope, dominated by low energy suspension fallout and highly bioturbated muds with thin lenses of sand resulting from turbidity currents (Buatois and Mángano, 2011).

Shelf deposits are dominated by the *Zoophycos* ichnofacies (MacEachern et al., 1999; Pemberton et al., 2001; Buatois and Mángano, 2011). Although shelf deposits are intensely bioturbated, ichnodiversity is low and assemblages typically include *Chondrites* (Ch), *Zoophycos* (Zo), and *Phycosiphon* (Ph) as common components, with ichnofabrics being dominated by deep-tier structures (MacEachern et al., 2010; Buatois and Mangano, 2011). Under anoxic conditions, the shelf is dominated by parallel-laminated black shale facies (Buatois et al., 2006; Angulo and Buatois, 2009; Buatois and Mángano, 2011).

3.4.2 Lower Offshore

The lower offshore is located above the storm wave base (MacEachern et al., 1999; Pemberton et al., 2001; Buatois and Mángano, 2011) dominated by low energy suspension fallout, highly bioturbated muds like the shelf. There is however an increase in the amount of thin sand lenses from turbidity currents and storm events. These sand lenses have sharp bases and oscillatory flow ripples (MacEachern et al., 2010) resulting from decreased proximity to the shoreline.

Lower offshore deposits are dominated by the distal *Cruziana* ichnofacies (MacEachern et al., 1999; Pemberton et al., 2001; Buatois and Mángano, 2011), showing an increase in ichnodiversity in comparison to the *Zoophycos* ichnofacies of the shelf (MacEachern et al., 2010). Ichnofauna includes *Phycosiphon* (Ph), *Chondrites* (Ch), *Zoophycos* (Zo), *Planolites* (Pl), *Teichichnus* (Te), *Asterosoma* (As), *Schaubcylindrichnus* (Sf), *Scolicia* (Sc), and *Thalassinoides* (Th) (MacEachern et al., 2010; Buatois and Mángano, 2011).

3.4.3 Upper Offshore

The upper offshore is located above the lower offshore (MacEachern et al., 1999; Pemberton et al., 2001; Buatois and Mángano, 2011) and is subject to more variable conditions than the lower offshore facies with periods of high energy being more frequent and longer in amongst the background of low energy suspension fallout. This results in bioturbated muds being punctuated more frequently by relatively coarser-grained silts and sands with lamination and ripples. Micro-hummocky, HCS, and planar lamination may even occur (Buatois and Mángano, 2011).

Upper offshore deposits are dominated by the archetypal *Cruziana* ichnofacies (MacEachern et al., 1999; Pemberton et al., 2001; Buatois and Mángano, 2011), showing a further increase in ichnodiversity in comparison to the distal *Cruziana* ichnofacies of the lower offshore (MacEachern et al., 2010), recorded in the heavily bioturbated fair-weather mudstone (Buatois and Mángano, 2011). Ichnofauna includes *Asterosoma* (As), *Arenicolites* (Ar), *Bergaueria* (Be), *Planolites* (Pl), *Curvolithus* (Cu), *Protovirgularia* (Pr), *Lockeia* (Lo), *Palaeophycus* (Pa), *Arthrophycus* (Art), *Phycodes* (Pc), *Thalassinoides* (Th), *Rhizocorallium*

(Rh), *Rosselia* (Ro), *Teichichnus* (Te), *Zoophycos* (Zo), and *Phycosiphon* (Ph) (MacEachern et al., 2010; Buatois and Mángano, 2011).

3.4.4 Transgressive Offshore Sandstones

Transgressive offshore sandstones are located below the fair-weather wave base within a low-gradient open-marine setting (Swift and Parsons, 1999) subject to consistent, predominantly unidirectional currents (Tillman and Martinsen, 1987; Tillman, 1999) representing a progradational dunefield that developed as a response to the onset of a tidal-transport system (Veiga and Schwarz, 2016). In previously studied deposits, this results in clean, cross-bedded (trough) and cross stratified (tangential and tabular), fine-grained sandstone interpreted as 3-D and 2-D subaqueous sand dunes that overlie the transgressive skeletal sandstones, representing the base of the sand dune. Ripple cross-laminated, very fine- to fine-grained sands may be dominant or grade vertically from cross-stratified beds representing distal expressions of the 2-D dunes, referred to as a sand wave. The resulting sequence includes floatstones and overlying wackestones above the clean sandstone unit representing late transgressive carbonates within the offshore sand body (Schwarz, 2012; Schwarz et al, 2016).

Trace fossils of transgressive offshore sandstones are different than those of shoreface deposits as few ichnotaxa are observed in comparison to most Cretaceous shoreface sandstones. In comparison to Cretaceous shoreface sandstones, transgressive offshore sandstones typically lack *Asterosoma*, *Rosselia*, *Rhizocorallium*, and readily abundant *Ophiomorpha* (Tillman and Martinsen, 1989; Tillman, 1999). The base of the transgressive offshore sandstones is commonly burrowed by *Thalassinoides* extending into the underlying substrate filled by the skeletal sandstone representing the *Glossifungites* ichnofacies. Within the cross-stratified clean sands, the *Skolithos* ichnofacies is observed; deposits have a low bioturbation index dominated by

horizontal burrows of *Ophiomorpha* (dominant)*, Palaeophycus*, and subordinate *Skolithos*. In more proximal locations of the sand dune, bioturbation is very high with few discrete trace fossils. A massive structure dominates with only the most robust elements of the *Skolithos* ichnofacies, *Ophiomorpha* being present (Tillman, 1999; Schwarz, 2012).

3.4.5 Offshore Transition

The offshore transition is located above the upper offshore and below the fair-weather wave base (MacEachern et al., 1999; Pemberton et al., 2001; Buatois and Mángano, 2011) with an identical alternation between high energy and low energy conditions, resulting in scoured based, HCS, very fine-grained sandstone with ripples at the top and bioturbated mudstones, respectively (Buatois and Mángano, 2011). Bioturbation of mudstone in the offshore transition decreases with decreasing proximity to the shoreline, resulting in lower bioturbation than in more distal facies.

Offshore transition deposits are dominated by the archetypal *Cruziana* ichnofacies (MacEachern et al., 1999; Pemberton et al., 2001; Buatois and Mángano, 2011), with storm-related *Skolithos* ichnofacies being displayed in the sandstone (Buatois and Mángano, 2011). The offshore transition includes a wide variety of ichnotaxa including *Cruziana* (Cr), *Rusophycus* (Ru), *Diplichnites*, *Gyrolithes*, *Arthrophycus* (Art), *Scolicia*, *Cylindrichnus*, *Rosselia* (Ro), *Phycosiphon* (Ph), *Lockeia* (Lo), *Protovirgularia* (Pr), *Siphonichus* (Si), *Teichichnus* (T), *Phycodes* (Pc), *Asterosoma* (As), *Schaubcylindrichnus* (Sf), *Taenidium* (Ta), *Rhizocorallium* (Rh*), Thalassinoides* (Th), *Chondrites* (Ch), *Paleophycus* (Pa), and *Planolites* (P). The *Skolithos* ichnofacies of the offshore transition includes predominantly *Skolithos* (Sk), *Ophiomorpha* (Op), and *Arenicolites* (Ar) (MacEachern et al., 2010; Buatois and Mángano, 2011).

3.4.6 Lower Shoreface

The lower shoreface is located above the fair-weather wave base (Reinson, 1984; Walker and Plint, 1992; MacEachern et al., 1999; Buatois and Mángano, 2011) with wave action being the dominant process (Buatois and Mángano, 2011). The lower shoreface therefore results in deposits of HCS very-fine grained sandstones (Plint, 2010).

Lower shoreface deposits are represented by combined proximal *Cruziana* and *Skolithos* ichnofacies (MacEachern et al., 1999; Pemberton et al., 2001; Buatois and Mángano, 2011) as these facies displays strong ichnologic variability resulting from variations in intensity and duration of storm events (MacEachern and Pemberton, 1992; Buatois and Mángano, 2011). In a weakly storm-affected lower shoreface there is a low amount of tempestites preserved, a high degree of bioturbation in fair-weather deposits (Buatois et al., 2002, 2003; Carmona et al., 2008), and an overall high biodiversity (Buatois and Mángano, 2011). In a moderately storm-effected shoreface, stacked tempestites with preserved burrow tops and fair-weather beds display a lam-scram appearance (MacEachern and Pemberton, 1992; Pemberton et al., 2012), whereas in a strongly storm-affected lower shoreface, deposits consist of amalgamated HCS sandstones (Plint, 2010) with little to no bioturbation, typical of high intensity and frequency of storms (Buatois and Mángano, 2011). With high energy storm conditions prevailing, only the deepest structures are preserved in the lower shoreface of a strandplain body succession (Plint, 2010) -- the post-storm *Skolithos* ichnofacies (e.g. *Skolithos* and *Ophiomorpha*) (Buatois and Mángano, 2011). This commonly results in lower shoreface and middle shoreface facies being classified together as the lower-middle shoreface (Mángano et al., 2005; Plint, 2010), as lack of fair-weather suite ichnofacies creates complications of using ichnofacies to categorize facies (MacEachern and Pemberton, 1992; Buatois and Mángano, 2011).

3.4.7 Middle Shoreface

The middle shoreface is located where shoaling and initial breaking of waves occur (Reinson, 1984; Clifton, 2006; Buatois and Mangano, 2011) under high energy conditions. The middle shoreface includes local amounts of cross-bedding passing down into wavy-planar amongst a background of SCS and HCS (Plint, 2010).

Middle shoreface deposits are represented by the *Skolithos* ichnofacies (MacEachern and Pemberton, 1992; MacEachern et al., 1999; Pemberton et al., 2001; MacEachern et al., 2010; Buatois and Mángano, 2011) as this facies experiences consistent high energy conditions; ichnodiversity, however, remains higher than in the more proximal facies of the *Skolithos* suite (MacEachern et al., 2010; Buatois and Mángano, 2011). Ichnofauna includes *Ophiomorpha* (Op), *Skolithos* (Sk), *Diplocraterion* (Di), *Arenicolites* (Ar), *Bergaueria* (Be), *Rosselia* (Ro), with vertically dominated components of *Thalassinoides* (Th) being susceptible for preservation as well. Similar to the lower shoreface in a strandplain body succession, only the deepest structures may be preserved (Plint, 2010) due to high rates of both erosion and deposition. This effectively removes evidence of a higher-ichnodiversity lower shoreface (MacEachern and Pemberton, 1992; Buatois and Mángano, 2011), facilitating a combined lower-middle shoreface facies (Mángano et al., 2005; Plint, 2010).

3.4.8 Upper Shoreface

The upper shoreface is located below the low-tide line, and is subjected to multidirectional current flows in the build-up and surf zone (Clifton et al., 1971; Komar, 1976; Walker and Plint, 1992; Buatois and Mángano, 2011) under high energy conditions depositing well-sorted

medium- to coarse-grained sandstone with large scale tabular and TCS, with minor amounts of low angle lamination (Plint, 2010).

Upper shoreface deposits are represented by the *Skolithos* ichnofacies (MacEachern and Pemberton, 1992; MacEachern et al., 1999; Pemberton et al., 2001; MacEachern et al., 2010; Buatois and Mángano, 2011) with sparse bioturbation and reduced ichnodiversity compared to the more distal middle and lower shoreface facies as a result of continuous bedform migration under high energy conditions (Buatois and Mángano, 2011). Ichnofauna may include *Skolithos* (Sk), *Arenicolites* (Ar), *Diplocraterion* (Di), *Ophiomorpha* (Op), local *Conichnus* (C) and *Macaronichnus segregatis* (Ms) (MacEachern et al., 2010; Buatois and Mángano, 2011). In modern environments, the upper shoreface features many tracks and trails; however, preservation potential in such a high energy environment, dictates that only the deeper structures of vertical domiciles remain preserved (Buatois and Mángano, 2011).

3.4.9 Foreshore

The foreshore is located in the intertidal area and is characterized by high-energy (Buatois and Mángano, 2011), well sorted, planar, low-angle laminated medium- to coarse-grained sandstones (Plint, 2010), commonly with parting lineation (Buatois and Mángano, 2011).

Foreshore deposits are represented by the *Macaronichnus* assemblage of the *Skolithos* ichnofacies (MacEachern and Pemberton, 1992; MacEachern et al., 1999; Pemberton et al., 2001; MacEachern et al., 2010; Buatois and Mángano, 2011). Low ichnodiversity characterizes the foreshore with zones of intense bioturbation by *Macaronichnus* (Ms) common amongst a background of sparse to no bioturbation (MacEachern and Pemberton, 1992; Pemberton et al., 2001; MacEachern et al., 2010; Buatois and Mángano, 2011). Deep tier dwelling structures such

as *Skolithos* (Sk) and *Ophiomorpha* (Op) may also be found in foreshore deposits (Buatois and Mángano, 2011).

3.4.10 Backshore

The backshore is located in the supralittoral area of the wave-dominated depositional profile as this subaerial facies is susceptible to periodic flooding during storm events and torrential rains (Frey and Pemberton, 1987; Buatois and Mángano, 2011). Bedforms of the backshore vary, from distinct sand dune cross bedding, to fine-grained sandstone with faint sub-horizontal stratification, root traces (rt), and insect burrows of the vegetated coastal dunes (Plint, 2010).

Backshore deposits are represented by the *Psilonichnus* ichnofacies (Frey and Pemberton, 1987; Pemberton et al., 2001; MacEachern et al., 2010; Buatois and Mángano, 2011) characterized by low ichnodiversity and low abundance produced by arthropods, vertebrates, and plants (Frey and Pemberton, 1987; Buatois and Mángano, 2011). Root traces (rt) produced by halophytic vegetation are common of the backshore as they are formed in many environments, are able to colonize dunes as they are ecological pioneers, and hardy enough to be able to survive environmental fluctuations (Brown and McLachlan, 1990; Buatois and Mángano, 2011). In addition, root traces (rt) are vertically dominated structures which have a greater preservation potential opposed to arthropod of vertebrate trackways which have a lower preservation potential (Curran, 1984; Frey et al, 1984; Plint, 2010). Like root traces, vertical J-, Y-, and U- shaped burrows produced by ghost crabs of the family Ocypodidae, ichnogenus *Psilonichnus* (Ps), which are diagnostic of the backshore facies (Frey et al., 1984; Buatois and Mángano, 2011).

More proximal to the backshore, and effectively out of the classification of a wave-dominated strandplain succession, the *Psilonichnus* ichnofacies grades into terrestrial ichnofacies such as the *Scoyenia*, and *Coprinisphaera* ichnofacies (Buatois and Mángano, 1995; Genise et al., 2000; Buatois and Mángano, 2011).

3.5 Ichnofabric Approach

The ichnofabric approach emphasizes the taphonomic aspects of the trace-fossil record and is a comprehensive way to analyze degrees of bioturbation leading to information about the sandstone reservoir properties, benthic paleoecology, and evolutionary paleoecology (Buatois and Mángano, 2011). However, only by evaluating the ichnofabrics ethologically in the context of the ichnofacies paradigm can they be utilized in any meaningful way to characterize the paleoenvironment (MacEachern et al., 2010). Ecological stratification within the ichnofabric approach is referred to as tiering, the vertical partitioning of the community in the substrate (Ausich and Bottjer, 1982; Bromely and Ekdale, 1986) controlled by consolidation of the substrate, organic matter, and oxygenation content (Bromley, 1990; Bromley, 1996). Trace fossils are categorized into shallow, mid and deep tiers and once tiers are assigned, a tiering diagram can be constructed and visually compared with bedding of a deposit to quantify bioturbation on a scale of BI=0 to BI=6 (Taylor and Goldring, 1993).

3.6 Shoreface Variability

Shallow marine wave-dominated clastic parasequences may display strong sedimentologic variability (Hart and Plint, 1995; Clifton, 2006; Plint, 2010; Pemberton et al., 2012) as a result of alternating and contrasting hydrodynamic energy levels due to overall storm intensity, storm frequency, and relative water depth (Pemberton et al., 2012), as well as ichnologic variability as the storms facilitate stress factors on the benthic communities (Buatois and Mángano, 2011).

Integration of sedimentology and ichnology can provide a high-resolution model to identify wave-dominated facies (Pemberton et al., 2012).

In a shallow marine wave-dominated coastline, there is a general proximal-distal energy gradient with a seaward decrease in wave energy (Yoshida et al., 2007) that results in the *Skolithos* ichnofacies being located in a more proximal location and the *Cruziana* ichnofacies being located in a more distal location (MacEachern et al., 1999; Buatois and Mángano, 2011). However, this does not account for storm intensity frequency and variability in a shallow marine clastic environment. The lower-middle shoreface contains the highest variability in terms of both ichnodiversity and sedimentology (Pemberton et al., 2012). These alternating storm events and fair-weather conditions are represented by contrasting *Skolithos* and *Cruziana* ichnofacies, respectively, with the *Skolithos* ichnofacies representing opportunistic colonization and the *Cruziana* ichnofacies representing a stable, climax community (MacEachern et al., 2010). Shoreface variations attributed to overall storm intensity, storm frequency, and relative water depth result in different taphonomic pathways facilitating categorization of three major types of shorefaces; (1) strongly storm-dominated, (2) moderately storm-affected, and (3) weakly storm-affected (Buatois and Mángano, 2011; Pemberton et al., 2012). Two types of tidal shorefaces have also been defined by different hydrodynamic conditions: (1) tidally influenced shorefaces (TIS), and (2) tidally modulated shorefaces (TMS) (Dashtgard et al., 2009; Frey and Dashtgard, 2011; Pemberton et al., 2012).

3.6.1 Strongly storm-dominated Shorefaces

Strongly storm-dominated shorefaces (Fig. 12A) lead to erosionally amalgamated tempestites with hummocky cross-stratification (HCS) and swaley cross-stratification (SCS) with few preserved biogenic structures (MacEachern and Pemberton, 1992; Pemberton et al., 2012).

They occur when there is a short-term colonization window because erosion is facilitated by repeated storm events resulting in preservation of only the deepest tiered structure of vertical domiciles of the *Skolithos* Ichnofacies (MacEachern et al., 2010; Plint, 2010; Buatois and Mángano, 2011).

3.6.2 Moderately storm-dominated Shorefaces

Moderately storm-dominated shorefaces lead to alternating stacked tempestites and fair-weather beds displaying a lam-scram appearance (MacEachern and Pemberton, 1992; Pemberton et al., 2012). This type of shoreface occurs when moderate to little erosion occurs on a climax community, followed by renewed storm deposition, resulting in alternating intervals of the storm primary fabric overprinted by elements of the *Skolithos* Ichnofacies, and bioturbated intervals containing representatives of the fair-weather suite *Cruziana* Ichnofacies (MacEachern and Pemberton, 1992; Buatois and Mángano, 2011).

3.6.3 Weakly storm-affected Shorefaces

Weakly storm-affected shorefaces lead to little to no preservation of tempestites and a succession dominated by fair-weather deposits that are heavily bioturbated (MacEachern and Pemberton, 1992; Pemberton et al., 2012), displaying high ichnodiversity and dominated by infaunal feeding structures of a climax community illustrating the *Cruziana* Ichnofacies. In addition to the already bioturbated fair-weather deposits, storm beds in weakly storm-affected shorefaces may be completely biogenically reworked (Buatois et al., 2002, 2003; Carmona et al., 2008; Buatois and Mángano, 2011). This type of shoreface occurs when there is a very long-term colonization window with little to no erosion (Buatois and Mángano, 2011). Conversely, in some cases, where only the highest energy conditions prevail in the lower and middle shorefaces, this

results in these facies being classified together as the lower-middle shoreface (MacEachern and Pemberton, 1992; Mángano et al., 2005; Plint, 2010).

3.6.4 Tidally influenced Shorefaces

Tidally influenced shorefaces (TIS) are relatively newly identified shorefaces produced on coast lines with strong tidal currents such as strait margins and embayments, with sedimentologic and ichnologic criteria indicative of the TIS being restricted to the lower shoreface and offshore (Frey and Dashtgard, 2011; Pemberton et al., 2012).

In tidally influenced shorefaces (TIS) (1) grain size remains constant or slightly increases seaward across the offshore to middle shoreface zone, having little mud content, (2) current generated structures and planar bedding dominate the lower shoreface and offshore if not obliterated by bioturbation, (3) archetypal *Skolithos* ichnofacies dominates, (4) there is increased preservation of wave generated structures (HCS and SCS) with limited preservation of bioturbated fair-weather beds towards the middle shoreface, and (5) the upper shoreface and foreshore are both sedimentologically and ichnologically similar to their wave-dominated counterparts (Frey and Dashtgard, 2011; Pemberton et al., 2012).

3.6.5 Tidally modulated Shorefaces

Tidally modulated shorefaces (TMS) like Tidally influenced shorefaces (TIS) are also relatively newly described (Dashtgard et al., 2009; Dashtgard et al., 2012) and occur on the end member for the wave-tidal spectrum settings, indicating tidal settings prone to strong wave energy resulting in lateral movement of wave zones across the shoreface-shelf profile in response to tidal action (Pemberton et al., 2012).

Tidally modulated shorefaces (TMS) are identified on the basis of (1) common interbedding of tidal sedimentary structures down the shoreface profile, (2) the notable absence of an obvious middle shoreface, (3) an anomalously thick foreshore, and (4) the presence of a low-diversity and low-density trace-fossil suite of simple vertical and horizontal burrows (Dashtgard et al., 2009; Pemberton et al., 2012).

CHAPTER 4.0: FACIES ASSOCIATIONS OF THE MULICHINCO FORMATION

4.1 Geological Background

4.1.1 Neuquén Basin

The Neuquén Basin (Fig. 5) is located east of the Andes in west-central Argentina and comprises approximately 6000 m of Upper Triassic to Paleogene strata formed in a back-arc basin covering over 120,000 km² (Leanza et al., 1977; Uliana et al., 1977; Legarreta and Uliana, 1991; Howell et al., 2005; Schwarz, 2012). During the Middle Jurassic to Early Cretaceous, as the Andes formed due to the eastward subduction of proto-Pacific oceanic crust beneath the western margin of Gondwana (Schwarz et al., 2006), the Neuquén Basin experienced thermal subsidence, interrupted by several episodes of structural inversion (Vergani et al., 1995; Schwarz and Howell, 2005). The basin later evolved into a shallow water epeiric seaway during the Late Jurassic and Early Cretaceous with ramp type margins in the east and south creating an aerial funnel morphology (Legarreta and Uliana, 1991). Within the basin, sedimentary infill from transgressive and regressive successions of the Mendoza Group (Tithonian–Barremian) (Groeber, 1946; Legarreta and Gulisano, 1989; Legarreta and Uliana, 1991; Schwarz et al., 2006) alternated as more distal deposits accumulated more proximally during the shoreline transgression forming retrogradational stacking patterns, and proximal sediments deposited more distally during shoreline regression forming progradational stacking patterns, facilitated by regional subsidence, tectonic inversion and uplift, as well as fault-controlled subsidence (Vergani et al., 1995; Schwarz et al., 2006). This infill reflecting the interaction between eustacy and tectonics (Vergani et al., 1995; Howell et al., 2005; Schwarz et al., 2006; Schwarz, 2012),

developed an extensive second-order highstand from Tithonian to early Valanginian, resulting in the funnel shaped morphology open to the north and west (Schwarz and Howell, 2005). During the early Valanginian, a tectonic inversion pulse occurred, accounting for a relative drop in sea-level (Vergani et al., 1995; Schwarz and Howell, 2005), which led to deposition of the Mulichinco Formation lowstand wedges in the central part of the basin (Schwarz et al., 2006).

Fig 5. Location map and approximate areal distribution of the Mulichinco Formation in the Neuquén Basin and study area (modified from Schwarz, 2012).

The study area is located within the central part of the Neuquén Basin (Fig. 5). The succession analyzed is within the second-order lowstand Mulichinco Formation wedge (Fig. 6), with the base of the unit overlying the Intra-Valanginian unconformity, separating the Mulichinco Formation from the anoxic shales of the Vaca Muerta Formation below (Gulisano et al., 1984; Schwarz and Howell, 2005; Schwarz et al., 2011; Schwarz and Buatois, 2012). The Intra-Valanginian unconformity represents a sequence boundary demarcated by alluvial deposits

overlying anoxic shale in proximal settings, and shallow marine carbonates above anoxic shale and marl in distal settings (Gulisano et al., 1984; Schwarz and Buatois, 2012). Capping the Mulichinco Formation is the dark gray to black, parallel-laminated shale of the Agrio Formation exhibiting a sharp base, directly above tabular or massive carbonates and siliciclastic successions at the top of the measured sections. Subdivision of these formations has been facilitated by observation of detailed biostratigraphic subdivisions of Lower Cretaceous (Berriasian–lower Barremian) strata through analysis of ammonite biozones and calcareous nanofossil bioevents within the Neuquén Basin (Aguirre-Urreta et al., 2005).

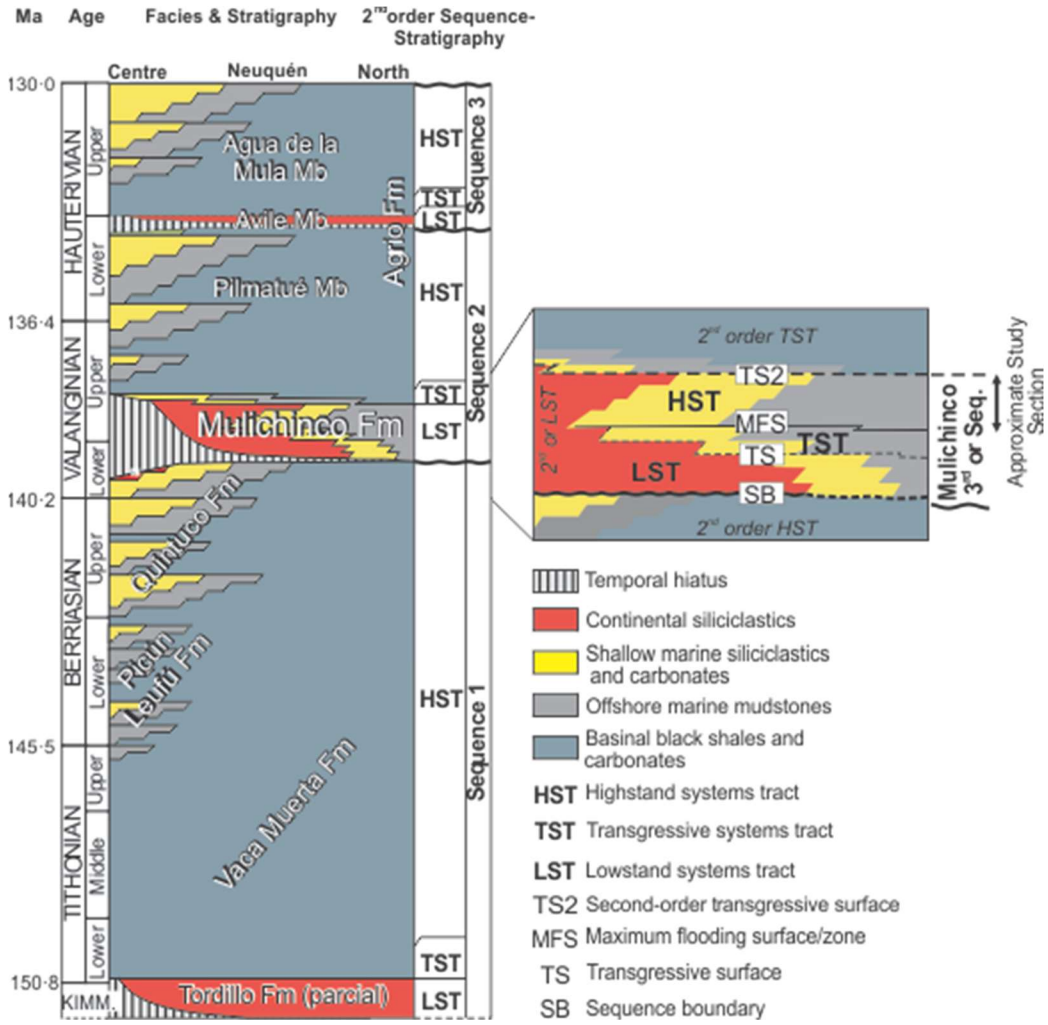

Fig. 6. Chronostratigraphic chart for the Tithonian-Huaterivian of the Neuquen Basin with age of units from Leanza (1993), Aguirre-Urreta et al. (2005) and Schwarz and Howell (2005). Time scale after Ogget al. (2004). The second-order lowstand Mulichinco Formation wedge was formed during relative sea-level drop facilitated by tectonic activity in the region. Schwarz and Howell (2005) identified third-order systems tracts (LST, TST, and HST), further refined by Schwarz et al. (2006) including key stratigraphic surfaces recognized within the Mulichinco strata (Fig. 6A), allowing classification of a third-order Mulichinco Lowstand Sequence (Schwarz et al., 2006; Schwarz, 2012; Schwarz et al., 2016). Approximate vertical dimension of the study section is shown within the Mulichinco third order sequence (modified from Schwarz, 2012).

4.1.2 Mulichinco Formation

The Mulichinco Formation is composed of three members: a lower, middle and upper (Fig. 7A), with as many as fourteen facies associations identified, ranging from continental, marginal marine, and shallow to outer-shelf marine settings (Schwarz and Howell, 2005). The lowermost

member of the formation is siliciclastic dominated, encompassing lower shoreface sandstone to offshore mudstone. The middle carbonate member of the formation ranges from offshore marl and wackestone to oyster-rich floatstone and boundstone (Schwarz and Howell, 2005; Schwarz et al., 2016). The upper member of the formation, the focus of this study, is a mixed siliciclastic-carbonate succession, comprising thin carbonates and thick, siliciclastic, open-marine deposits, stacked to form the parasequences discussed in this paper. In more proximal position south of the study area, marginal-marine deltaic, as well as fluvial systems (Schwarz and Howell, 2005), are interpreted to have acted as the sediment source for the uppermost part of the formation (Schwarz et al., 2008; Liberman et al., 2014; Schwarz et al., 2016). Provenance of the Mulichinco Formation sands is located in the southern hinterland, 100-120 km to the south of Puerta Curaco. These hinterlands would have provided the source for the proximal and distal braidplains, with clastics being continually transported northward and subsequently reworked, eventually effected by longshore currents and wave action on the shoreface (Schwarz and Howell, 2005).

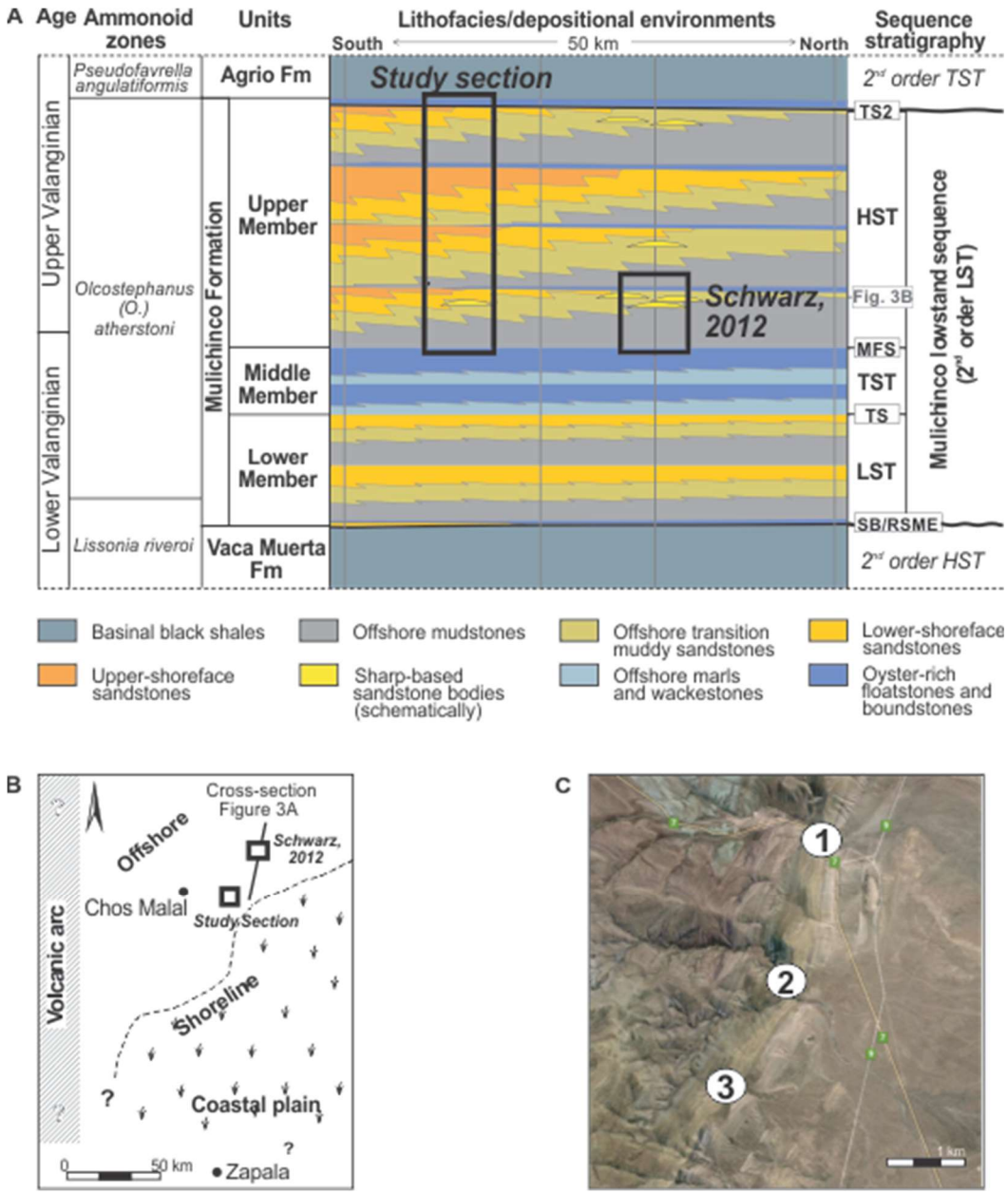

Fig. 7. (A). Cross-section showing age, facies, depositional systems and sequence stratigraphic framework of the Mulichinco Formation in the central region of the Neuquén Basin based on four sedimentological logs (gray vertical lines) (after Schwarz, 2012). See Fig. 1 for location of cross-section and extrapolated cross section perpendicular to it including the outcrops of this study. Note the north-east to south-west proximal to distal trend defined for the upper member of the Mulichinco Formation. The sharp-based sandstone bodies which are described in Schwarz (2012) and identified within the measured sections in this study are shown schematically, found within a succession dominated by offshore and offshore transition strata. (B). Highly schematic paleogeographical reconstruction of the Upper Member of the Mulichinco Formation from a time slice indicated in (A). Reconstruction is based on previously reported data (Schwarz and Howell, 2005; Schwarz et al., 2006; Schwarz, 2012; Schwarz and Buatois, 2012; Schwarz et al, 2016) and this paper. (C). Close up of the location of the study section outcrops; PCS1 (1), PCS2 (2), and PCS3 (3) within the Neuquén Basin.

4.1.3 Transgressive Offshore Sandstone Bodies

Isolated sandstone bodies have been described in detail since the 1970s resulting in interpretations that have evolved over time (Snedden and Bergman, 1999). Based on multiple datasets, new facies associations and architectural elements, recent re-analysis of previously interpreted shoreface facies associations in the Mulichinco Formation (Schwarz and Howell, 2005; Schwarz et al., 2006) call for a different sequence-stratigraphic model and the possibility that some of the sandstone-dominated intervals may represent transgressive offshore sandstone bodies (Schwarz, 2012; Schwarz et al., 2016). This model is similar to that proposed for the Shannon Sandstone of the Salt Creek Anticline (Wyoming, USA), indicative of transgressive deposition in an open marine setting (Tillman and Martinsen, 1987; Tillman, 1999; Swift and Parsons, 1999).

Offshore sandstone bodies are interpreted as being deposited by seaward migration of shore-detached 2-D and 3-D dunes formed below fair-weather wave base within a low-gradient open-marine setting during a transgression. The bases of the sandstone bodies represent both sequence boundaries and transgressive ravinement surfaces (SB/TRS) (Schwarz, 2012). Tabular and massive carbonate beds below these transgressive offshore sandstone bodies have also been interpreted to have been deposited during transgression. Where carbonates cap the sandstone bodies, those sandstones are interpreted as having been deposited during early transgression. In contrast, the carbonates are interpreted as having been deposited during late transgression. These transgressive deposits are subsequently overlain again by regressive highstand siliciclastic deposits (Schwarz et al., 2016).

4.2 Facies Associations

Within the research area, a total of 9 facies associations were identified in this study of the Mulichinco Formation: carbonate ramp oyster accumulations (FA1), lower offshore (FA2), upper offshore (FA3), storm-dominated offshore transition (FA4), weakly storm-affected offshore transition (FA5), storm-dominated lower shoreface (FA6), weakly storm-affected lower shoreface (FA7), upper shoreface (FA8), and offshore sand ridge (FA9).

4.2.1 FA1: Carbonate ramp oyster accumulations

Description: This facies association consists of massive, bioturbated nodular wackestone, bivalve shell bed floatstone (Fig. 8A), and packstone which are laterally extensive for hundreds of metres before pinching out. Beds are 0.05-0.5 m thick, forming intervals up to 5.5 m thick. Contact between FA1 and underlying facies association is typically scoured into FA2 and FA3. Tangential cross stratification may be locally observed with in the packstone with the tops of the beds capped with wave ripples. Fossils include articulated and disarticulated shallow-infaunal bivalves (*Trigonia* sp.), deep-infaunal bivalves (*Panopea* sp.), cemented oysters (*Ceratostreon* sp.), a few polychaetes (serpulids) and ammonoid shell fragments. Carbonate ramp oyster accumulations were used as the base of the study sections as they are easily recognizable across the study area.

Monospecific suites of *Thalassinoides* isp. are present. The degree of bioturbation is high (BI = 5-6). FA1 is commonly associated within offshore (FA3 and FA4) deposits, occurring at the top of a coarsening upwards succession at the base of the study sections, constituting the middle member of the Mulichinco Formation, and capping the top of the formation, above more proximal facies associations.

Interpretation: This facies association is interpreted as transgressive deposits within high frequency mixed carbonate–siliciclastic successions produced by changes in sediment supply facilitated by orbitally induced climate fluctuations (Schwarz, 2012). During intervals of extreme arid temperatures, low to minor amounts of siliciclastic influx were introduced to the system resulting in carbonate (FA1) deposition on the shelf and subsequent transgression of the carbonate ramp (James, 1997; Schwarz and Howell, 2005; Schwarz, 2012; Hönig and John, 2015; Navarro-Ramirez et al., 2015; Schwarz et al., 2016). Dominance of wackestone and packstone suggests siliciclastic starvation in a low energy system on a ramp-type open-marine setting. Low energy conditions are further supported by abundant articulated bivalves. The floatstone, though indicative of a low energy system, has coarser grains hosting an assemblage of fossils similar to the wackestone and is composed predominantly of siliciclastic and lime mud in an offshore (Burchette et al., 1990) or muddy middle ramp (Christ et al., 2012; Schwarz et al., 2016) setting. In the most proximal settings of the carbonate system within FA1, packstone having the same fossil composition as the floatstone but with a greater fragmentation indicates further reworking of sediment by wave action found above fair-weather wave base in inner-ramp settings (Burchette et al., 1990; Christ et al., 2012; Rankey, 2014; Schwarz et al., 2016). Benthic fauna largely consisting of bivalves (*Trigonia* sp., *Panopea* sp.) further supports a well oxygenated mobile substrate and under conditions of a high stressed, sediment starved environment; a low diversity of cemented oysters (*Ceratostreon* sp.) dominated the sediment-water interface (Schwarz and Howell, 2005).

4.2.2 FA2: Lower Offshore

Description: This facies association consists of dark gray, bioturbated mudstone locally interbedded with thin, very fine-grained silty sandstone exhibiting faint parallel lamination (Fig.

8B). Sandstone / mudstone ratios are very low (typically > 1:20). Silty sandstone beds are very thin (< 0.02 m); mudstone intervals are 0.3-0.5 m thick; overall thickness of FA2 intervals is 2-15 m. Contact of FA2 with the underlying facies association is invariably sharp. Fossils include articulated bivalves (*Trigonia* sp., *Panopea* sp.) and ammonoids.

Intensity of bioturbation in background mudstone is high (BI = 5-6), commonly evidenced by a mottled texture, whereas intensity of bioturbation in silty sandstone beds is low (BI = 0-1) with discrete *Thalassinoides* isp., *Teichichnus rectus*, and *Phycosiphon incertum* occurring in sandstone beds. FA2 is deposited above and below tabular or massive carbonates (FA1), and grades up into upper offshore (FA3) deposits.

Interpretation: This facies association is interpreted as being deposited by low energy, suspension fallout mud, punctuated infrequently by storm events. FA2 was formed well beneath the fairweather wave base and thus, these deposits have only been modified by the strongest storm events. At such depths, these thin, parallel laminated sandstones are not affected by fair-weather waves, providing a high preservation potential for primary fabric (Dott, 1983, 1988; Wheatcroft, 1990; Pemberton et al., 2012).

4.2.3 FA3: Upper Offshore

Description: This facies association consists of dark gray, bioturbated mudstone locally interbedded with very thin, very fine-grained sandstone with parallel and wave-ripple cross-lamination. Sandstone / mudstone ratios vary from 1:5 to 1:2. Individual very fine-grained sandstone beds are thicker (0.02-0.1 m) than in the underlying facies association. Mudstone intervals are 0.1-0.4 m thick. Thickness of FA3 intervals is 1.0-5.5 m. The contact of FA3 is gradational from FA2 and is demarcated by an increase in thickness and abundance of sandstone

beds. Similar, yet relatively fewer, body fossils are observed in in this facies association (*Trigonia* sp., *Panopea* sp.) in comparison to FA2.

Thalassinoides isp. and *Teichichnus rectus* occur in the sandstone. Bioturbation intensity is low (BI = 0-1) in the sandstone and high (BI = 5-6) in the mudstone, exhibiting a mottled texture, whereas sandstone beds exhibit sharp boundaries. FA3 is situated above lower offshore (FA2), and below offshore transition deposits (FA4 and FA5).

Interpretation: This facies association is interpreted as low energy, suspension fallout mud punctuated frequently by higher energy storm events. FA3, representing deposition in the upper offshore, exhibits increased and thicker storm beds as the storm induced oscillation maintains greater energy in these relatively shallower waters. Wave-ripple cross-lamination, occurring in addition to parallel lamination, represents the waning stage of storm activity at the sediment-water interface (Pemberton et al., 2012). Hydrodynamics of symmetrical ripples dictate conditions of low to moderate oscillatory flow speed with at most superimposed unidirectional flow, whereas weakly asymmetrical ripples suggest combined flow conditions with similar oscillatory flow conditions, but a moderate to strong unidirectional flow component (Dumas et al., 2005). The storm-induced tempestites contain no fossils, and display low bioturbation intensities (BI = 0-1), supporting high energy conditions that were suboptimal for colonization of organisms. This is in stark contrast to the fair-weather mudstone that represents low energy suspension fallout characterized by high degree of bioturbation (BI = 5-6), similar to the more distal lower offshore deposits (FA2) (MacEachern and Pemberton, 1992).

4.2.4 FA4: Storm-dominated Offshore Transition

Description: This facies association consists of interbedded silty mudstones and very fine-grained sandstone with hummocky cross stratification and parallel lamination (Fig. 8C).

Sandstone / mudstone ratios vary from 1:2 to 1:1. Very fine-grained sandstone beds are thicker than facies association FA3 (0.1-2.5 m), mudstone intervals are 0.1-2.5 m thick, and total thickness of FA4 intervals is 2.0-5.0 m. A sharp base is present on the bottom of the sandstone beds; however, this facies association is overall gradational from the underlying upper offshore (FA3) deposits. If uninterrupted by a by a change in the degree of storm influence, FA4 will grade upwards into the storm-dominated lower shoreface (FA6) deposits.

The trace-fossil association includes *Thalassinoides* isp. and *Ophiomorpha irregulaire* being dominant, escape trace fossils and equilibrium structures subordinate, and *Gyrochorte comosa*, *Lockeia siliquaria*, and *Hillichnus* isp. as accessory components. Degree of bioturbation in background mudstone is high (BI = 5-6), but with lower intensities in the interbedded tempestite sandstones (BI = 2).

Interpretation: This facies association is interpreted as regular alternation of low energy, suspension fallout with higher energy storm events, lying directly underneath the fair-weather wave base (Pemberton et al. 2001). Experimental work showed that HCS is formed under under high oscillation speeds with at most weak unidirectional flow speed (Dumas et al., 2005; Dumas and Arnott, 2006). During these high-energy storm events, eroded sand would be transported distally towards the offshore transition (FA4), deposited as tempestites within the offshore (FA2 and FA3) (Walker and Plint, 1992). At depths beneath the fair-weather wave base, there is almost equivalence between fair-weather and storm-induced deposition. Fair-weather deposits consist of intensely bioturbated (BI = 5-6) silty mudstone displaying high ichnodiversity where as storm-induced, sparsely bioturbated (BI = 0-1), hummocky cross stratified and parallel laminated sandstone deposits display low ichnodiversity (MacEachern and Pemberton, 1992; Buatois and Mángano, 2011).

4.2.5 FA5: Weakly storm-affected Offshore Transition

Description: This facies association consists of muddy and silty sandstone with faint parallel laminations, or faint wave- and combined-flow ripple cross-laminations. Where bioturbation is high (BI = 5-6), the primary sedimentary fabric is not preserved, being completely obliterated by bioturbation (Fig. 8D). Beds are 0.1-2.5 m thick. Total thickness of FA5 single section intervals is 1.0-9.0 m.

Degree of bioturbation is high (BI = 3-6). *Thalassinoides* isp. and *Gyrochorte comosa* are dominant, *Teichichnus rectus* and equilibrium trace fossils are subordinated, and *Lockeia siliquaria* and escape trace fossils accessory. The base of FA5 is gradational with underlying upper offshore (FA3).

Interpretation: This facies association is interpreted as low energy, mud suspension fallout with low intensity and low frequency of storms, directly beneath the fair-weather wave base. In comparison to the storm-dominated offshore transition (FA4), the reduced intensity and frequency of storm events results in a long-term colonization window and pervasive bioturbation. Through bioturbation, the mudstone and silty sandstone were thoroughly mixed and original primary fabric is commonly completely obliterated (Kachel and Smith, 1986; Wheatcroft, 1990) reflecting fair-weather deposition (Pemberton et al., 1992) in a well-oxygenated, fully marine setting (MacEachern and Pemberton, 1992).

4.2.6 FA6: Storm-dominated Lower Shoreface

Description: This facies association consists of amalgamated, hummocky cross-stratified, very fine-grained sandstone (Fig. 8E). Beds are 0.1-0.15 m thick, whereas amalgamated

sandstone intervals are 0.6-6 m thick. No mudstone interbedding is present throughout FA6 intervals.

Bioturbation intensity is low (BI = 0-2) with *Ophiomorpha irregulaire* dominant, *Skolithos* isp. subordinate, and *Sinusichnus* isp. and *Gyrochorte comosa* accessory. The base of FA6 is gradational with the storm-dominated offshore transition (FA4), and sharp when overlying the weakly storm-affected offshore transition (FA5).

Interpretation: This facies association is interpreted as high energy, oscillatory and combined flow above the fair-weather wave base (Walker and Plint, 1992; Schwarz and Howell, 2005). Water depths for the formation of HCS are estimated to range from 13 to 50 m (Dumas and Arnott, 2006). Long period waves can form with fine-grained sediments readily available in unrestricted open-water conditions (Dumas et al., 2005). As the high-energy conditions persisted, only organisms with primarily the most robust dwelling structures were able to colonize the substrate (MacEachern and Pemberton, 1992), representing opportunistic populations in a sandy storm-dominated environment (Echevarría et al., 2012).

4.2.7 FA7: Weakly storm-affected Lower Shoreface

Description: This facies association consists of very fine-grained sandstone with wave-, current-, and combined-flow ripple cross-lamination. Individual rippled laminae are < 0.01 m thick, commonly amalgamated with overlying and underlying rippled beds to produce thicker ripple cross-laminated beds (< 0.04 m thick) (Fig. 8F). Facies intervals are 0.4 - 9 m thick. A sharp base is present when overlying the storm-dominated lower shoreface (FA6); however, the base is gradational where overlying the weakly storm-affected offshore transition (FA5).

Degree of bioturbation is low (BI = 2) with *Gyrochorte comosa* dominant, *Thalassinoides* isp., ?*Scolicia* isp., *Lockeia siliquaria*, *Ophiomorpha irregulaire, Spongeliomorpha isp.*

subordinate, and *Hillichnus* isp., *Arenituba verso*, *Teichichnus rectus*, and *Protovirgularia* isp. accessory.

Interpretation: This facies association is interpreted as a low energy environment with low intensity and low frequency of storms above the fair-weather wave base (Schwarz and Howell, 2005). Under reduced intensity and frequency of storm events, wave and combined-flow ripple cross lamination were pervasive, resulting from the migration symmetrical and weakly asymmetrical ripples produced by combined low oscillatory and weak unidirectional flows (Myrow and Southard, 1996; Schwarz and Howell, 2005; Zecchin, 2007; Schwarz et al., 2016). Within this facies association at more distal locations, symmetrical wave-ripples may be preferentially formed due to the small size of the wave orbitals. In contrast, the wave orbitals increase in size as wave orbital motion becomes more asymmetric in a proximal direction, generating asymmetric bedforms (Clifton, 1976) as the result of the frictional component of the sediment acting on the stronger wave orbital moving sediment locally shoreward (Swift et al., 1991; Dumas and Arnott, 2006). Under pervasive low oscillatory and weak unidirectional conditions, fair-weather waves reworked the underlying storm deposits of the storm-dominated lower shoreface (FA6). As the weakly storm-affected lower shoreface (FA7) is adjacent to the offshore transition (FA5) and deposited under the same marine regime, the ichnoassemblage of FA7 more closely resembles FA5 than FA4, with ichnodiversity remaining high.

4.2.8 FA8: Upper Shoreface

Description: This facies association consists of amalgamated, tabular and trough cross-stratified, very fine- to fine-grained sandstone (Fig. 9A-B). Facies intervals are 5.5-14.0 m thick with individual beds ranging 0.25-0.5 m in thickness.

Bioturbation intensity is low (BI = 0-1) with *Ophiomorpha irregulaire* dominant, *Gyrolithes* isp. and *Gyrochorte comosa* accessory. The base of FA8 is sharp when overlying both strongly storm-dominated (FA6) and weakly storm-affected (FA7) lower shoreface deposits.

Interpretation: This facies association is interpreted as the upper shoreface deposited under high-energy, current conditions beneath the low tide line. Sediments representing the upper shoreface (FA8) are interpreted to be deposited laterally adjacent to the storm-dominated and weakly storm-affected lower shoreface facies associations, FA6 and FA7 respectively. High energy, fair-weather and longshore currents result in two- and three-dimensional dunes (Clifton et a., 1971; Greenwood and Mittler, 1985) where their migration forms tabular and trough cross-bedding (Walker and Plint, 1992) formed under a unidirectional flow velocity of ~ 40 cm/s (Dumas et al., 2005). Only the most robust organisms are able to colonize under these conditions (MacEachern and Pemberton, 1992; Buatois and Mángano, 2011).

4.2.9 FA9: Offshore Sand Ridge

Description: This facies association consists of skeletal, trough to planar cross-stratified, fine-grained sandstones. Beds are 0.2-0.5 m thick with facies intervals ranging 3.5-9.0 m thick (Fig. 9C-E). Current ripple cross-lamination is locally present and some beds appear massive.

Bioturbation ranges from absent to moderate (BI = 0-4) with *Ophiomorpha* isp. being the only visible ichnotaxon. In cases of more intense bioturbation, bed boundaries are only visible providing insight on an overall tabular bed geometry. FA9 is associated within offshore (FA2 and FA3) sediments, having a scoured base beneath the skeletal sandstone, and demonstrates various degrees of proximity to storm-wave base (FA6 and FA7).

Interpretation: This facies association is interpreted as high energy, mostly two-dimensional dune migration in an open shallow marine environment with well oxygenated, clean

waters, moving in an offshore direction. The offshore sand ridge has been estimated <7 m thick, <3km wide, and >3 km long (Schwarz, 2012). A skeletal sandstone demarcating a shell-rich transgressive lag, showing mixing of the benthic fauna, is diagnostic of this facies association. In places this lag is mantling a transgressive ravinement surface and sequence boundary (TRS/SB) where mixing of the benthic fauna occurred. Directly above the skeletal sandstones, transgressive cross-bedded sandstones are deposited. Finally, highly bioturbated sandstones with only bed boundaries being visible cap the cross-bedded sandstones at the top of FA9, deposited under more fair-weather conditions where colonization and bioturbation can take place (Schwarz, 2012). Similar to FA1, FA9 will not undergo further analysis in the study presented here.

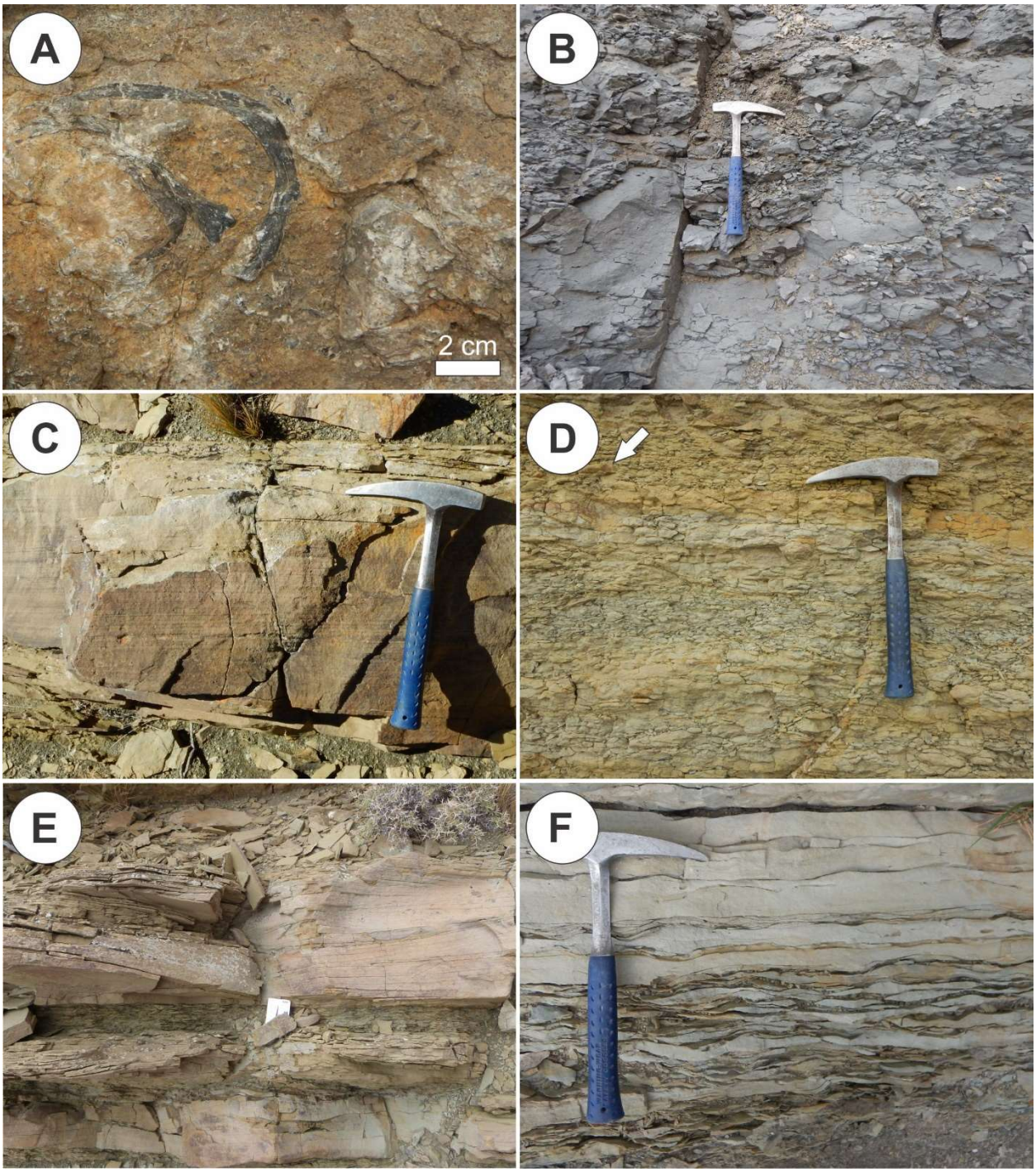

Fig. 8. Facies Associations 1-7. (A). Facies Association 1. Close up of floatstone in outcrop with a large oyster belonging to *Ceratostreon* sp. (B). Facies Association 2. Thoroughly bioturbated mudstones. (C). Facies Association 4. Bedding plane view of a storm bed with HCS interbedded with offshore mudstones. (D). Facies Association 5. Detailed view of bioturbated muddy-silty sandstone with *Thalassinoides* isp. (white arrow). (E). Facies Association 6. Bedding plane view of HCS dominated outcrop. (F). Facies Association 7. Generalized bedding plane view with showing thin mud drapes between wave rippled fine-grained sandstone.

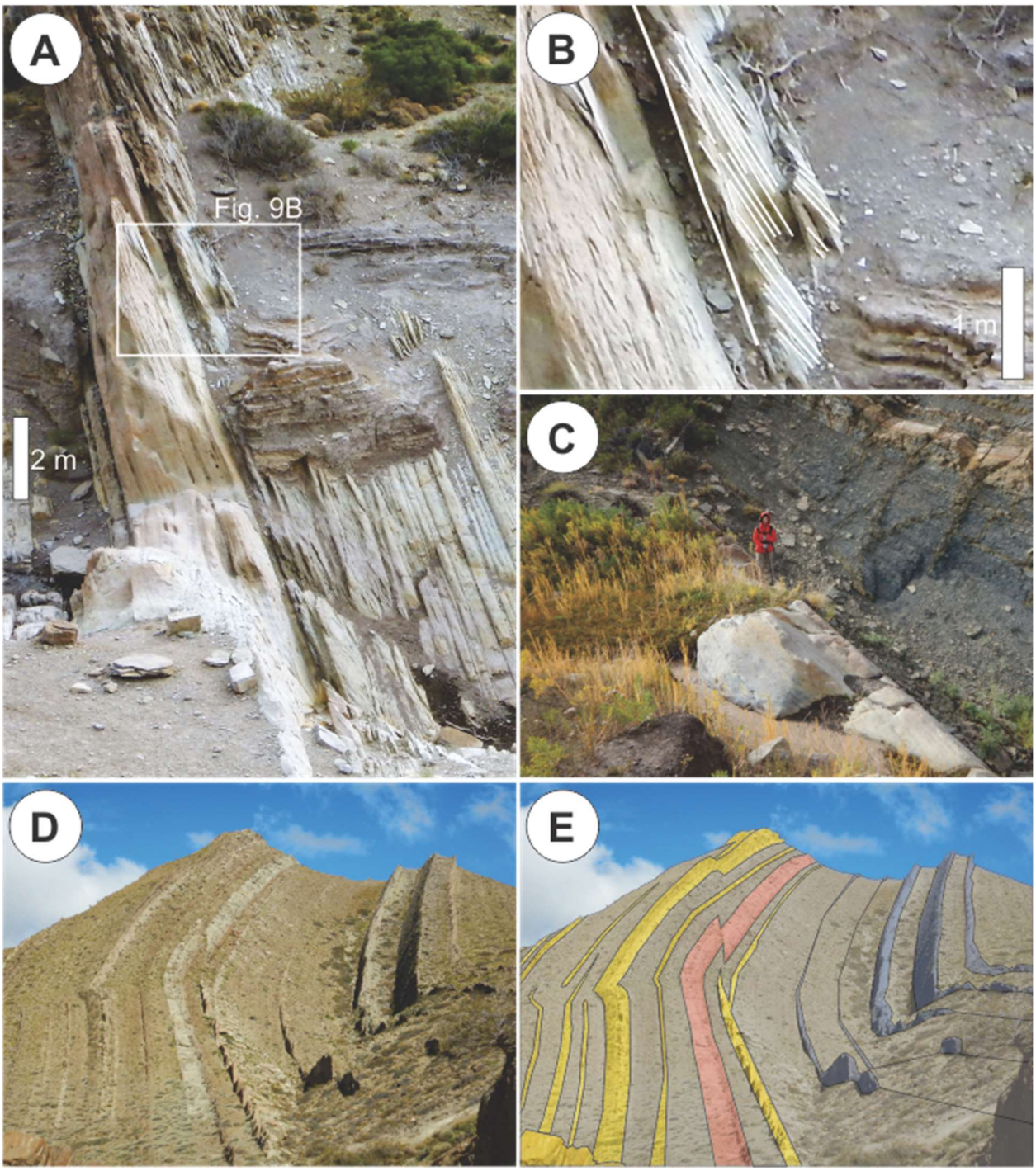

Fig. 9. Facies Associations 8-9. (A). Facies Association 8. Outcrop photograph of cross-stratified deposits. (B). Close up of cross-bedded stratification depicting the low angle surface at the base with the foresets angled above. (C). Facies Association 9. Outcrop photograph of the top of an offshore sandstone ridge capped by offshore mudstones (FA 2 and FA 3). (D). Panoramic view of FA 9 physically separated from shoreface sandstones by offshore mudstones. (E). Panoramic view with shading representative of depositional environment. Offshore sand ridge (red). Shoreface sandstones (yellow). Carbonate ramp oyster accumulations (blue). Offshore muds and offshore transition heteroliths (gray).

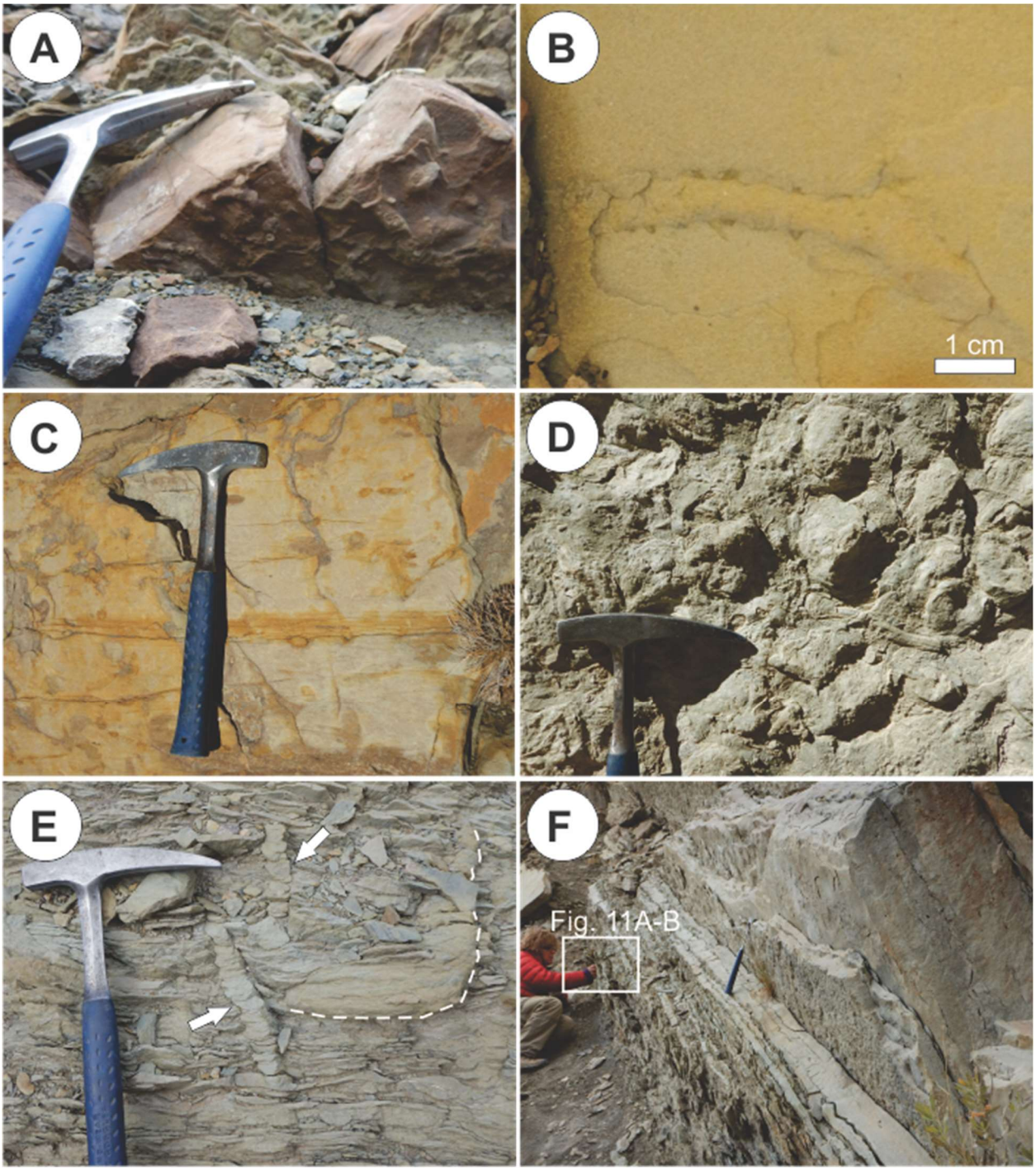

Fig. 10. Representative trace fossils. (A). Facies Association 4. Base of storm bed hosting three dimensional burrow systems of *Ophiomorpha irregulaire* indicative of high energy conditions. (B). Facies Association 6. *Ophiomorpha irregulaire* at the top of a cross stratified bed. (C). Cross sectional view of a HCS bed exhibiting horizontal and vertical shafts of *Ophiomorpha irregulaire*. (D). Facies Association 7. Base of ripple cross laminated bed with bivalve resting trace *Lockeia siliquaria* and *Thalassinoides* isp. (E). Wave rippled fine-grained sandstone with two different vertical expressions (white arrows and white hashed line) of the deposit feeding trace *Teichichnus rectus*. (F). Outcrop of FA 7 showing location of (Fig. 11A-B).

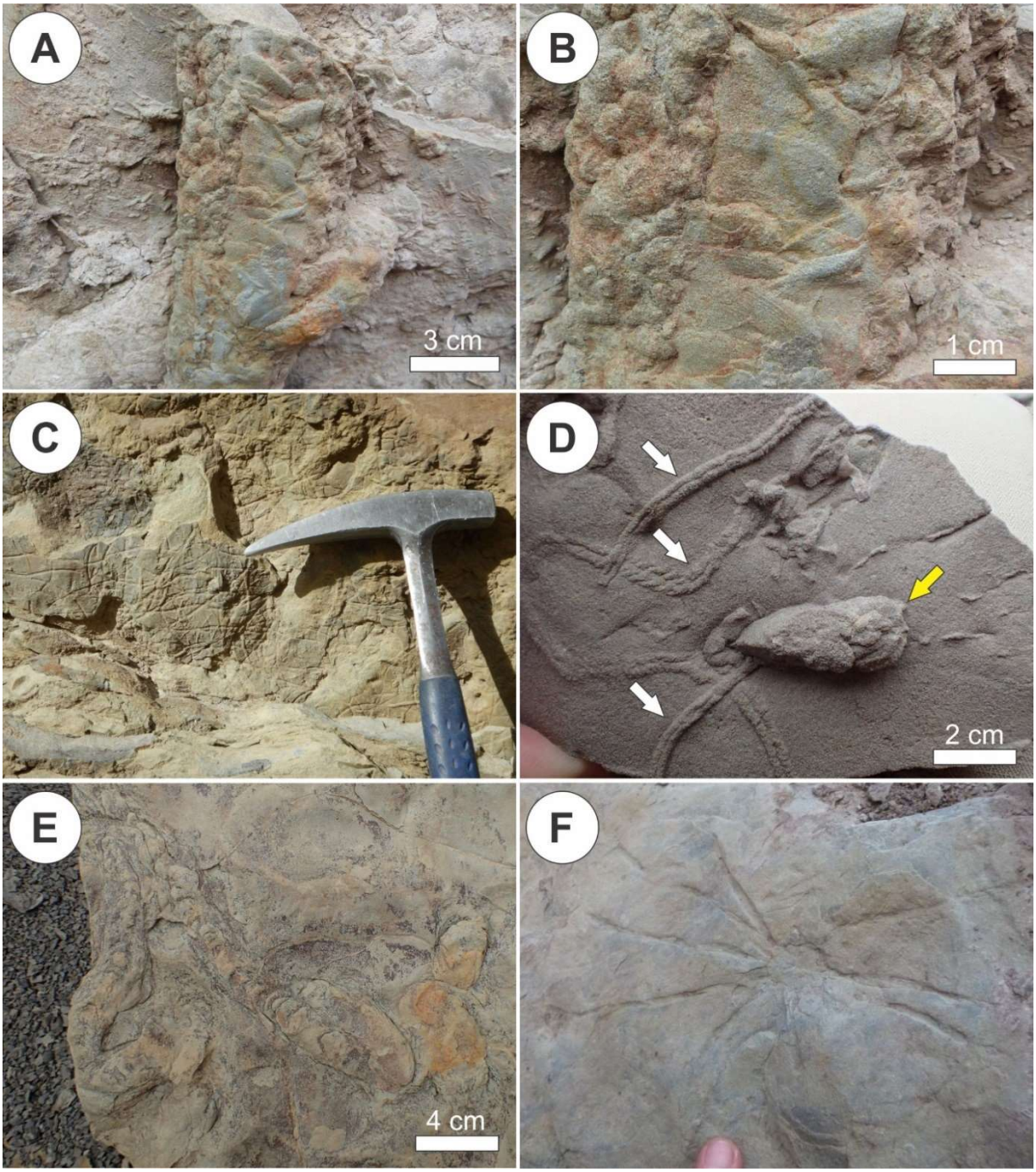

Fig. 11. Representative trace fossils. (A). Facies Association 7. Bedding plane view of a highly ornamented three dimensional crustacean burrow system, *Spongeliomorpha* isp. penetrating the wave rippled fine-grained sandstone with a smaller specimen cross cutting the original. (B). Close up of *Spongeliomorpha* isp. with scratch marks resulting in an heavily ornamented ventral surface, and bubbly-like texture on the lateral sides of the structure. (C). Base of a ripple cross laminated bed with dense, horizontal detritus feeding trails belonging to *Gyrochorte comosa*. (D). Close up of a bedding plane view displaying bilobate epichnial ridge and an underlying hypichnial groove of *Gyrochorte comosa* (white arrows) as well as a specimen of *Lockeia siliquaria* (yellow arrow). (E). Top of bedding plane view featuring echinoid deposit feeding trail, ?*Scolicia* isp. displaying internal menisci. (F). *Arenituba verso*, a system of radially branched tubes around a larger tube, at the base of a sandstone bed and probably produced by worm-like organisms.

Table 1. Facies Associations.

Facies Association	Lithology	Inorganic Sedimentary Structures	Thickness	Ichnology	Distribution and Vertical Facies Transition	Interpretation
FA1: Carbonate ramp oyster accumulations	Bioturbated, nodular wackestones, tabular and massive densely packed bivalve shell bed (± serpulids) floatstone and packstones.	Massive with tangential cross stratification locally in packstones. Tabular geometry.	0.05-0.5 m thick beds; 0.5-5.5 m thick facies intervals.	BI = 5-6. *Thalassinoides* isp.	PCS1, PCS2, and PCS3. Associated within, above, or below lower offshore (FA3) sediments, or below euxinic basinal deposits (FA2).	Transgressive conditions within high-frequency cycles on a low energy, siliciclastic starved, ramp-type open-marine carbonate system.
FA2: Lower Offshore	Mudstone locally interbedded with very thin, very fine-grained silty sandstone. Sandstone / mudstone ratios very low (typically > 1 : 20).	Parallel laminations.	<0.02 m thick silty sandstone beds; 0.3-0.5 m thick mudstone beds; 2-15 m thick facies intervals.	BI = 5-6 in background mudstones (mottled texture). Sandstone with *Thalassinoides* isp. *Teichichnus rectus*, and *Phycosiphon incertum*.	PCS1, PCS2, and PCS3. Deposited above and below tabular or massive carbonates (FA1), and grades up into upper offshore (FA4) sediments.	Low energy, suspension fallout punctuated infrequently by higher energy storm events, and lies directly above the storm wave base.
FA3: Upper Offshore	Mudstone locally interbedded with very thin, very fine-grained sandstone. Sandstone / mudstone ratio vary from 1 : 5 to 1 : 2.	Parallel laminations and wave-ripple cross lamination.	0.02-0.1 m thick very fine-grained sandstone beds; 0.1-0.4 m thick mudstone beds; 1-5.5 m thick facies intervals.	BI = 5-6 in background mudstones (mottled texture). Sandstone with *Thalassinoides* isp., and *Teichichnus rectus*.	PCS1, PCS2, and PCS3. Situated above lower offshore (FA3), and underneath offshore transition deposits (FA5 and FA6).	Low energy, suspension fallout punctuated frequently by higher energy storm events.
FA4: Storm-dominated Offshore Transition	Interbedded silty mudstones and very fine-grained sandstone. Sandstone / mudstone ratio vary from 1 : 2 to 1 : 1.	HCS and parallel laminations.	0.1-2.5 m thick very fine-grained sandstone beds; 0.1-2.5 m thick mudstone beds; 2-5 m thick facies intervals.	BI = 3-4 in background mudstones, and BI = 0-2 in sandstones. *Thalassinoides* isp., *Ophiomorpha irregulaire,* escape traces, equilibrium structures, *Gyrochorte comosa*, *Lockeia siliquaria*, and *Hillichnus* isp.	PCS1, PCS2, and PCS3. Deposited between upper offshore (FA4) and storm-dominated lower shoreface (FA7) sediments.	Regular alteration of low energy, suspension fallout with higher energy storm events, lying directly underneath the fair-weather wave base.
FA5: Weakly storm-affected Offshore Transition	Muddy-silty sandstone	Parallel laminations, wave-, and current-ripple cross-lamination faint, to primary sedimentary fabric not preserved. Tabular geometry.	0.1-2.5 m thick beds; 1-9 m thick facies intervals.	BI = 3-6. *Thalassinoides* isp., *Gyrochorte comosa, Teichichnus rectus*, equilibrium structures, *Lockeia siliquaria*, and escape traces.	PCS1, PCS2, and PCS3. Located above upper offshore (FA4) sediments and below weakly storm-affected lower shoreface (FA8) deposits.	Low energy, suspension fallout with low intensity and low frequency of storms, directly beneath the fair-weather wave base.
FA6: Storm-dominated Lower Shoreface	Amalgamated, very fine-grained sandstone	HCS.	0.1-0.15 m thick beds; 0.6-6 m thick facies intervals.	BI = 0-2. *Ophiomorpha irregulaire, Skolithos* isp., *Sinusichnus* isp., and *Gyrochorte comosa*.	PCS1, PSC2, and PCS3. Grading up from storm-dominated offshore transition (FA5) deposits into weakly storm-affected lower shoreface (FA7), or upper shoreface (FA9) deposits.	High energy, oscillatory and combined flow above the fair-weather wave base.
FA7: Weakly storm-affected Lower Shoreface	Very fine-grained sandstone	Wave-, and current-ripple cross-lamination. Tabular geometry.	< 0.01 m thick individual ripple laminae amalgamated to produce < 0.04 m thick ripple cross-laminated beds. 0.4-9 m thick facies intervals.	BI = 2. *Gyrochorte comosa, Thalassinoides* isp., ?*Scolicia* isp., *Lockeia siliquaria, Ophiomorpha irregulaire, Spongeliomorpha* isp., escape traces, *Hillichnus isp., Arenituba verso, Teichichnus rectus, and Protovirgularia* isp.	PCS1, PCS2, and PCS3. Situated above weakly storm-affected offshore transition (FA6), or storm-dominated lower shoreface (FA7), and below upper shoreface deposits (FA9).	Low energy environment with low intensity and low frequency of storms above the fair-weather wave base. May also include low energy reworking of storm-dominated lower shoreface (FA7) deposits, exhibiting relict *Skolithos* ichnofacies.
FA8: Upper Shoreface	Amalgamated, very fine- to fine-grained sandstone	Trough cross-stratification.	0.25-0.5 m thick beds; 5.5-14 m thick facies intervals.	BI = 0-1. *Ophiomorpha irregulaire, Gyrolithes* isp. and *Gyrochorte comosa*.	PCS1, PCS2, and PCS3. Grading out of the underlying lower shoreface deposits (FA7 and FA8).	High energy, wave and current action, beneath the low tide.
FA9: Offshore Sand Ridge	Skeletal sandstones, fine-grained sandstones, and bioturbated sandstones.	Cross-stratified (planar-tangential or trough), current ripple cross-lamination, and massive.	0.2-0.5 m thick beds; 3.5-9 m thick facies intervals.	BI = 0-4. *Ophiomorpha irregulaire* (?).	PCS1, and PCS2. Associated within offshore (FA3 and FA4) sediments, having various degrees of proximity to storm-wave base (FA7 and FA8).	High energy, mostly 2-D dune migration in an open shallow marine environment with well oxygenated, clean waters, moving in an offshore direction.

CHAPTER 5.0: DISCUSSION

5.1 Shorefaces

Shorefaces are open-marine, low gradient (1:200), seaward-sloping sediment ramps situated between the basal fair-weather wave base and the upper low-tide line, partitioned into three regions; the lower, middle and upper (Walker and Plint, 1992). In each region of the typical shoreface-shelf profile, different processes affect the sediment water interface. In the lower shoreface, located above the fair-weather wave base (Reinson, 1984; Walker and Plint, 1992), wave action is the dominant process (Walker and Plint, 1992). In the middle shoreface, shoaling and initial breaking of waves occur (Reinson, 1984; Clifton, 2006) under high energy conditions, sustaining migration of longshore bars (Walker and Plint, 1992). In the upper shoreface, beneath the low-tide line, multidirectional current flows in the build-up and surf zone are the dominant process, reflecting the highest energy conditions (Clifton et al., 1971; Komar, 1976; Walker and Plint, 1992).

During storm activity, storm-driven shelf current systems occur as the storm-induced onshore winds causing nearshore waters at the sediment-water interface to move seawards and deflected due to the Coriolis effect migrating along and offshore via combined flow (Swift et al., 1986; Duke, 1990; Walker and James, 1992; Plint, 2010). These types of storm-driven shelf currents include (1) relatively slow-moving unidirectional, coast-parallel to coast-oblique geostrophic flows culminating from wind stress on the water surface, and (2) fast-moving oscillatory flows resulting from wave motion propagation reaching depths of the sediment-water interface (Swift et al., 1986; Plint, 2010). Interaction between the resulting storm waves in the shallow waters and the sediment results in symmetrical elliptical patterns that preferentially moves the finer sand seaward towards the storm-wave base; however, during fair-weather,

normal conditions, strongly asymmetrical elliptical conditions dominate, moving coarser sands preferentially landwards (Clifton, 2006; Plint, 2010).

Shoreface variability, assessed by both sedimentologic and ichnologic variation, is greatest within the lower-middle shoreface (MacEachern and Pemberton, 1992). This variation results in different taphonomic pathways for emplacement and preservation of biogenic structures (Fig. 12) (Buatois and Mángano, 2011), facilitating categorization of three major types of shorefaces for storm-induced variability; (1) strongly storm-dominated (high energy), (2) moderately storm-dominated (intermediate energy), and (3) weakly storm-affected (low energy) (MacEachern and Pemberton, 1992) as previously discussed in Sections 3.6.1-3.6.3 as well as Tidally influenced shorefaces (TIS) and Tidally modulated shorefaces (TMS) discussed in Sections 3.6.4 and 3.6.5, respectively.

5.2 Facies Association Variations

Energy variations vertically throughout the parasequence also affect other factors exhibited by the ichnofauna, including the degree of oxygenation, sand content, amount of organic particles in suspension, and mobility of the substrate (Pemberton et al., 1992; Buatois and Mangano, 2011). Within the study section, four main types of parasequences have been identified on the basis of parasequence architecture: (1) Strongly storm-dominated parasequence, (2) Moderately storm-affected parasequence, (3) Moderately storm-affected – Strongly fair-weather reworked parasequence, and (4) Weakly storm-affected parasequence (Fig. 13). Variability within parasequence architecture includes changes in both the offshore transition (FA4 and FA5), and lower shoreface (FA6 and FA7) facies associations.

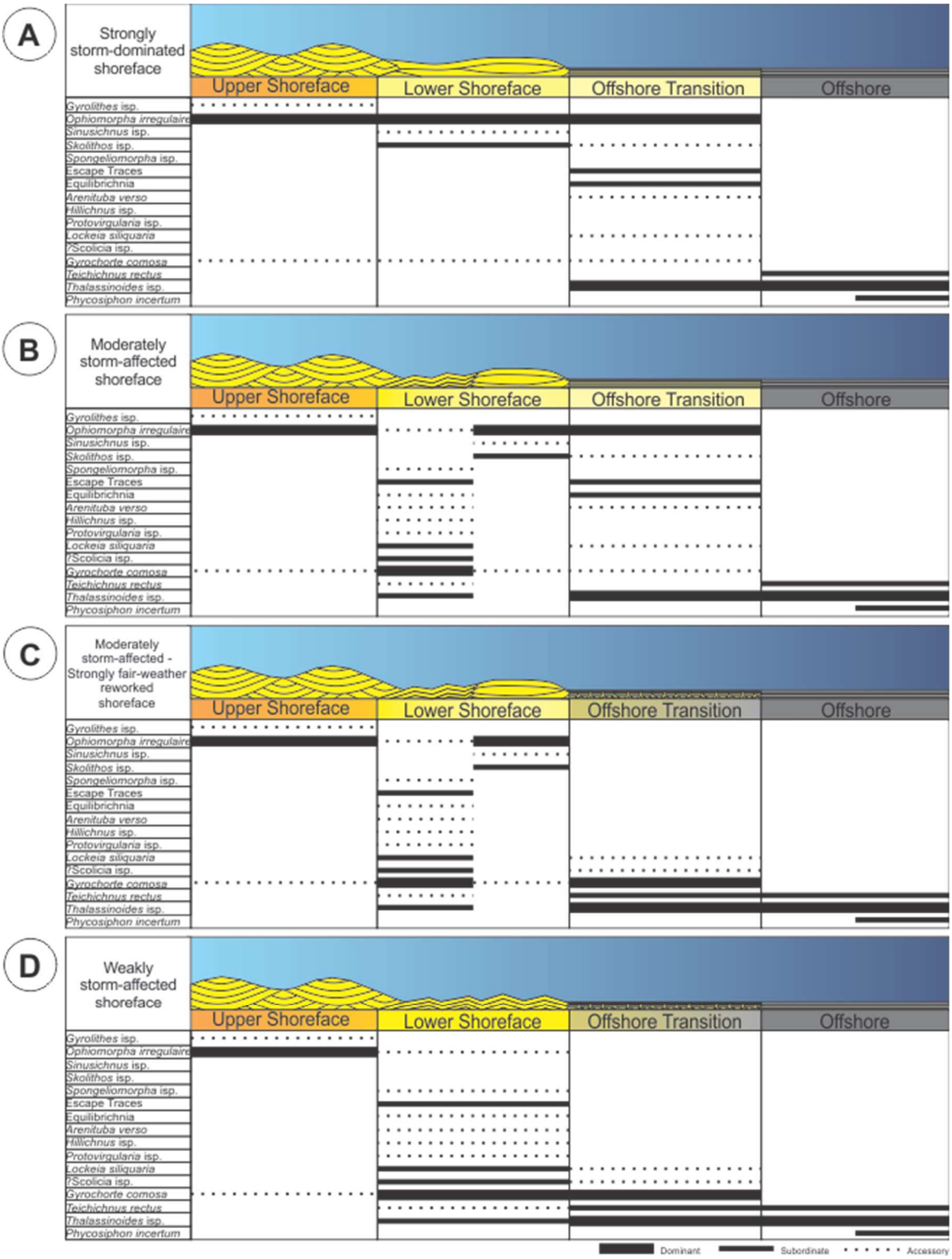

Fig. 12. Ichnoassemblages from shoreface complexes. (A). Strongly storm-dominated shoreface. (B) Moderately storm-affected shoreface. (C). Moderately storm-affected – strongly fair-weather reworked shoreface. (D) Weakly storm-affected shoreface, partitioned into the offshore, offshore transition, lower shoreface, and upper shoreface. Intensity of ichnofauna present from highest to lower; dominant, subordinate, and accessory (modified from Veiga and Schwarz, 2016).

5.2.1 Offshore Transition Variations

The offshore transition, also referred to as the distal lower shoreface by some authors (MacEachern and Bann, 2008; Pemberton et al., 2012), is located directly below the fair-weather wave base (Pemberton et al., 2001). Under storm-dominated conditions, the offshore transition (FA4) (Fig. 8C) reflects roughly equal alternation between high-energy storm event sandstones and fair-weather mud deposition (Buatois and Mángano, 2011), having *Skolithos* and *Cruziana* Ichnofacies, respectively (MacEachern and Pemberton, 1992). Within the storm-dominated offshore transition (FA4), the dominant ichnoassemblage includes *Thalassinoides* isp. and *Ophiomorpha irregulaire*, with escape traces and equilibrium structures subordinate, and *Gyrochorte comosa*, *Lockeia siliquaria*, and *Hillichnus* isp. as accessory elements (Fig. 12, and Fig. 13).

In contrast, the offshore transition in weakly storm-affected conditions (FA5) (Fig. 8D) consists of bioturbated muddy-silty sandstone (Morris et al., 2006; Schwarz, 2012; Schwarz et al., 2016) illustrating the *Cruziana* Ichnofacies (MacEachern and Pemberton, 1992), and hosting endo-byssate bivalves (Schwarz, 2012, 2016), where conditions reflect thorough fair-weather bioturbation of the sediment. The weakly storm-affected offshore transition (FA5) ichnoassemblage reflects the lower energy conditions and intense bioturbation of the substrate; *Thalasinoides* isp., *Gyrochorte comosa*, and *Teichichnus rectus* (Fig. 12, and Fig. 13).

5.2.2 Lower Shoreface Variations

The lower shoreface, located directly above the offshore transition and correspondingly above the fair-weather wave base (Reinson, 1984; Walker and Plint, 1992), also ranges from being strongly storm-dominated (FA6) to weakly storm-affected (FA7). In the strongly storm-dominated lower shoreface (FA6) (Fig. 8E) where wave action is the prevailing physical process,

hummocky cross stratification is the dominant sedimentary structure under high oscillatory flow velocities of ~ 50-90 cm/s with low unidirectional flow velocities < ~ 12 cm/s (Dumas et al., 2005; Dumas and Arnott, 2006). Continuous storm induced oscillations blocked fair-weather deposition and facilitated subsequent erosion and amalgamation throughout this setting. Within the strongly storm-dominated lower shoreface (FA6), only the deepest biogenic structures of the *Skolithos* Ichnofacies are present (MacEachern and Pemberton, 1992), with the ichnoassemblage dominated by *Ophiomorpha irregulaire* (Fig. 10A-C).

In the weakly storm-affected lower shoreface (FA7) (Fig. 8F), the frequency and magnitude of storms were not as dominant as compared to FA6, resulting in wave and combined-flow ripple cross lamination preservation, representative of the migration of symmetrical and weakly asymmetrical ripples produced by combined low oscillatory and weak unidirectional flows (Myrow and Southard 1996; Schwarz and Howell, 2005; Dumas and Arnott, 2006; Zecchin, 2007; Schwarz et al., 2016). Conditions necessary for formation of symmetrical ripples include an oscillatory velocity ~ 40 cm/s with a superimposed unidirectional velocity of < 10 cm/s, while hydrodynamics of weakly asymmetrical ripples reveal combined oscillatory conditions formed by an oscillatory velocity of 0 to 40 cm/s with a superimposed unidirectional velocity of 10-25 cm/s (Dumas et al., 2005). In previous studies, similar deposits have also been referred to as “rippled sand sheets” (Anderton 1976; Belderson et al. 1982; Reynaud and Dalrymple 2012; Veiga and Schwarz, 2016), although in these cases, they are associated with primarily relatively persistent unidirectional currents and colonized by elements of the *Skolithos* Ichnofacies. However, similarities between the weakly storm-dominated lower shoreface and “rippled sand sheets” arise as both are transitional with heterolithic deposits (FA5) (Veiga and Schwarz, 2016). Intervals within a strongly storm-dominated lower shoreface (FA6) without

significant erosion may experience low energy reworking preserving wave and combined ripples (Buatois and Mángano, 2011; Pemberton et al., 2012), suggesting a waning-flow stage where both purely oscillatory and combined (oscillatory and unidirectional) flows are recorded (Myrow and Southard, 1991; 1996; Schwarz, 2012) and categorized within FA7.

Within the weakly storm-dominated lower shoreface (FA7), the ichnoassemblage is dominated by *Gyrochorte comosa* (Fig. 11C-D); however, the weakly storm-dominated lower shoreface (FA7) also exhibits the highest ichnodiversity in the study with subordinate traces including other members within the ichnoassemblage, namely *Thalassinoides* isp., ?*Scolicia* isp. (Fig. 11E), *Lockeia siliquaria* (Fig. 10D and Fig. 11D), *Ophiomorpha irregulaire*, and *Spongeliomorpha* isp. (Fig. 11A-B), as well as accessory ichnotaxa, such as *Hillichnus* isp., *Arenituba verso* (Fig. 11F), *Teichichnus rectus* (Fig. 10E), and *Protovirgularia* isp. Overall, the ichnofauna of the weakly storm-affected lower shoreface (FA7) illustrates the archetypal *Cruziana* Ichnofacies, in contrast to the *Skolithos* Ichnofacies of the strongly storm-dominated lower shoreface (FA6) (MacEachern and Pemberton, 1992).

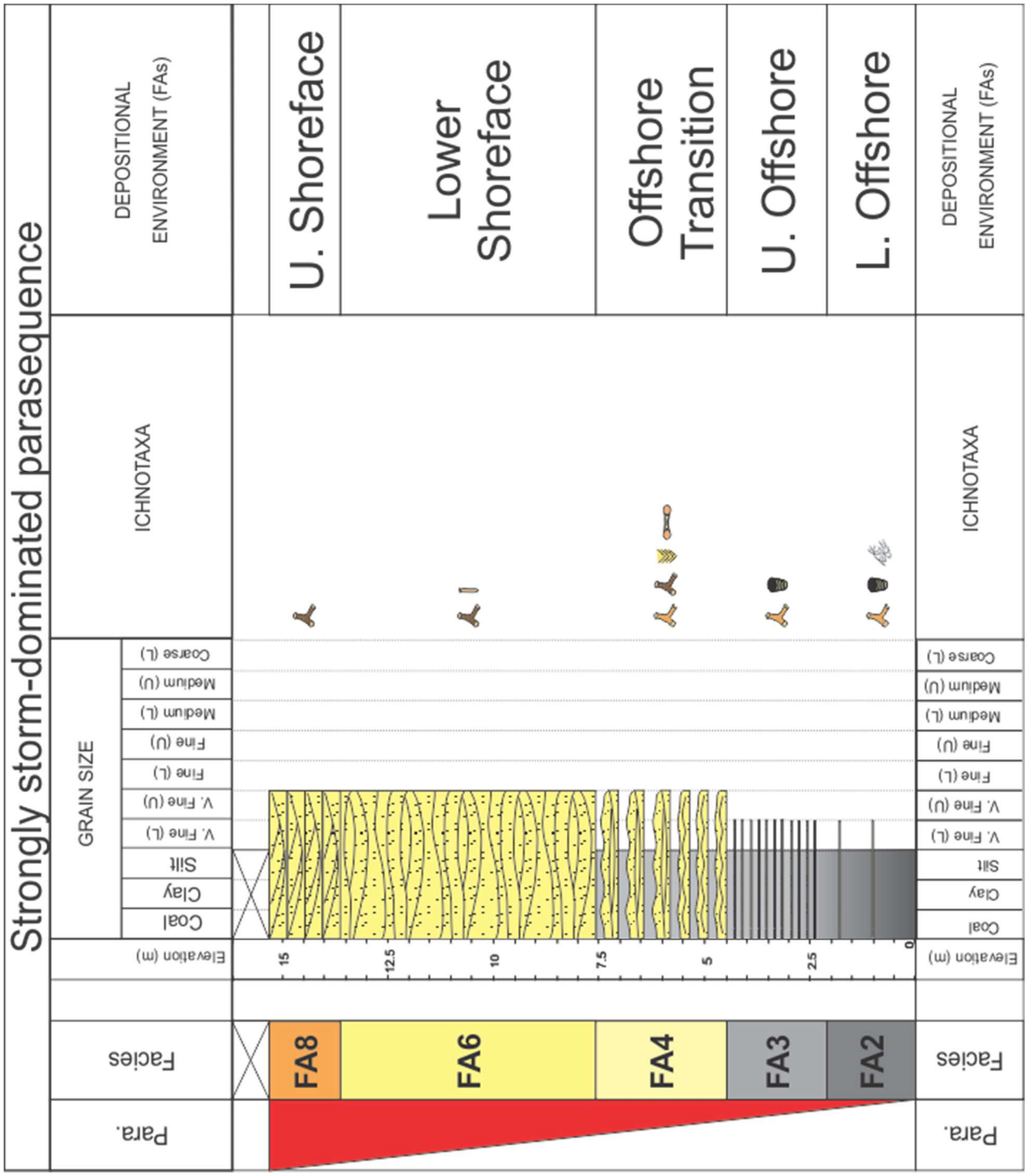

Fig. 13. (A). Strongly storm-dominated parasequence and intra-parasequence architecture. Accessory ichnotaxa not included. Within the lower offshore (FA2), *Thalassinoides* isp. dominates, with *Teichichnus rectus* and *Phycosiphon incertum* subordinate. Upper offshore (FA3); *Thalassinoides* isp. dominant, and *Teichichnus rectus* subordinate. Storm-dominated offshore transition (FA4); *Thalassinoides* isp. and *Ophiomorpha irregulaire* dominant, escape traces and equilibrium structures subordinate. Storm-dominated lower shoreface (FA6); *Ophiomorpha irregulaire* dominant, and *Skolithos* isp. subordinate. Upper shoreface (FA8); *Ophiomorpha irregulaire* dominant.

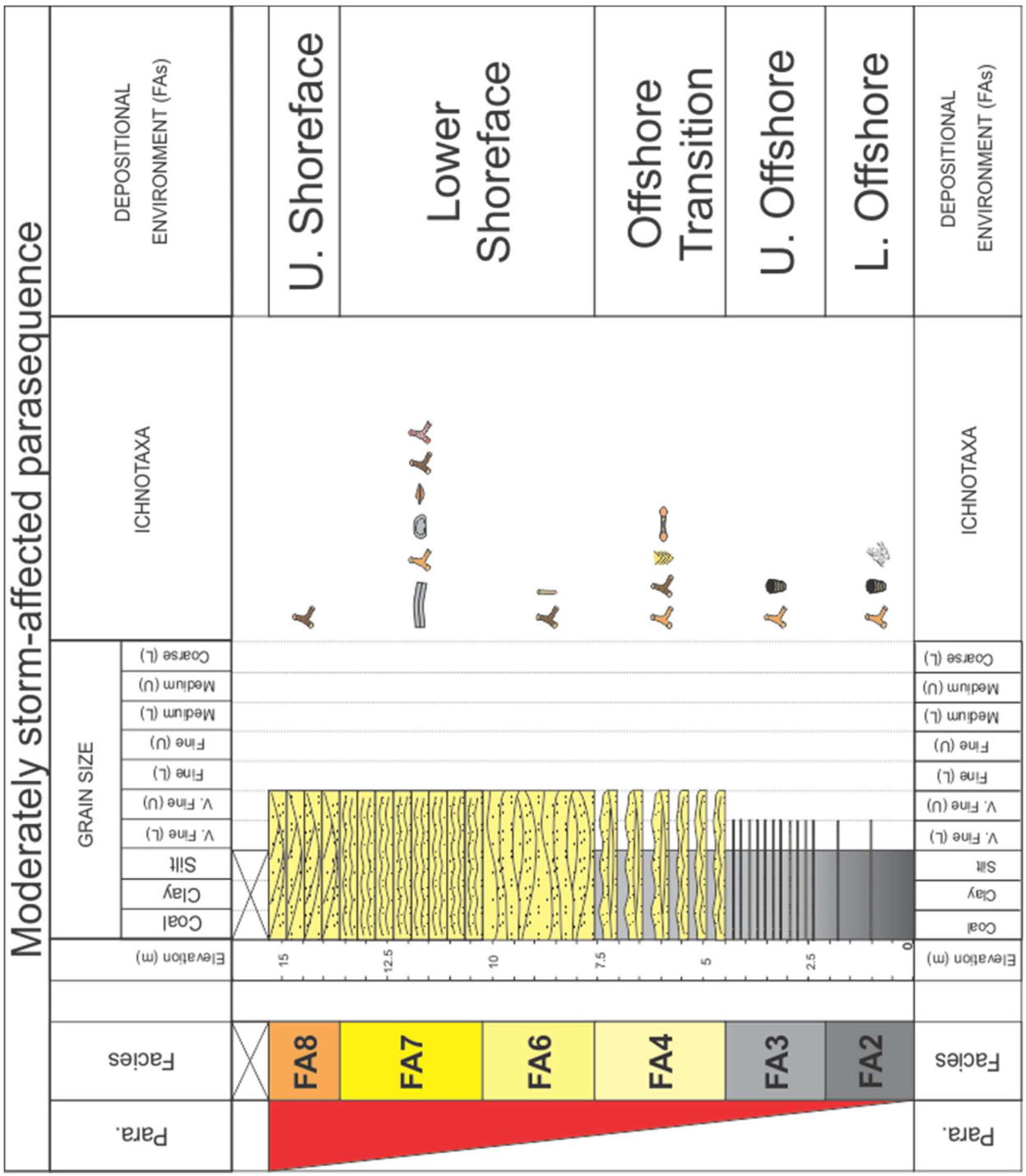

Fig. 13. (B). Moderately storm-affected parasequence and intra-parasequence architecture. Accessory ichnotaxa not included. Within the lower offshore (FA2), *Thalassinoides* isp. dominates, with *Teichichnus rectus* and *Phycosiphon incertum* subordinate. Upper offshore (FA3); *Thalassinoides* isp. dominant, and *Teichichnus rectus* subordinate. Storm-dominated offshore transition (FA4); *Thalassinoides* isp. and *Ophiomorpha irregulaire* dominant, escape traces and equilibrium structures subordinate. Storm-dominated lower shoreface (FA6); *Ophiomorpha irregulaire* dominant, and *Skolithos* isp. subordinate. Weakly storm-affected lower shoreface (FA7); *Gyrochorte comosa* dominant, *Thalassinoides* isp., ?*Scolicia* isp., *Lockeia siliquaria*, *Ophiomorpha irregulaire*, *Spongeliomorpha* isp. and escape trace fossils subordinate. Upper shoreface (FA8); *Ophiomorpha irregulaire* dominant.

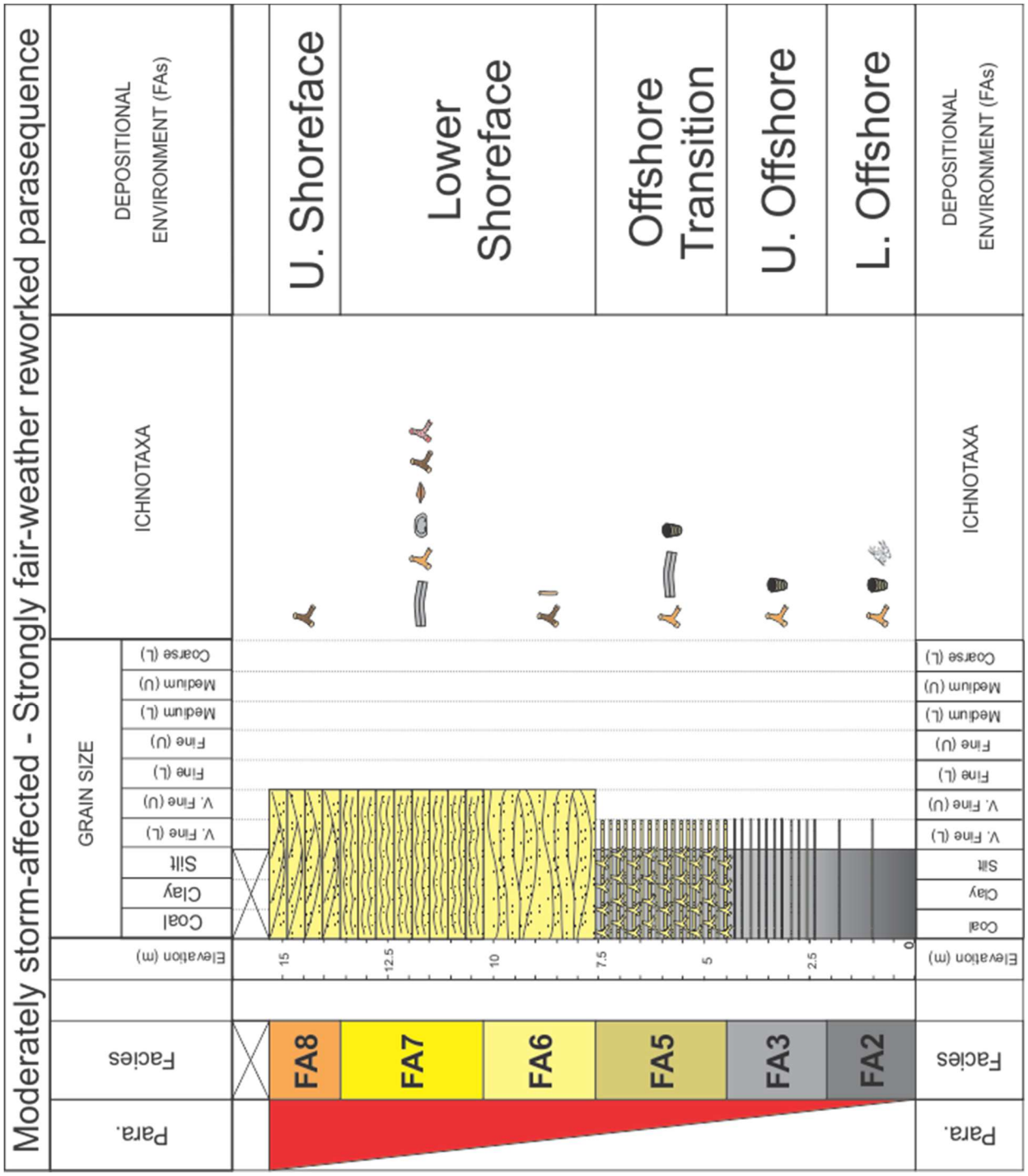

Fig. 13. (C). Moderately storm-affected – strongly fair-weather reworked parasequence and intra-parasequence architecture. Accessory ichnotaxa not included. Within the lower offshore (FA2), *Thalassinoides* isp. dominates, with *Teichichnus rectus* and *Phycosiphon incertum* subordinate. Upper offshore (FA3); *Thalassinoides* isp. dominant, and *Teichichnus rectus* subordinate. Weakly storm-affected offshore transition (FA5); *Thalassinoides* isp. and *Gyrochorte comosa* dominant, *Teichichnus rectus* subordinate. Storm-dominated lower shoreface (FA6); *Ophiomorpha irregulaire* dominant, and *Skolithos* isp. subordinate. Weakly storm-affected lower shoreface (FA7); *Gyrochorte comosa* dominant, *Thalassinoides* isp., ?*Scolicia* isp., *Lockeia siliquaria*, *Ophiomorpha irregulaire*, *Spongeliomorpha* isp. and escape trace fossils subordinate. Upper shoreface (FA8); *Ophiomorpha irregulaire* dominant.

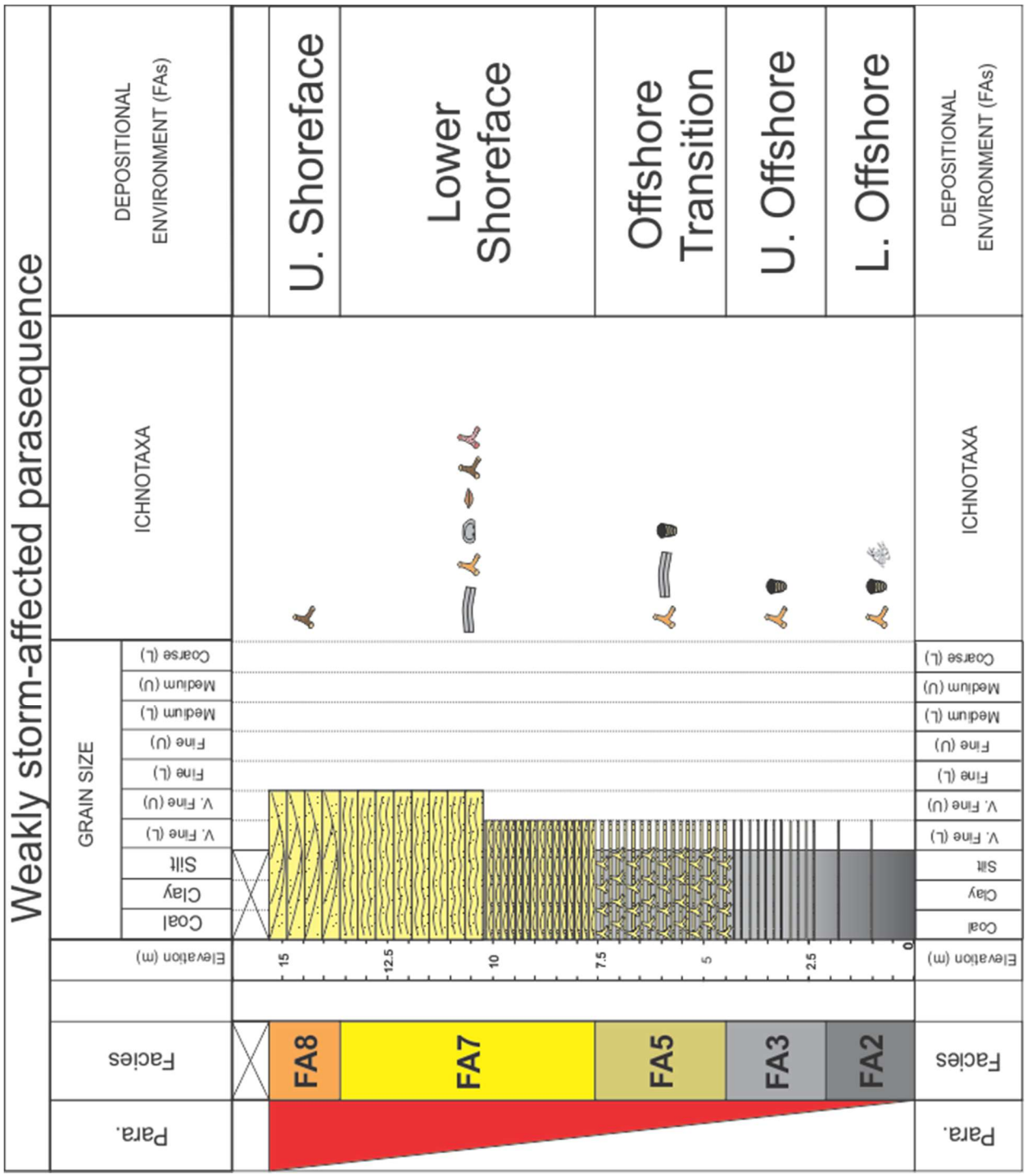

Fig. 13. (D). Weakly storm-affected parasequence and intra-parasequence architecture. Accessory ichnotaxa not included. Within the lower offshore (FA2), *Thalassinoides* isp. dominates, with *Teichichnus rectus* and *Phycosiphon incertum* subordinate. Upper offshore (FA3); *Thalassinoides* isp. dominant, and *Teichichnus rectus* subordinate. Weakly storm-affected offshore transition (FA5); *Thalassinoides* isp. and *Gyrochorte comosa* dominant, *Teichichnus rectus* subordinate. Weakly storm-affected lower shoreface (FA7); *Gyrochorte comosa* dominant, *Thalassinoides* isp., ?*Scolicia* isp., *Lockeia siliquaria*, *Ophiomorpha irregulaire*, *Spongeliomorpha* isp. and escape trace fossils subordinate. Upper shoreface (FA8); *Ophiomorpha irregulaire* dominant.

5.3 Intra-parasequence Architecture

Intra-parasequence architecture has been studied in detail over the years, evolving with the use of technology, as seen in numerical modeling utilizing the BARSIM (barrier simulation) model, allowing evaluation of causational mechanisms of intra-parasequence variability; changes in sea level, sediment supply, and wave-height regime (O'Bryne and Flint; 1995; Pattison, 1995; Hampson, 2000; Hampson and Storms, 2003; Hampson and Howell, 2005; Storms and Hampson, 2005; Sømme et al. 2008; Charvin et al., 2010; Hampson, 2010; Charvin et al., 2011; Hampson, 2016). Intra-parasequence architecture can be affected by both allogenic (i.e. tectonic subsidence, sea-level, and sediment influx) and autogenic (i.e. hydrodynamic) controls (Hampson, 2016) that commonly result in rearrangement of shoreline geometry that has a direct effect on local sediment supply and storm-wave influence (Charvin et al., 2010).

5.4 Parasequence Variability

5.4.1 Strongly storm-dominated parasequence

In a strongly storm-dominated parasequence (Fig. 13A and Fig. 14A), deposition occurs under pervasive high energy conditions where storm waves are the dominant physical process, resulting in a parasequence including lower offshore (FA2), upper offshore (FA3) storm-dominated offshore transition (FA4), storm-dominated lower shoreface (FA6), and upper shoreface (FA8) deposits. Within the strongly storm-dominated parasequence, paleoenvironmental controls dictate presence of the *Skolithos* Ichnofacies (MacEachern and Pemberton, 1992) with the observed ichnoassemblage dominated by *Thalassinoides* isp. and *Ophiomorpha irregulaire* (Fig. 10A) within the tempestites of the storm-dominated offshore transition (FA4), and overwhelmingly by *Ophiomorpha irregulaire* (Fig. 10B-C) in the storm-dominated lower shoreface (FA6). Under pervasive fully marine conditions, oxygen remains

high throughout progradation with high degrees of turbulence at the sediment water interface, increasing with reduced proximity to the shoreline. As a result of these conditions, a high abundance of *Ophiomorpha irregulaire* throughout the storm-dominated offshore transition (FA4) to upper shoreface (FA8) is observed in these shallow marine, high energy environments (Frey et al., 1978; Curran, 2007; Buatois et al., 2016).

5.4.2 Weakly storm-affected parasequence

The weakly storm-affected parasequence (Fig. 13D and Fig. 14D) is associated with lower energy conditions where storm influence is subordinate to combined low oscillatory and weak to absent unidirectional flows (Dumas and Arnott, 2006). Complete parasequence architecture consists of lower offshore (FA2), upper offshore (FA3), weakly storm-affected offshore transition (FA5), weakly storm-affected lower shoreface (FA7), and upper shoreface (FA8). Within the weakly storm-affected parasequence, paleoenvironmental controls in this scenario favor the establishment of the *Cruziana* Ichnofacies (MacEachern and Pemberton, 1992). The ichnoassemblage observed here is dominated primarily by *Thalassinoides* isp. and *Gyrochorte comosa* in the offshore transition, and by *Gyrochorte comosa* within the lower shoreface, and similar to the storm-dominated offshore transition and lower shoreface, waters were fully marine with relatively high degrees of oxygen, only differing in reduced turbulence within the weakly storm-affected parasequence.

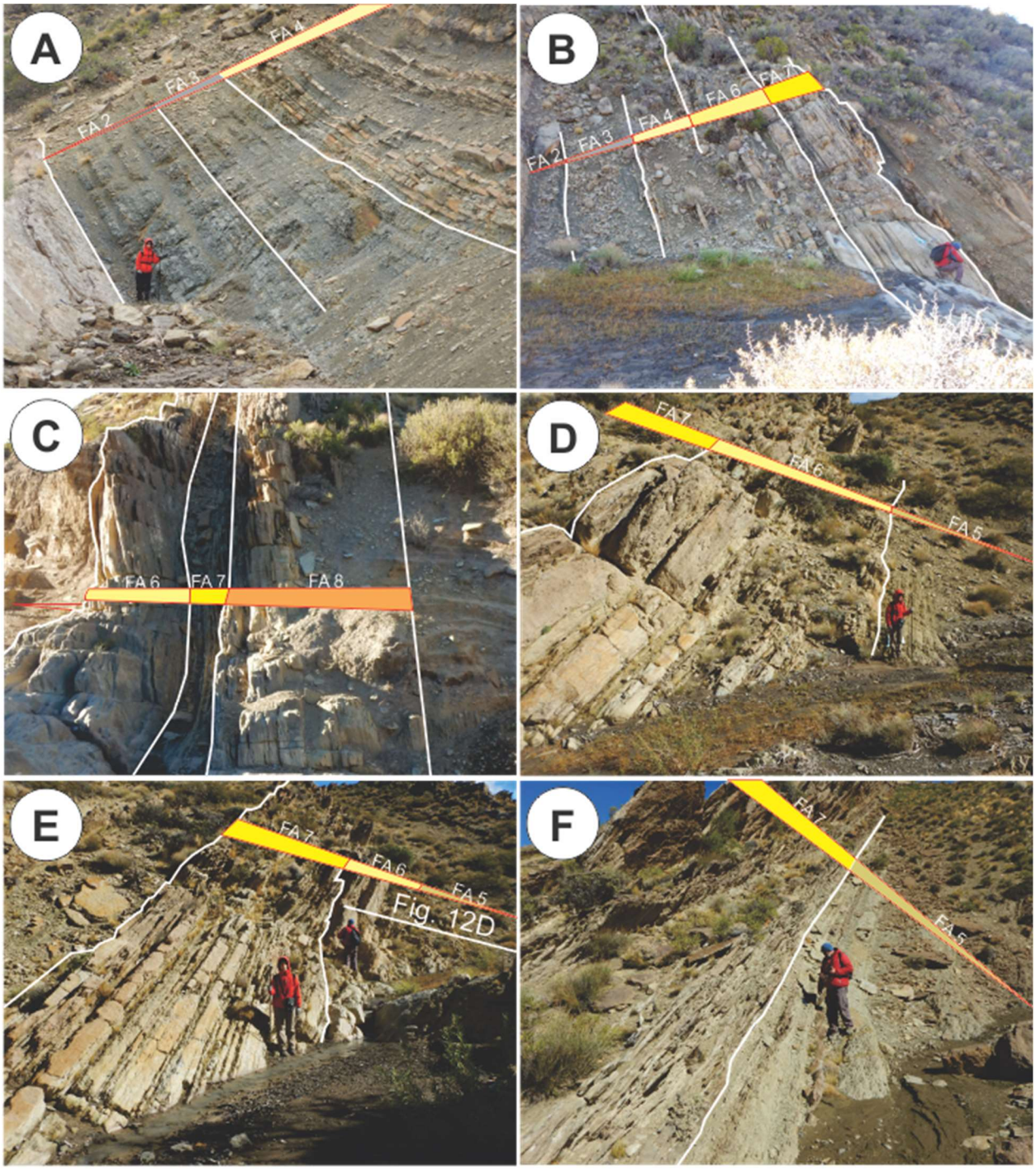

Fig. 14. Outcrop view of parasequences architecture. (A). Strongly storm-dominated parasequence. Lower offshore to offshore transition (FA 2, FA 3, and FA 4). FA 9 located beneath the parasequence. (B). Moderately storm-affected parasequence. Offshore (FA 2, FA 3), offshore transition (FA 4), and lower shoreface (FA 6, FA 7). (C). Lower shoreface (FA 6, FA 7) to upper shoreface (FA 8). (D). Moderately storm-affected – strongly fair-weather reworked parasequence. Offshore transition (FA 4), to lower shoreface (FA 6) in foreground. (E). Lower shoreface (FA 7) in foreground. (F). Weakly storm-affected parasequence. Offshore transition (FA 5) to lower shoreface (FA 7).

5.4.3 Moderately storm-affected parasequence

At present, the shoreface ternary diagram has been developed to distinguish fair-weather waves, storm waves, and tides (Dashtgard et al., 2012; Pemberton et al., 2012); however, storm-affected, storm-influenced, and storm-dominated shorefaces represent the spectrum of wave-dominated shoreface settings, facilitating a classification scheme based on storm wave action alone (cf. MacEachern and Pemberton, 1992; Dashtgard et al., 2012). The tripartite spectrum of wave-dominated shorefaces in correspondence with the relatively newly designated tide-influenced and tidally modulated shorefaces (Dashtgard et al., 2009) provide increased resolution in shorefaces exposed to a range of storm-waves and tides. However, this scheme cannot fully accommodate the broad range of shoreface variability (Dashtgard et al., 2012). In particular, shorefaces shaped by fair-weather waves have remained understudied because standard classification schemes for wave-dominated shorefaces have been formulated based on storm wave action alone (cf. MacEachern and Pemberton, 1992; Dashtgard et al., 2012). A newly identified shoreface, previously overlooked by past literature, consists of a shoreface comprising storm deposits reworked thoroughly by fair-weather waves, here referred to as the moderately storm-affected – strongly fair-weather reworked shoreface (Fig. 12C), and included in the moderately storm-affected – strongly fair-weather reworked parasequence (Figs. 13C, 15).

In contrast to the strongly storm-dominated (Fig. 13A) and weakly storm-affected parasequences (Fig. 13D), which both have been shaped by distinct depositional processes, the moderately storm-affected (Fig. 13B) and moderately storm-affected – strongly fair-weather reworked parasequences (Fig. 13C) have architectural elements of both the storm-dominated and weakly storm-affected parasequences. The moderately storm-affected parasequence comprises the lower offshore (FA2), upper offshore (FA3), storm-dominated offshore transition (FA4),

storm-dominated lower shoreface (FA6), weakly storm-affected lower shoreface (FA7), and upper shoreface (FA8) deposits. Storm wave action is pervasive until undergoing a waning-flow stage, represented by the weakly storm-affected lower shoreface (FA7), where both purely oscillatory and combined (oscillatory and unidirectional) flows developed (Fig. 12C). This moderately storm-affected parasequence bears resemblance to several intervals of alternating weakly storm-affected and strongly storm-dominated shorefaces in the Spring Canyon and Sunnyside members of the Blackhawk Formation in the shallow-marine, epeiric Western Interior Seaway deposits of Utah (MacEachern and Pemberton, 1992; O'Bryne and Flint; 1995; Pattison, 1995). Intra-parasequence scale autogenic variation (hydrodynamic energy) of the Aberdeen and Sunnyside members indicates that more proximally, localized fluvial deposits underwent variation in sediment input and current velocity, facilitating deltaic lobe switching during progradation, modifying the local wave climate by redistributing sand via waves and longshore currents (Hampson and Howell, 2005; Storms and Hampson, 2005; Sømme et al., 2008; Charvin et al., 2010; Hampson et al., 2010; Hampson, 2016). Sands that were redistributed alongshore formed spits and barriers, protecting certain locations of the shoreface where weakly storm-affected lower shorefaces (FA7) could be deposited in an otherwise storm-dominated environment in lieu of the storm-dominated lower shoreface (FA6). Longshore drift currents supplied the sediment from the gradual erosion of the abandoned fluvially fed promontory and as sands filled the protected, topographic low behind the spits and barriers, they were once again subject to wave and current processes switching back to a strongly storm-dominated shoreface (Charvin et al., 2011), as seen in the moderately storm-affected parasequence (Fig. 13B). Like the Blackhawk Formation with deltaic sands coming from the west, in the Mulichinco Formation, high volumes of sands were transported distally down the relatively steep fluvial and

shelf gradient producing river-dominated deltaic deposits, associated with broad coeval fluvial deposit to the south and eastern portion of the Neuquén Basin (Schwarz et al., 2006).

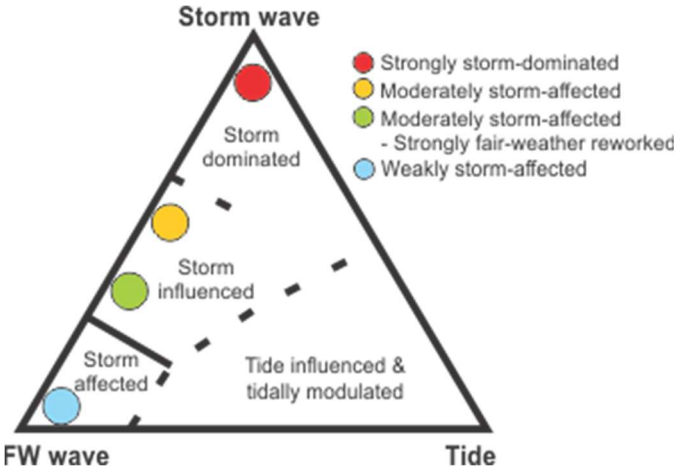

Fig. 15. Conceptual shoreface model ternary diagram designed to illustrate the three main influences on deposition at the sediment substrate interface: storm waves, fair-weather (FW) waves, and tides, with locations of all shorefaces described here spatially represented on the diagram. The newly observed moderately storm-affected – strongly fair-weather reworked shoreface, displays a dominance of fair-weather waves that thoroughly reworks preceding storm-wave beds (modified from Dashtgard et al., 2012).

5.4.4 Moderately storm-affected – strongly fair-weather reworked

In the newly described shoreface presented here, the moderately storm-affected – strongly fair-weather reworked shoreface (Fig. 12C), the shoreface features storm deposits reworked thoroughly by fair-weather waves. Within this shoreface, the moderately storm-affected – strongly fair-weather reworked parasequence (Fig. 13C) records fair-weather oscillatory and combined flows dominated in the weakly storm-affected offshore transition (FA5), followed by an increase in storm activity depicted by deposition of storm-dominated lower shoreface (FA6), before being reclaimed by fair-weather oscillatory and combined flows of the waning-flow stage of the weakly storm-affected lower shoreface (FA7). Fair-weather waves thoroughly reworked the underlying storm-dominated lower shoreface deposits and are diagnostic in the classification as fair-weather waves are dominant to storm-waves in this type of shoreface (Fig. 15). Vertical

facies patterns suggest that this type of shoreface records high intensity but low frequency of storms in an environment regularly affected by vigorous fair-weather waves. The Mulichinco Formation is characterized by both an overarching allogenic tectonic inversion controlling or intensifying sea level and sediment influx variation (Vergani et al., 1995; Veiga et al., 2002), as well as autogenic control. Autogenic controls pertain to internal hydrodynamics of the individual and combined depositional environments (Muto et al., 2007; Hampson, 2010), and together with allogenic tectonic inversion, act together in synergy creating the diagnostic parasequence and intra-parasequence architecture of the strongly storm-dominated, moderately storm-affected, moderately storm-affected – strongly fair-weather reworked and weakly storm-affected shoreface.

CHAPTER 6.0: CONCLUSIONS

1. Shorefaces can display strong sedimentologic and ichnological variability. Integration of sedimentology and ichnology can provide a high-resolution model to identify variations between storm-dominated and weakly storm-affected facies. In addition, to help determine shoreface variability, ichnology can be used to help delineate parasequences by the fact that trace-fossil associations are excellent indicators of environmental conditions that typically change along the depositional profile. Shallow-marine parasequences of the Mulichinco Formation within the Neuquén Basin of western Argentina, were mapped to evaluate stress factors exhibited by parasequence architecture.

2. Four distinct types of parasequence architecture were described within the study sections. All four variants of parasequences are capped by an upper shoreface (FA8), and are underlain by lower and upper offshore deposits; FA2 and FA3, respectively.

1) Strongly storm-dominated parasequence; storm wave action is pervasive throughout the parasequence represented by storm-dominated offshore transition (FA4), and storm-dominated lower shoreface (FA6) deposits.

2) Moderately storm-affected parasequence; wave action is the dominant physical process followed by a waning-flow stage where both purely oscillatory and combined (oscillatory and unidirectional) flows occur. This is represented in the studied parasequences by a storm-dominated offshore transition (FA4), storm-dominated lower shoreface (FA6) succession diverging from the storm-dominated parasequence, as weakly storm-affected lower shoreface (FA7) strata is located directly above the storm-dominated lower shoreface (FA6).

3) Moderately storm-affected – strongly fair-weather reworked parasequence; storm-wave action is subordinate to fair-weather waves. Wave action initially holds a decreased influence on

the sediment substrate, represented by a weakly storm-affected offshore transition (FA5), eventually increasing with an increased storm presence and frequency in the lower shoreface characterized by storm-dominated lower shoreface (FA6), before moving back to a fair-weather dominated scheme undergoing pervasive fair-weather wave action which reworked the previously deposited storm-dominated lower shoreface into the weakly storm-affected lower shoreface (FA7).

4) Weakly storm-affected parasequence; storm wave action operates at both a lower magnitude and duration, where deposits are indicative of fair-weather combined oscillatory and unidirectional flows represented by weakly storm-affected offshore transition (FA5), and weakly storm-affected lower shoreface (FA7) strata.

3. Within each idealized parasequence, parasequence and intra-parasequence architecture dictates varying degrees of storm and fair-weather wave influence on the sediment substrate interface, affected by both allogenic (i.e. tectonic subsidence, sea-level, and sediment influx) and autogenic (i.e. hydrodynamic) controls within the Neuquén Basin on both a parasequence and intra-parasequence time scale. The new type of shoreface described here, the moderately storm-affected – strongly fair-weather reworked shoreface, illustrates fair-weather wave dominance to storm waves, as the fair-weather deposits thoroughly rework the higher energy, storm-dominated lower shoreface sandstones. The previous classification scheme, which was focused on the role of storm-waves, has been modified to encompass this newly defined shoreface.

LITERATURE CITED

Aguirre-Urreta, M.B., Rawson, P.F., Concheyro, G.A., Bown, P.R., Ottone, E.G., 2005. Lower Cretaceous biostratigraphy of the Neuquén Basin, in: Veiga, G.D., Spalletti, L.A., Howell, J.A., Schwarz, E. (Eds.), The Neuquén Basin, Argentina: A Case Study in Sequence Stratigraphy and Basin Dynamics. Geol. Soc. Lond. Spec. Publ. 252, pp. 57-81.

Anderton, R., 1976. Tidal-shelf sedimentation: an example from the Scottish Dalradian. Sedimentology 23, 429-458.

Angulo, S., Buatois, L.A., 2009. Sedimentological and ichnological aspects of a sandy low-energy coast: Upper Devonian-Lower Mississippian Bakken Formation, Williston Basin, Southeastern Saskatchewan. In Summary of Investigations 2009, Volume 1, Saskatchewan Geological Survey, Saskatchewan Ministry of Energy and Resources, Miscellaneous Report 2009-4.1, Paper A-5, 17.

Ausich, W.I., Bottjer, D.J., 1982. Tiering in suspension-feeding communities on soft substrata throughout the Phanerozoic. Science 216, 173-174.

Belderson, R.H., Johnson, M.A., Kenyon, N.H., 1982. Bedforms, in: Stride, A.H. (Eds.), Offshore tidal sands: processes and deposits. Chapman & Hall, London, pp. 27-57.

Bromley, R.G., Ekdale, A.A., 1986. Composite ichnofabrics and tiering of burrows. Geological Magazine 123, 59-65.

Bromley, R.G., 1990. Trace Fossils. Biology and Taphonomy. Unwin Hyman, London, pp. 280.

Bromley, R.G. 1996. Trace Fossils. Biology, Taphonomy, and Applications, second ed. Chapman & Hall, London, pp. 361.

Buatois, L.A., Mángano, M.G., Alissa, A., Carr, T.R., 2002. Sequence stratigraphic and sedimentologic significance of biogenic structures from a late Paleozoic marginal to open-marine reservoir, Morrow Sandstone, subsurface of southwest Kansas, USA. Sedimentary Geology 152, 99-132.

Buatois, L.A., Bromley, R.G., Mángano, M.G., Bellosi, E., Carmona, N.B., 2003. Ichnology of shallow marine deposits in the Miocene Chenque Formation of Patagonia: Complex ecologic structure and niche partitioning in Neogene ecosystems, in: Buatois, L.A., Mángano, M.G. (Eds.), Icnología: Hacia una convergencia entre geología y biología. Publicación Especial de la Asociación Paleontológica Argentina 9, 85-95.

Buatois, L.A., Netto, R.G., Mángano, M.G., Balistieri, P., 2006. Extreme freshwater release during the Late Paleozoic Gondwana deglaciation and its impact on coastal ecosystems. Geology 34, 1021-1024.

Buatois, L.A., Mángano, M.G., 2011. Ichnology: Organism-Substrate Interactions in Space and Time. Cambridge University Press. Cambridge, UK.

Buatois, L.A., Carmona, N.B., Curran, H.A., Netto, R.G., Mángano, M.G., Wetzel, A., 2016. The Mesozoic marine revolution, in: Mángano, M.G., Buatois, L.A. (Eds.), The trace-fossil record of major evolutionary events. Springer Netherlands., pp. 24-27.

Burchette, T.P., Wright, V.P., Faulkner, T.J., 1990. Oolitic sandbody depositional models and geometries, Mississippian of southwest Britain: implications for petroleum exploration in carbonate ramp settings. Sedimentary Geology 68, 87-115.

Carmona, N.B., Buatois, L.A., Mángano, M.G., Bromley, R.G., 2008. Ichnology of the Lower Miocene Chenque Formation, Patagonia, Argentina: animal–substrate interactions and the Modern Evolutionary Fauna. Ameghiniana 45, 93-122.

Carmona, N.B., Ponce, J.J., Wetzel, A., Bournod, C.N., Cuadrado., D.G., 2012. Microbially induced sedimentary structures in Neogene tidal flats from Argentina: Paleoenvironmental, stratigraphic and taphonomic implications. Palaeogeography, Palaeoclimatology, Palaeoecology 353, 1-9.

Charvin, K., Hampson, G.J., Gallagher, K.L., Labourdette, R., 2010. Intraparasequence architecture of an interpreted asymmetrical wave-dominated delta. Sedimentology, 57, 760-785.

Charvin, K., Hampson, G.J., Gallagher, K.L., Storms, J.E.A., Labourdette, R., 2011. Characterization of controls on high-resolution stratigraphic architecture in wave-dominated

shoreface–shelf parasequences using inverse numerical modelling. Journal of Sedimentary Research, 81, 562-578.

Cheel, R.J., Leckie, D.A., 1993. Hummocky cross-stratification. Sedimentology Review 1, 103-122.

Christ, N., Immenhauser, A., Amour, F., Mutti, M., Tomas, S., Agar, S.M., Alway, R., Kabiri, L., 2012. Characterization and interpretation of discontinuity surfaces in a Jurassic ramp setting (High Atlas, Morocco): Sedimentology 59, 249-290.

Clifton, H.E., Hunter, R.E., Phillips, R.L., 1971. Depositional structures and processes in the non-bar high energy nearshore. Journal of Sedimentary Petrology 41, 651-670.

Clifton, H.E., 1976. Wave-formed sedimentary structures - A conceptual model, in: Davis, R.A., Jr., Ethington, R.L. (Eds). Beach and Nearshore Sedimentation. Society for Sedimentary Geology (SEPM), Special Publications 24, 126-148.

Clifton, H.E., 2006. A re-examination of facies models for clastic shorefaces, in: Posamentier, H.W., Walker, R.G. (Eds.), Facies Models Revisited, Special Publication No. 84. SEPM (Society for Sedimentary Geology), Tulsa, USA, pp. 293-337.

Curran, H.A., 2007. Ichnofacies, ichnocoenoses and ichnofabrics of Quaternary shallow-marine to dunal tropical carbonates: a model and implications, in: Miller, W. III (Eds.) Trace Fossils: Concepts, Problems, Prospects, Amsterdam, pp. 232-247.

Dalrymple, R.W., 2010. Tidal depositional systems, in: Dalrymple, R.W., James, N.P. (Eds.), Facies Models, fourth edition. Geological Association of Canada, St. John's, Newfoundland, pp. 201-231.

Dashtgard, S.E., Gingras, M.K., MacEachern, J.A., 2009. Tidally modulated shorefaces. Journal of Sedimentary Research 79, 793-807.

Dashtgard, S.E., MacEachern, J.A., Frey, S.E., Gingras, M.K., 2012. Tidal effects on shorefaces: Towards a conceptual framework. Sedimentary Geology 279, 42-61.

Dott Jr., H.R., 1983. Episodic sedimentation - how normal is average? How rare is rare? Does it matter? Journal of Sedimentary Petrology 53, 5-23.

Dott Jr., H.R., 1988. An episodic view of shallow marine classic sedimentation, in: Debor, P.L., Van Gelder, A., Nio, S.D. (Eds.), Tide-Influenced Sedimentary Environments and Facies. D. Reidel Publishing, Dordrecht, pp. 3-12.

Duke, W.L., 1990, Geostrophic circulation or shallow marine turbidity currents? The dilemma of paleoflow patterns in storm-influenced prograding shoreline systems. Journal of Sedimentary Petrology 60, 870-883.

Dumas, S., Arnott, R.W.C., Southard, J.B., 2005. Experiments on oscillatory-flow and combined-flow bedforms: Implications for interpreting parts of the shallow-marine sedimentary record. Journal of Sedimentary Research 75, 501-513.

Dumas, S., Arnott, R.W.C., 2006. Origin of hummocky and swaley cross-stratification - The controlling influence of unidirectional current strength and aggradation rate. Geology 34, 1073-1076.

Echevarría, J., Damborenea, S.E., Manceñido, M.O., 2012. Palaeodemecological Analysis of Infaunal Bivalves "Lebensspuren" from the Mulichinco Formation, Lower Cretaceous, Neuquén Basin, Argentina. Ameghiniana 49, 47-59.

Frey, R.W., Howard, J.D., Pryor, W.A., 1978. *Ophiomorpha*: its morphologic, taxonomic and environmental significance. Palaeogeography, Palaeoclimatology, Palaeoecology 23, 199-229.

Frey, R.W., Curran, H.A., Pemberton, S.G., 1984. Tracemaking activities of crabs and their environmental significance; the ichnogenus *Psilonichnus*. Journal of Paleontology 58, 333-350.

Frey, R.W., Pemberton, S.G., 1987. The *Psilonichnus* ichnocoenose, and its relationship to adjacent marine and nonmarine ichnocoenoses along the Georgia coast. Bulletin of Canadian Petroleum Geology 35, 333-357.

Frey, S.E., Dashtgard, S.E., 2011. Sedimentology, ichnology and hydrodynamics of strait-margin, sand and gravel beaches and shorefaces: Juan de Fuca Strait, British Columbia, Canada. Sedimentology 58, 1326-1346.

Genise, J.F., Mángano, M.G., Buatois, L.A., Laza, J., Verde, M., 2000. Insect trace fossil associations in paleosols: The *Coprinisphaera* ichnofacies. Palaios 15, 33-48.

Greenwood, B., Mittler, P.R., 1985. Vertical sequence and lateral transitions in the facies of a barred nearshore environment. Journal of Sedimentary Petrology 55, 366-375.

Groeber, P., 1946. Observaciones geológicas a lo largo del meridiano 70. 1. Hoja Chos Malal. Soc. Geol. Argentina Rev. 20, 177–208.

Gulisano, C.A., Gutiérrez Pleimling, A.R., Digregorio, R.E., 1984. Análisis estratigráfico del intervalo Tithoniano–Valanginiano (Formaciones Vaca Muerta, Quintuco y Mulichinco) en el suroeste de la Provincia de Neuquén. IX Congreso Geológico Argentino 1, 221-235.

Hampson G.J., 2000. Discontinuity surfaces, clinoforms, and facies architecture in a wave-dominated, shoreface-shelf parasequence. Journal of Sedimentary Research 70, 325-340.

Hampson, G.J., 2010. Sediment dispersal and quantitative stratigraphic architecture across an ancient shelf. Sedimentology 57, 96-141.

Hampson, G. J., 2016. Towards a sequence stratigraphic solution set for autogenic processes and allogenic controls: Upper Cretaceous strata, Book Cliffs, Utah, USA. Journal of the Geological Society 173, 817-836.

Hampson, G.J., Howell, J.A., 2005. Sedimentologic and geomorphic characterization of ancient wave-dominated shorelines: examples from the Late Cretaceous Blackhawk Formation, Book Cliffs, Utah. in: Bhattacharya, J.P., Giosan, L. (Eds.), Deltas Old and New. SEPM Spec. Publ. 83, 133-154.

Hampson, G.J., Storms, J.E.A., 2003. Geomorphological and sequence stratigraphic variability in wave-dominated, shoreface–shelf parasequences. Sedimentology 50, 667-701.

Hart, B.S., Plint, A.G., 1995. Gravelly Shoreface and Beachface Deposits, in: Plint, A.G. (Eds.), Sedimentary Facies Analysis: A Tribute to the Research and Teaching of Harold G. Reading, Blackwell Publishing Ltd., Oxford, UK., pp. 75-99.

Hönig, M. R., John, C. M., 2015. Sedimentological and isotopic heterogeneities within a Jurassic carbonate ramp (UAE) and implications for reservoirs in the Middle East. Marine and Petroleum Geology 68, 240-257.

Howell, J.A., Schwarz, E., Spalletti, L.A., Veiga, G.D., 2005. The Neuquén Basin: an overview, in: Veiga, G.D., Spalletti, L.A., Howell, J.A., Schwarz, E. (Eds.), The Neuquén Basin,

Argentina: A Case Study in Sequence Stratigraphy and Basin Dynamics. Geol. Soc. Lond. Spec. Publ. 252, pp. 1-14.

James, N.P., 1997. The cool-water carbonate depositional realm, in: James, N.P., Clarke, J.A.D. (Eds.), Cool-Water Carbonates. Society for Sedimentary Geology (SEPM), Special Publications 56, 1-20.

Kachel, N.B., Smith, J.D., 1986. Geological impact of sediment transporting events on the Washington continental shelf, in: Knight, R.J., McLean, J.R. (Eds.), Shelf sands and sandstones. Canadian Society of Petroleum Geologists Memoir 11, 145-162.

Komar, P.D., 1976. Beach processes and sedimentation: Englewood Cliffs. Upper Saddle River, NJ. Prentice Hall, pp. 429.

Leanza, H.A., Marchese, H.G., Riggi, J.C., 1977. Estratigrafía del Grupo Mendoza con especial referencia a la Formación Vaca Muerta entre los Paralelos 35° y 40° l.s. Cuenca Neuquina-Mendocina. Revista de la Asociación Geológica Argentina 32, 190-208.

Leanza, H.A., 1993. Estratigrafía del Mesozoico posterior a los Movimientos Intermálmicos en la comarca del Cerro Chachil, provincia del Neuquén. Revista de la Asociación Geológica Argentina 48, 71-84.

Legarreta, L., Gulisano, C.A., 1989. Análisis estratigráfico secuencial de la Cuenca Neuquina (Triásico Superior-Terciario inferior), in: Chebli, G., Spalletti, L.A. (Eds.), Cuencas Sedimentarias Argentinas, Ser. Correlac. Geol. 6, 221-243.

Legarreta, L., Uliana, M.A., 1991. Jurassic-Cretaceous marine oscillations and geometry of a back-arc basin fill, central Argentine Andes, in: MacDonald, D.I.M. (Eds.), Sedimentation, Tectonics and Eustasy. Sea level Changes at Active Margins. Int. Assoc. Sedimentol. Spec. Publ. 12, 429-450.

Liberman, A., Schwarz, E., Veiga, G.D., 2014. Caracterización Paleoambiental y secuencial de reservorios de la Formación Mulichinco en el yacimiento Aguada del Chivato (sector nororiental de Cuenca Neuquina, Argentina): su contribución para el desarrollo de un campo aún inmaduro: IX Congreso de Exploración y Desarrollo de Hidrocarburos, Trabajos Técnicos, pp. 351-373.

MacEachern, J.A, Bann, K.L., 2008. The role of ichnology in refining shallow marine facies models, in: Hampson, G., Steel, R., Burgess, P., Dalrymple, R. (Eds.), Recent Advances in Models of Siliciclastic Shallow-Marine Stratigraphy. Society for Sedimentary Geology (SEPM), Special Publications 90, 73-116.

MacEachern, J.A., Pemberton, S.G., 1992. Ichnological aspects of Cretaceous shoreface successions and shoreface variability in the Western Interior Seaway of North America, in: Pemberton S.G. (Eds.), Applications of Ichnology to Petroleum Exporation: A Core Workshop. Society for Sedimentary Geology Core Workshop 17, 57-84.

MacEachern, J.A., Zaitlin, B.A., Pemberton, S.G., 1999. A sharp-based sandstone of the Viking Formation, Joffre Field, Alberta, Canada: criteria for recognition of transgressively incised shoreface complexes. Journal of Sedimentary Research 69, 876-892.

MacEachern, J.A., Pemberton, S.G., Gingras, M.K., Bann, K.L., 2010. Ichnology and Facies Models, in: Dalrymple, R.W., James, N.P. (Eds.), Facies Models, fourth edition. Geological Association of Canada, St. John's, Newfoundland, pp. 19-58.

Mángano, M.G., Buatois, L.A., West, R.R., Maples, C.G., 2002. Ichnology of Pennsylvanian Equatorial Tidal Flat: the Stull Shale Member at Waverly, Eastern Kansas. Kansas Geological Survey 245, 1-133.

Mángano, M.G., Buatois, L.A., Muniz-Guinea, F., 2005. Ichnology of the Alfarcito Member (Santa Rosita Formation) of northwestern Argentina: animal-substrate interactions in a lower Paleozoic wave-dominated shallow sea. Amerghiniana 42, 641-668.

Morris, J.E., Hampson, G.J., Johnson, H.D., 2006. A sequence stratigraphic model for an intensely bioturbated shallow-marine sandstone: the Bridport Sand Formation, Wessex Basin, UK. Sedimentology 53, 1229-1263.

Muto, T., Steel, R.J., Swenson, J.B., 2007. Autostratigraphy: a framework norm for genetic stratigraphy. Journal of Sedimentary Research 77, 2-12.

Myrow, P.M., Southard, J.B., 1991. Combined flow model for vertical stratification sequences in shallow marine storm-deposited beds. Journal of Sedimentary Petrology 61, 202-210.

Myrow, P.M., Southard, J.B., 1996. Tempestite deposition. Journal of Sedimentary Petrology 66, 875-887.

Navarro-Ramirez, J. P., Bodin, S., Heimhofer, U., Immenhauser, A., 2015. Record of Albian to early Cenomanian environmental perturbation in the eastern sub-equatorial Pacific. Palaeogeography, Palaeoclimatology, Palaeoecology 423, 122-137.

O'Byrne, C.J., Flint, S.S., 1995. Sequence, parasequence and intra-parasequence architecture of the Grassy Member, Blackhawk Formation, Book Cliffs, Utah, USA, in: Van Wagoner, J.C., Bertram, G.T. (Eds.), Sequence Stratigraphy of Foreland Basin Deposits: Outcrop and Subsurface Examples from the Cretaceous of North America. AAPG Mem. 64, 225-255.

Ogg, J.G., Agterberg, F.P., Gradstein, F.M., 2004. The Cretaceous period, in: Gradstein, F.M., Ogg, J.G., Smith, A.G. (Eds.), A Geologic Time Scale. Cambridge University Press, Cambridge, pp. 344–383.

Pattison, S.A.J., 1995. Sequence stratigraphic significance of sharp-based lowstand shoreface deposits, Kenilworth Member, Book Cliffs, Utah. AAPG Bull. 79, 444-462.

Pemberton, S.G., MacEachern, J.A., Frey, R.W., 1992. Trace fossil facies models: environmental and allostratigraphic significance, in: Walker, R.G., James, N.P. (Eds.), Facies Models and Sea Level Changes. Geological Association of Canada, St. John's, Newfoundland, pp. 47-72.

Pemberton, S.G., MacEachern, J.A., Dashtgard, S.E., Bann, K.L., Gingras, M.K., Zonneveld, J.P., 2012. Shorefaces, in: Knaust, D., Bromley, R.G. (Eds.), Trace fossils as indicators of sedimentary environments. Elsevier, pp. 563-603.

Pemberton, S.G., Spila, M., Pulham, A.J., Saunders, T., MacEachern, J.A., Robbins, D., Sinclair, I.K., 2001. Ichnology & Sedimentology of Shallow to Marginal Marine Systems. Ben Nevis and Avalon Reservoirs, Jeanne d' Arc Basin. Geological Association of Canada Short Course Notes, 15, pp. 343.

Plint, A.G., 2010. Wave- and storm-dominated shoreline and shallow-marine systems, in: Dalrymple, R.W., James, N.P. (Eds.), Facies Models, fourth edition. Geological Association of Canada, St. John's, Newfoundland, pp. 167-199.

Peters, S.A., Loss, D.P., 2012. Storm and fair-weather wave base: A relevant distinction? Geology 40, 511-514.

Rankey, E.C., 2014, Contrasts between wave-and tide-dominated oolitic systems: Holocene of Crooked–Acklins Platform, southern Bahamas. Facies 60, 405-428.

Reinson, G.E., 1984. Barrier island and associated strand-plain systems, in: Walker, R.G. (Eds.), Facies Models, second edition. Geological Association of Canada, Geoscience Canada Reprint Series 1, pp. 119-140.

Reynaud J-Y., Dalrymple, R.W., 2012. Shallow-marine tidal deposits, in: Davis, R.A., Dalrymple, R.W. (Eds.), Principles of tidal sedimentology. Springer, Dordrecht, pp. 335-369.

Savrda, C.E., 1992. Trace fossil and benthic oxygenation, in: Maples, C.G., West, R.R. (Eds.), Trace Fossils: Paleontological Society, Short Course, 5, pp. 172–196.

Savrda, C.E., 2007. Trace fossils and marine benthic oxygenation, in: Miller III, W. (Eds.), Trace Fossils. Concepts, Problems, Prospects. Amsterdam, Elsevier, pp. 149–156.

Schwarz, E., 1999. Facies sedimentarias y modelo deposicional de la Formación Mulichinco (Valanginiano), Cuenca Neuquina Septentrional. Asociación Argentina de Sedimentología Revista 6, 37–59.

Schwarz, E., 2012. Sharp-based marine sandstone bodies in the Mulichinco Formation (Lower Cretaceous), Neuquén Basin, Argentina: remnants of transgressive offshore sand ridges. Sedimentology 59, 1478–1508.

Schwarz, E., Howell, J.A., 2005. Sedimentary evolution and depositional architecture of a Lowstand Sequence Set: Lower Cretaceous Mulichinco Formation, Neuquén Basin, Argentina,

in: Veiga, G.D., Spalletti, L.A., Howell, J.A., Schwarz, E. (Eds.), The Neuquén Basin, Argentina: A Case Study in Sequence Stratigraphy and Basin Dynamics. Geol. Soc. Lond. Spec. Publ. 252, pp. 109-138.

Schwarz, E., Spalletti, L.A., Howell J.A., 2006. Sedimentary response to a tectonically-induced sea-level fall in a shallow back-arc basin: the Mulichinco Formation (Lower Cretaceous), Neuquén Basin, Argentina. Sedimentology 53, 55–81.

Schwarz, E., Veiga, G.D., Vela, R., Canalis, R., 2008. Paleoambientes y estratigrafía de la Formación Mulichinco en el yacimiento Volcán Auca Mahuida (Cuenca Neuquina, Argentina). Implicancias para la caracterización de sellos locales: VII Congreso de Exploración y Desarrollo de Hidrocarburos, Trabajos Técnicos, pp. 1-17.

Schwarz, E., Spalletti, L.A., Veiga, G.D., 2011. La Formación Mulichinco (Valanginiano), in: Leanza, H., Vallés, J., Arregui, C., Danieli, J.C. (Eds.), Relatorio del XVIII Congreso Geológico Argentino: Geología y Recursos Naturales de la provincia del Neuquén, pp. 131-144.

Schwarz, E., Buatois, L.A., 2012. Substrate-controlled ichnofacies along a marine sequence boundary: The Intra-Valanginian Discontinuity in central Neuquén Basin (Argentina). Sedimentary Geology 277, 72-87.

Schwarz, E., Veiga, G.D., Trentini, G.A., Spalletti, L.A., 2016. Climatically versus eustatically controlled, sediment-supply-driven cycles: Carbonate-siliciclastic, high-frequency sequences in

the Valanginian of the Neuquén Basin (Argentina). Journal of Sedimentary Research 86, 312-335.

Snedden, J.W., Bergman, K.M., 1999. Isolated shallow marine sand bodies: deposits for all interpretations, in: Bergman, K.M., Snedden, J.D. (Eds.), Isolated Shallow Marine Sand Bodies: Sequence Stratigraphic Analysis and Sedimentologic Interpretation. Society for Sedimentary Geology (SEPM), Special Publications 64, 1-11.

Sømme, T.O., Howell, J.A., Hampson, G.J., Storms, J.E.A., 2008. Architecture and genesis of intra-parasequence discontinuity surfaces in wave-dominated deltaic deposits: Upper Cretaceous Sunnyside Member, Blackhawk Formation, Book Cliffs, Utah, USA, in: Hampson, G.J., Steel, R.J., Burgess, P.M., Dalrymple, R.W. (Eds), Recent Advances in Models of Siliciclastic Shallow-Marine Stratigraphy. Society for Sedimentary Geology (SEPM), Special Publications 90, 421-441.

Storms, J.E.A., Hampson, G.J., 2005. Mechanisms for forming discontinuity surfaces within shoreface–shelf parasequences: Sea level, sediment supply, or wave regime? Journal of Sedimentary Research 75, 67-81.

Swift, D.J., Han, G., Vincent, C.E., 1986. Fluid Processes and Sea-Floor Response on a Modern Storm-Dominated Shelf: Middle Atlantic Shelf of North America. Part I: The Storm-Current Regime, in: Knight, R. J., McLean, J. R. (Eds.), Shelf Sands and Sandstones. Canadian Society of Petroleum Geologists, Memoir II, 99-119.

Swift, D.J.P., Oertel, G., Tillman, R., Thorne, J., 1991. Shelf sand and sandstone bodies; geometry, facies and sequence stratigraphy. International Association of Sedimentologists Special Publication 14, 532.

Swift, D.J.P., Parsons, B.S., 1999. Shannon Sandstone of the Power River Basin: Orthodoxy and Revisionism in Stratigraphic Thought, in: Bergman, K.M., Snedden, J.D. (Eds.), Isolated Shallow Marine Sand Bodies: Sequence Stratigraphic Analysis and Sedimentologic Interpretation. Society for Sedimentary Geology (SEPM), Special Publications 64, 55-84.

Taylor, A.M., Goldring, R., 1993. Description and analysis of bioturbation and ichnofabric. Journal of the Geological Society 150, 141-148.

Tillman, R.W., 1999. The Shannon Sandstone: A Review of the Sand-Ridge and Other Models, in: Bergman, K.M., Snedden, J.D. (Eds.), Isolated Shallow Marine Sand Bodies: Sequence Stratigraphic Analysis and Sedimentologic Interpretation. Society for Sedimentary Geology (SEPM), Special Publications 64, 29-53.

Tillman, R.W., Martinsen, R.S., 1987. Sedimentologic Model and Production Characteristics of Hartzog Draw Field, Wyoming. Shannon Shelf-Ridge Sandstone, in: Tillman, R.W., Weber, K. (Eds.), Reservoir Sedimentology. Society for Sedimentary Geology (SEPM), Special Publications 40, 15-114.

Uliana, M.A., Dellape, D.A., Pando, G.A., 1977. Análisis estratigráfico y evaluación del potencial petrolífero de las Formaciones Mulichinco, Chachao y Agrio, Cretácico Inferior de las Provincias de Neuquén y Mendoza. Petrotecnia 1-2, 41-46.

Van Wagoner, J.C., Mitchum, R.M., Campion, K.M., Rahmanian, V.D., 1990. Siliciclastic Sequence Stratigraphy in Well Logs, Cores, and Outcrops: Association of Petroleum Geologists. Methods in Exploration 7, pp. 55.

Veiga, G.D., Schwarz, E., 2017. Facies characterization and sequential evolution of an ancient offshore dunefield in a semi-enclosed sea: Neuquén Basin, Argentina. Geo-marine Letters 37, 411-426.

Veiga, R., Pángaro, F., Fernández, M., 2002. Modelado bidimensional y migración de hidrocarburos en el ámbito occidental de la Dorsal de Huincul, Cuenca Neuquina - Argentina. V Congr. Expl. Des. Hidroc. Electronic Format.

Vergani, G.D., Tankard, A.J., Belotti, H.J., Welsink, H.J., 1995. Tectonic evolution and paleogeography of the Neuquén Basin, Argentina, in: Tankard, A.J., Suarez Soruco, R., Welsink, H.J. (Eds.), Petroleum Basins of South America. AAPG Memoir 62, 383-402.

Walker, R.G., Plint, A.G., 1992. Wave- and storm-dominated shallow marine systems, in Walker, R.G., James, N.P. (Eds.), Facies Models, response to sea level change. Geological Association of Canada St. John's, Newfoundland, pp. 219-238.

Wheatcroft, R.A., 1990. Preservation potential of sedimentary event layers. Geology 18, 843–845.

Zecchin, M., 2007. The architectural variability of small-scale cycles in shelf and ramp clastic systems: the controlling factors. Earth-Science Reviews 84, 21–55.

APPENDIX I

- PCS 1

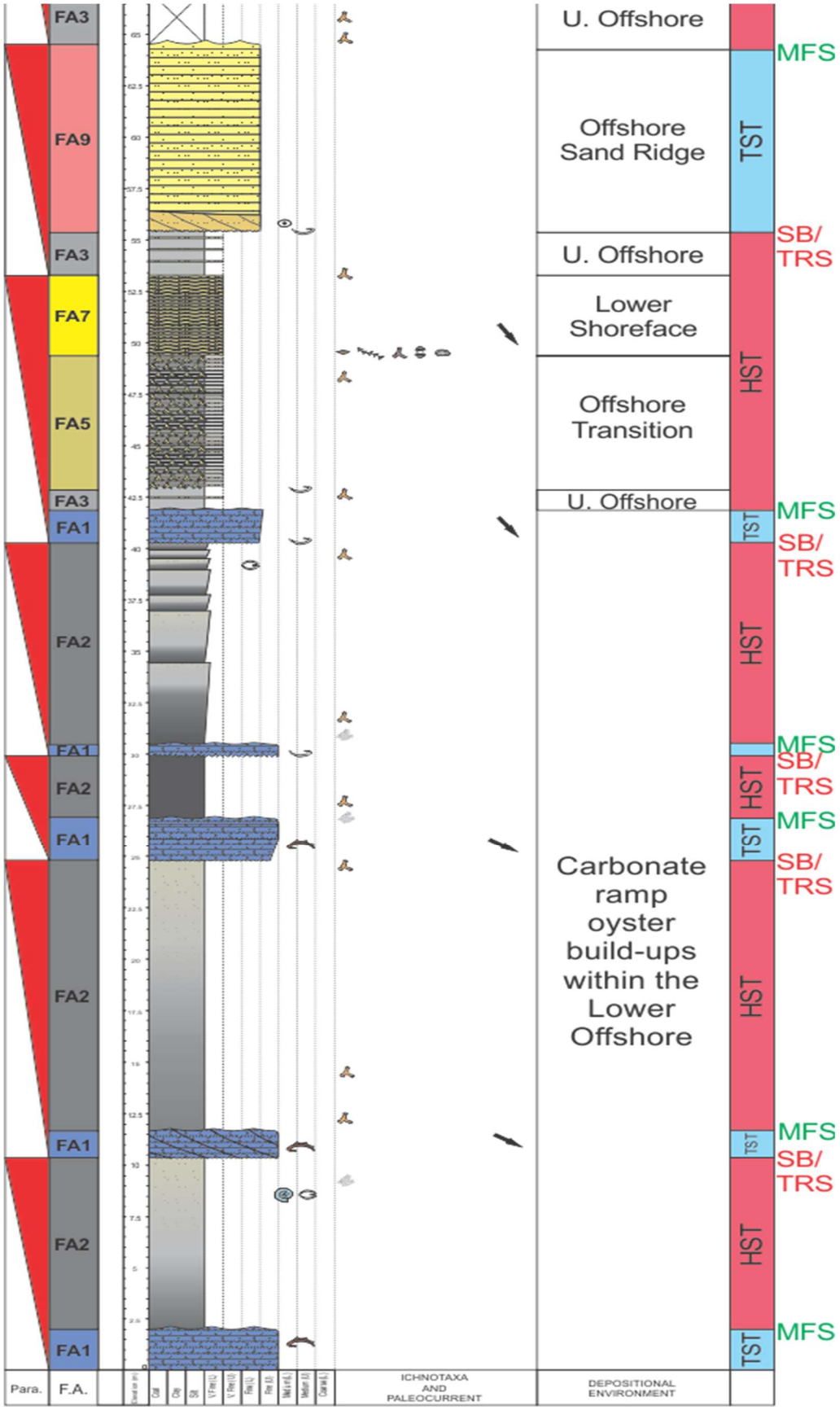
FA3
FA9
FA3
FA7
FA5
FA3
FA1
FA2
FA1
FA2
FA1
FA2
FA1
FA2
FA1
U. Offshore
Offshore Sand Ridge
U. Offshore
Lower Shoreface
Offshore Transition
U. Offshore
Carbonate ramp oyster build-ups within the Lower Offshore
MFS
SB/ TRS
MFS
SB/ TRS
MFS
SB/ TRS
MFS
SB/ TRS
MFS
SB/ TRS
MFS
TST
HST
HST
TST
HST
TST
HST
TST
Para.
F.A.
ICHNOTAXA AND PALEOCURRENT
DEPOSITIONAL ENVIRONMENT

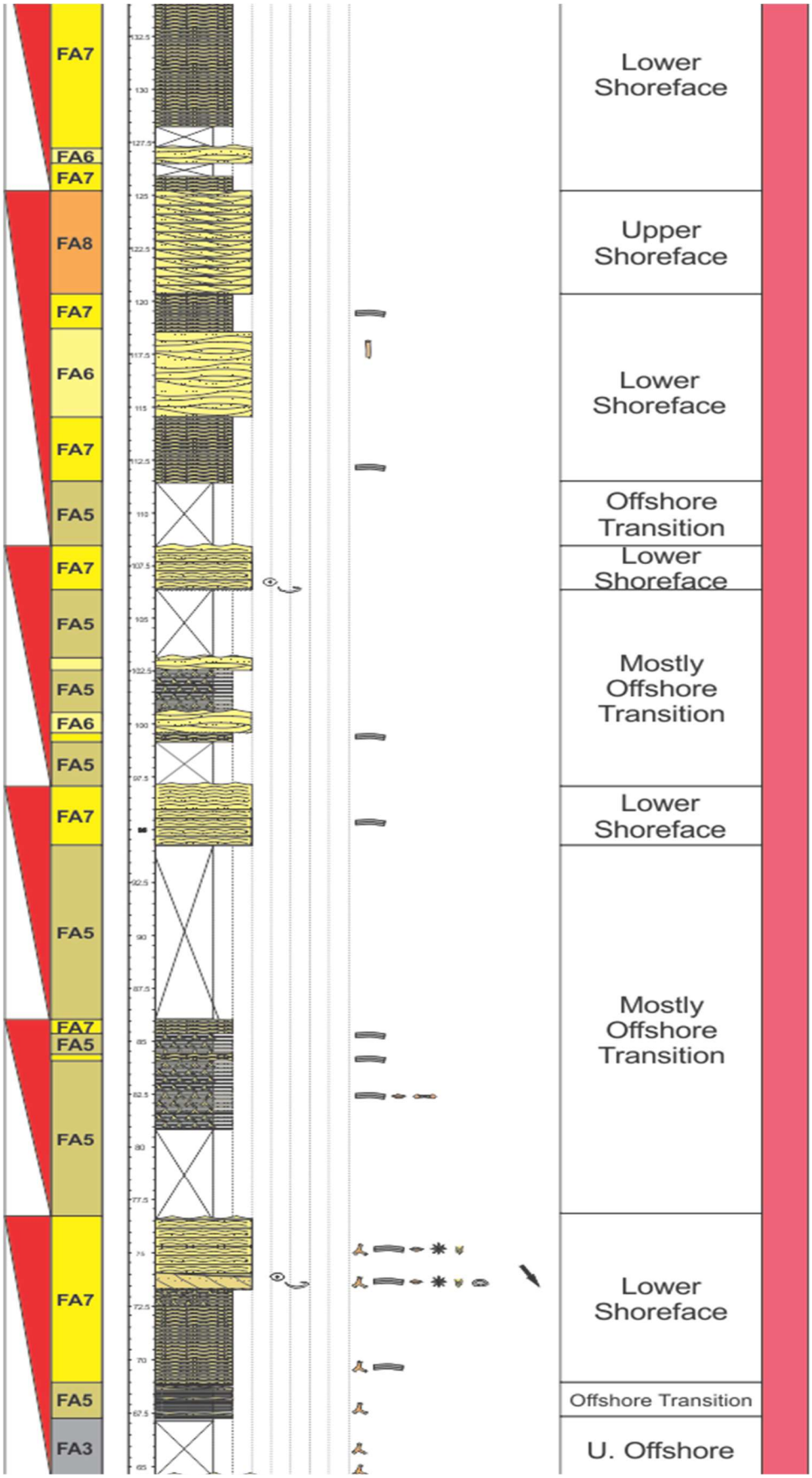
FA7
FA6
FA7
FA8
FA7
FA6
FA7
FA5
FA7
FA5
FA5
FA6
FA5
FA7
FA5
FA7
FA5
FA5
FA3
Lower Shoreface
Upper Shoreface
Lower Shoreface
Offshore Transition
Lower Shoreface
Mostly Offshore Transition
Lower Shoreface
Mostly Offshore Transition
Lower Shoreface
Offshore Transition
U. Offshore

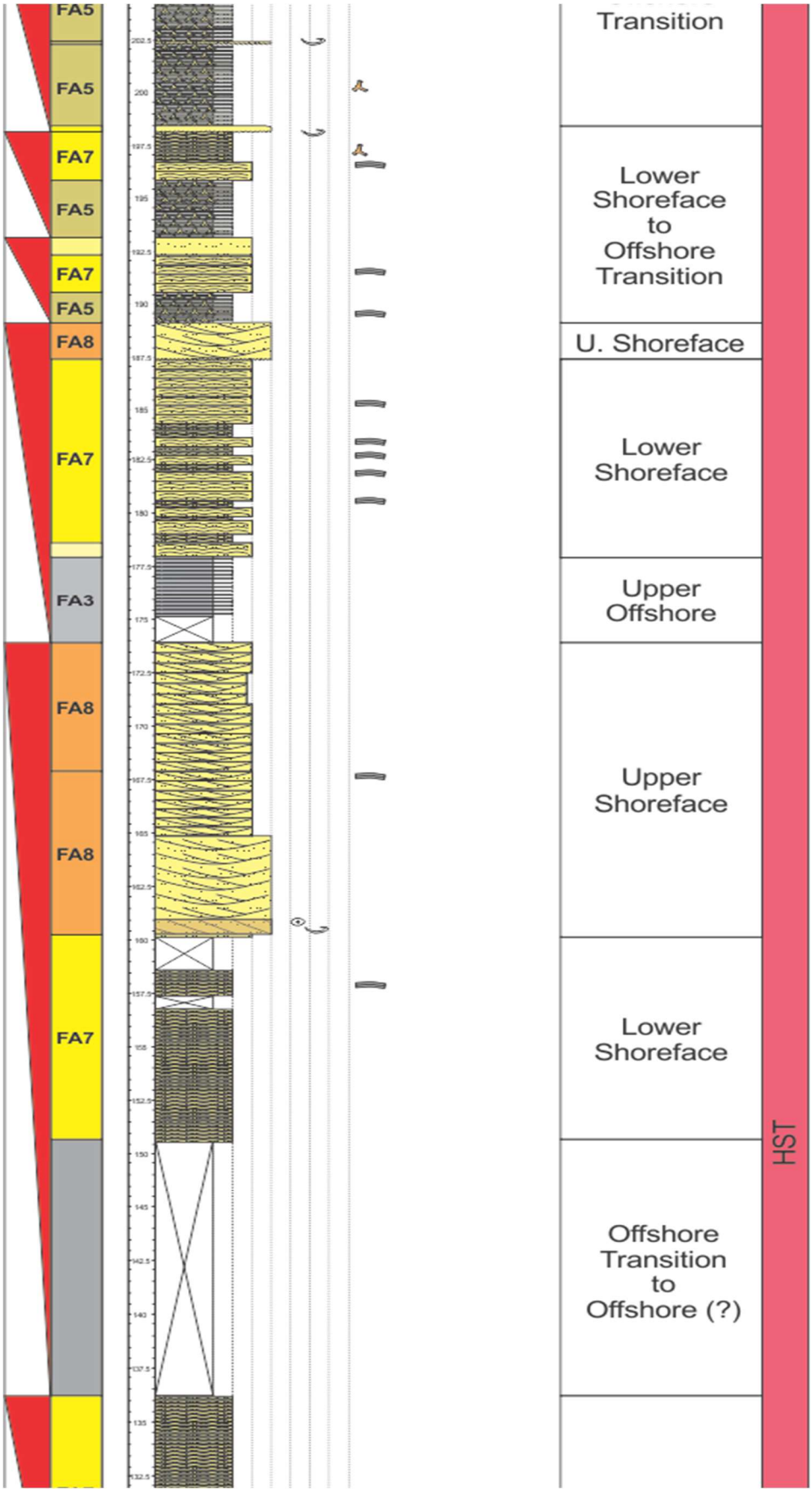
FA5
FA5
FA7
FA5
FA7
FA5
FA8
FA7
FA3
FA8
FA8
FA7
Transition
Lower Shoreface to Offshore Transition
U. Shoreface
Lower Shoreface
Upper Offshore
Upper Shoreface
Lower Shoreface
Offshore Transition to Offshore (?)
HST

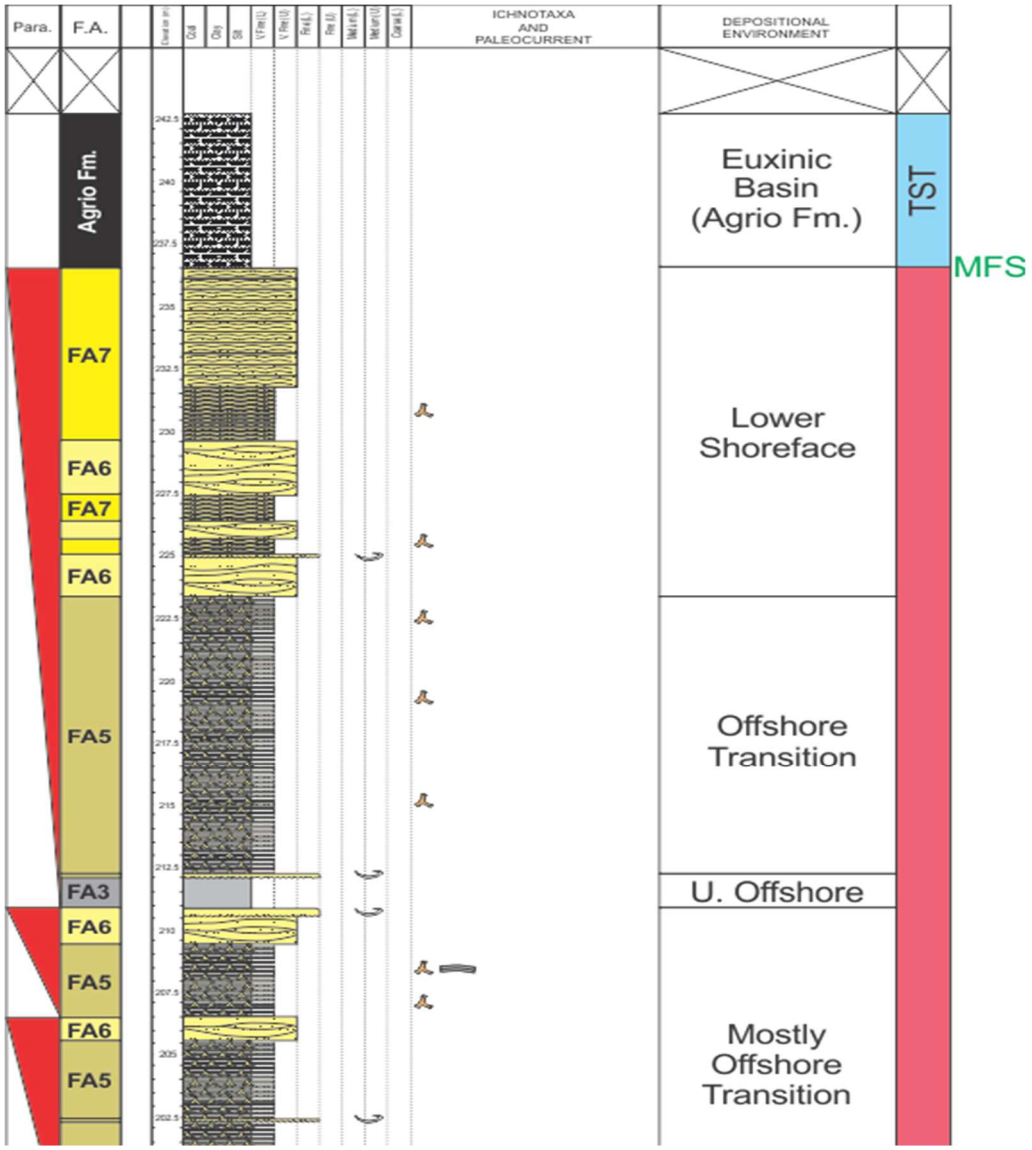
Para.
F.A.
ICHNOTAXA AND PALEOCURRENT
DEPOSITIONAL ENVIRONMENT
Agrio Fm.
FA7
FA6
FA7
FA6
FA5
FA3
FA6
FA5
FA6
FA5
Euxinic Basin (Agrio Fm.)
Lower Shoreface
Offshore Transition
U. Offshore
Mostly Offshore Transition
TST
MFS

APPEXNDIX II

- PCS2

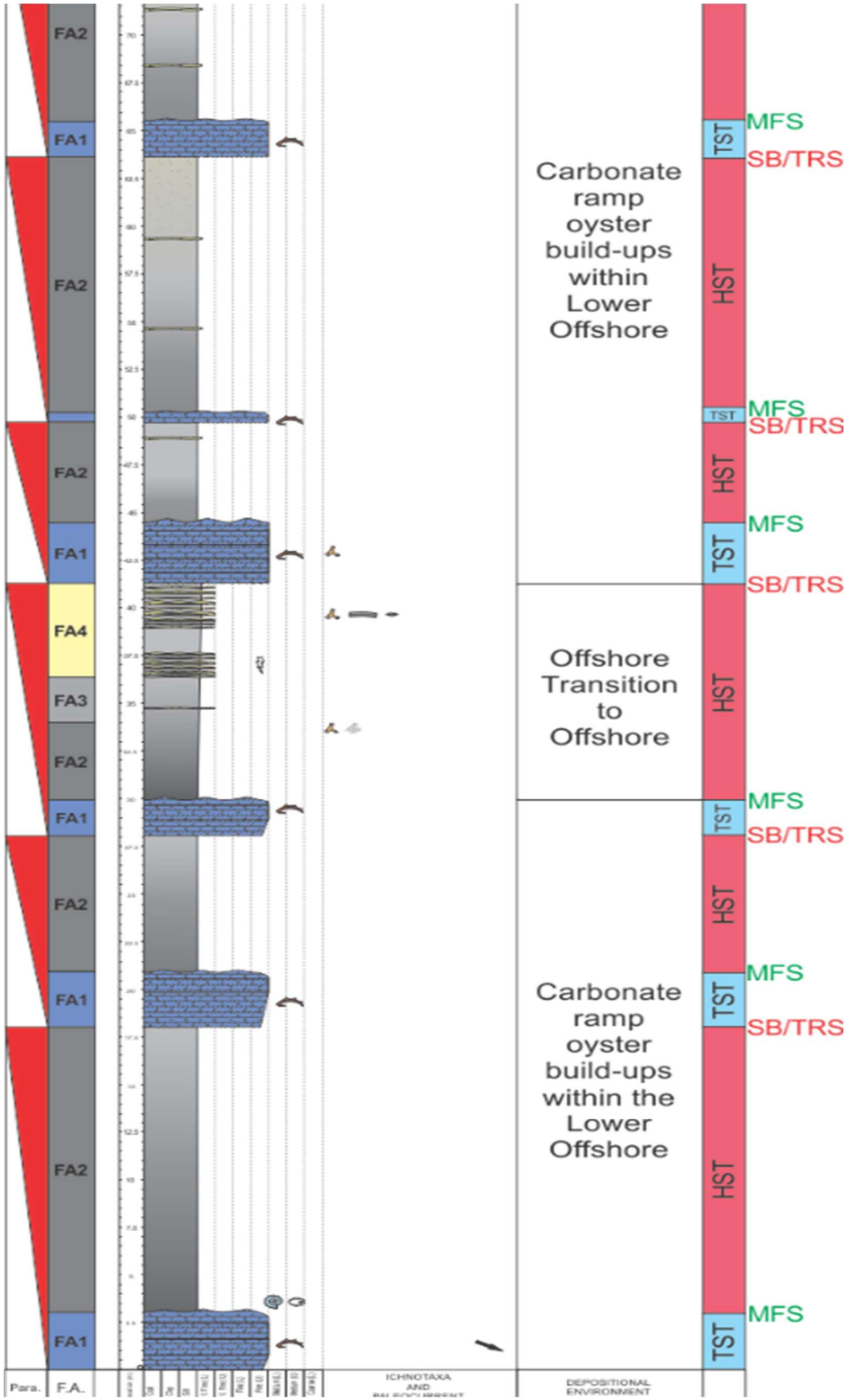
FA2
FA1
FA2
FA2
FA1
FA4
FA3
FA2
FA1
FA2
FA1
FA2
FA1
Para.
F.A.
ICHNOTAXA
AND
DEPOSITIONAL
ENVIRONMENT
Carbonate ramp oyster build-ups within Lower Offshore
Offshore Transition to Offshore
Carbonate ramp oyster build-ups within the Lower Offshore
TST
HST
MFS
SB/TRS

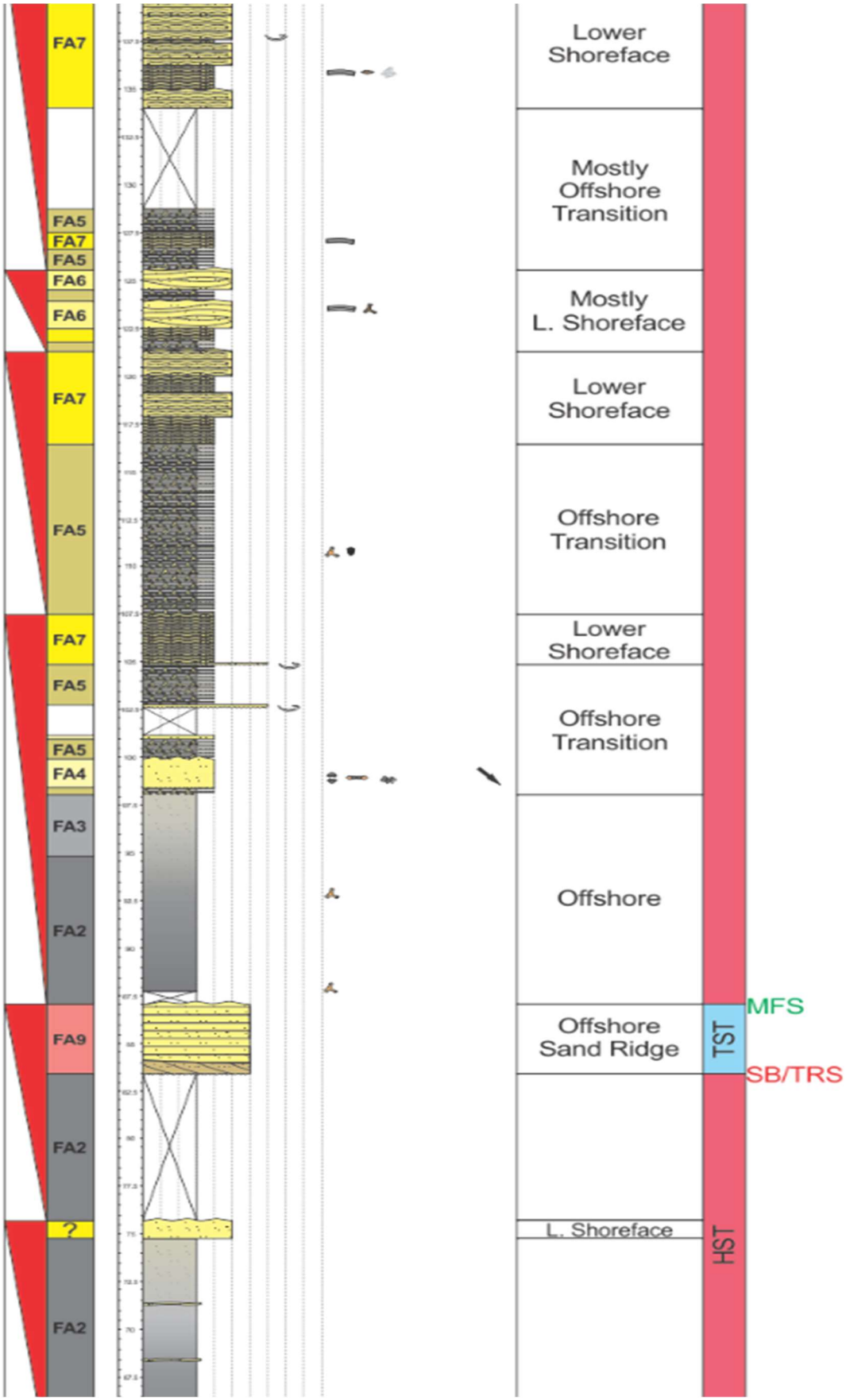
FA7
FA5
FA7
FA5
FA6
FA6
FA7
FA5
FA7
FA5
FA5
FA4
FA3
FA2
FA9
FA2
?
FA2
Lower Shoreface
Mostly Offshore Transition
Mostly L. Shoreface
Lower Shoreface
Offshore Transition
Lower Shoreface
Offshore Transition
Offshore
Offshore Sand Ridge
L. Shoreface
TST
HST
MFS
SB/TRS

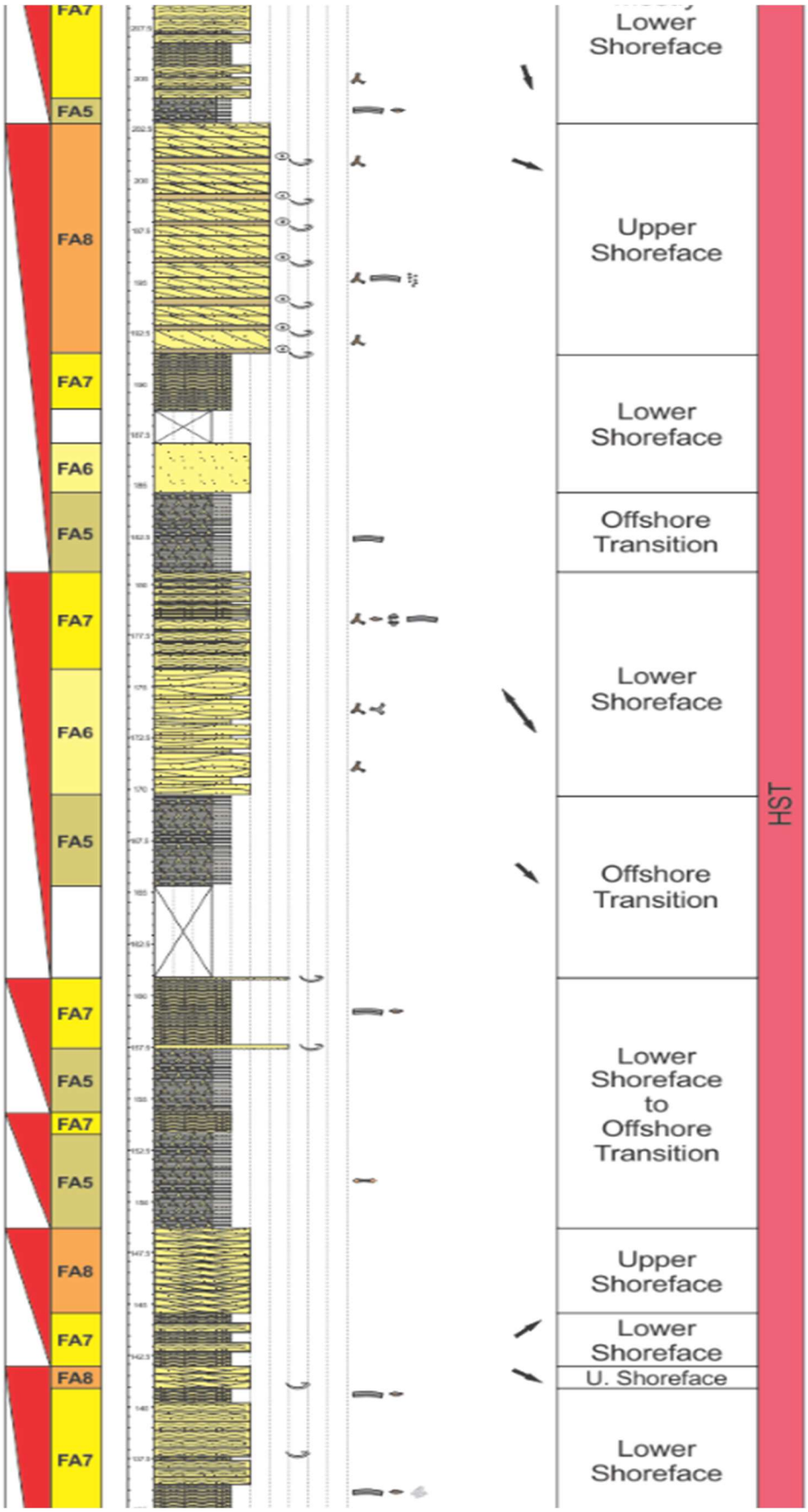
FA7
FA5
FA8
FA7
FA6
FA5
FA7
FA6
FA5
FA7
FA5
FA7
FA5
FA8
FA7
FA8
FA7
Lower Shoreface
Upper Shoreface
Lower Shoreface
Offshore Transition
Lower Shoreface
Offshore Transition
Lower Shoreface to Offshore Transition
Upper Shoreface
Lower Shoreface
U. Shoreface
Lower Shoreface
HST

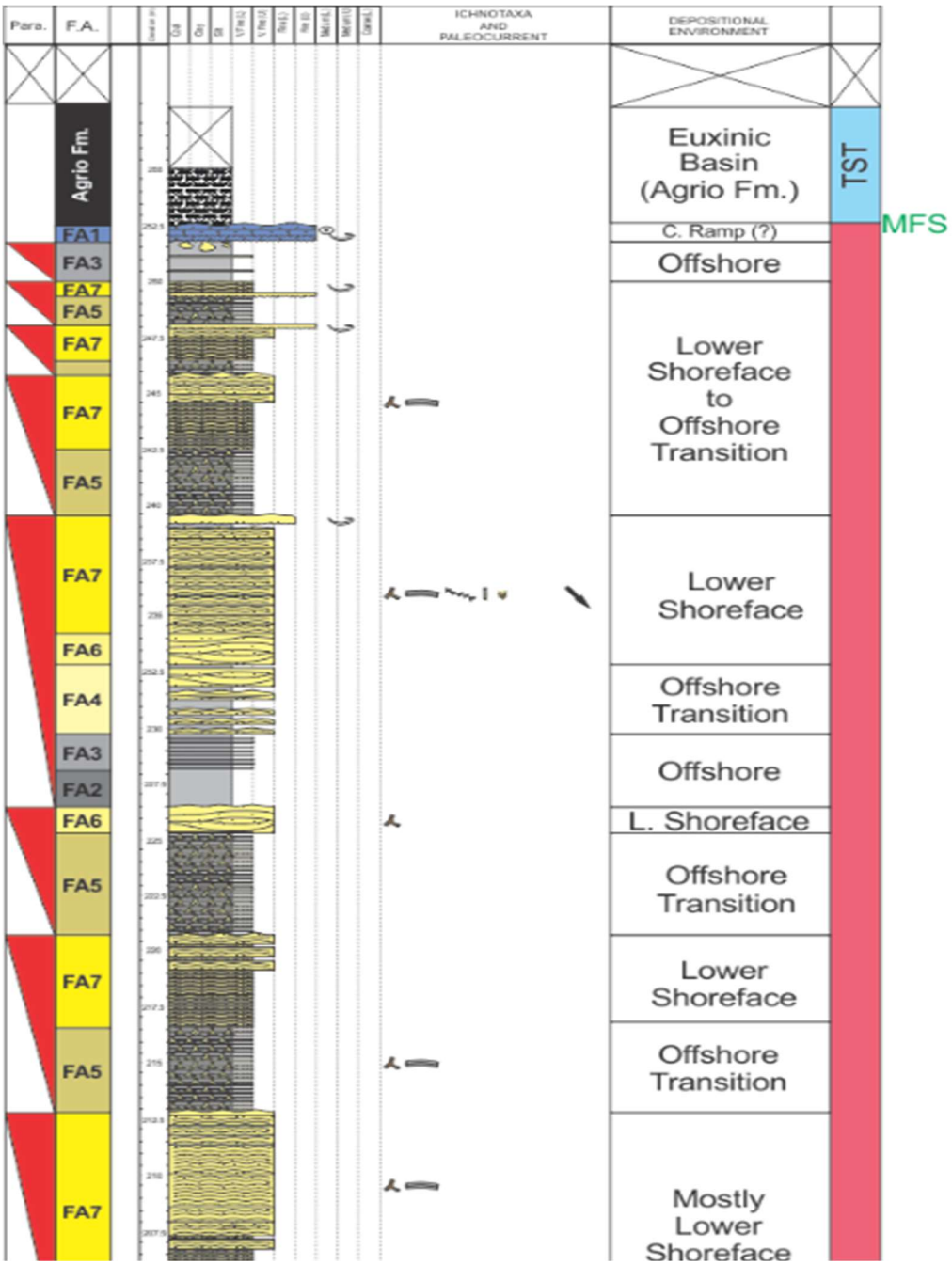
Para.
F.A.
ICHNOTAXA AND PALEOCURRENT
DEPOSITIONAL ENVIRONMENT
Agrio Fm.
FA1
FA3
FA7
FA5
FA7
FA7
FA5
FA7
FA6
FA4
FA3
FA2
FA6
FA5
FA7
FA5
FA7
Euxinic Basin (Agrio Fm.)
C. Ramp (?)
Offshore
Lower Shoreface to Offshore Transition
Lower Shoreface
Offshore Transition
Offshore
L. Shoreface
Offshore Transition
Lower Shoreface
Offshore Transition
Mostly Lower Shoreface
TST
MFS

APPENDIX III

- PCS3

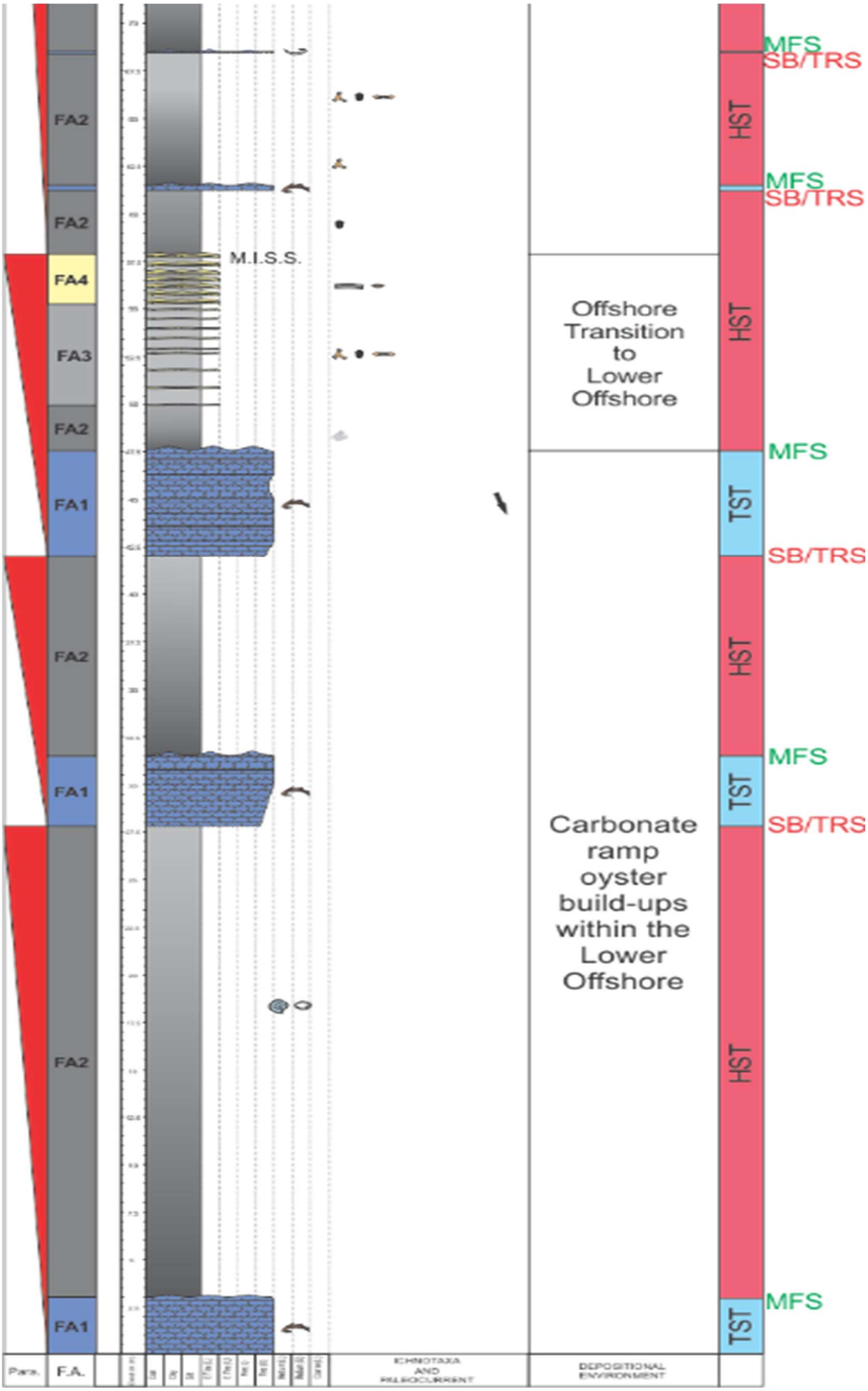
FA2
FA2
FA4
FA3
FA2
FA1
FA2
FA1
FA2
FA1
M.I.S.S.
Offshore Transition to Lower Offshore
Carbonate ramp oyster build-ups within the Lower Offshore
MFS
SB/TRS
HST
MFS
SB/TRS
HST
MFS
TST
SB/TRS
HST
MFS
TST
SB/TRS
HST
MFS
TST
Para.
F.A.
ICHNOTAXA AND PALEOCURRENT
DEPOSITIONAL ENVIRONMENT

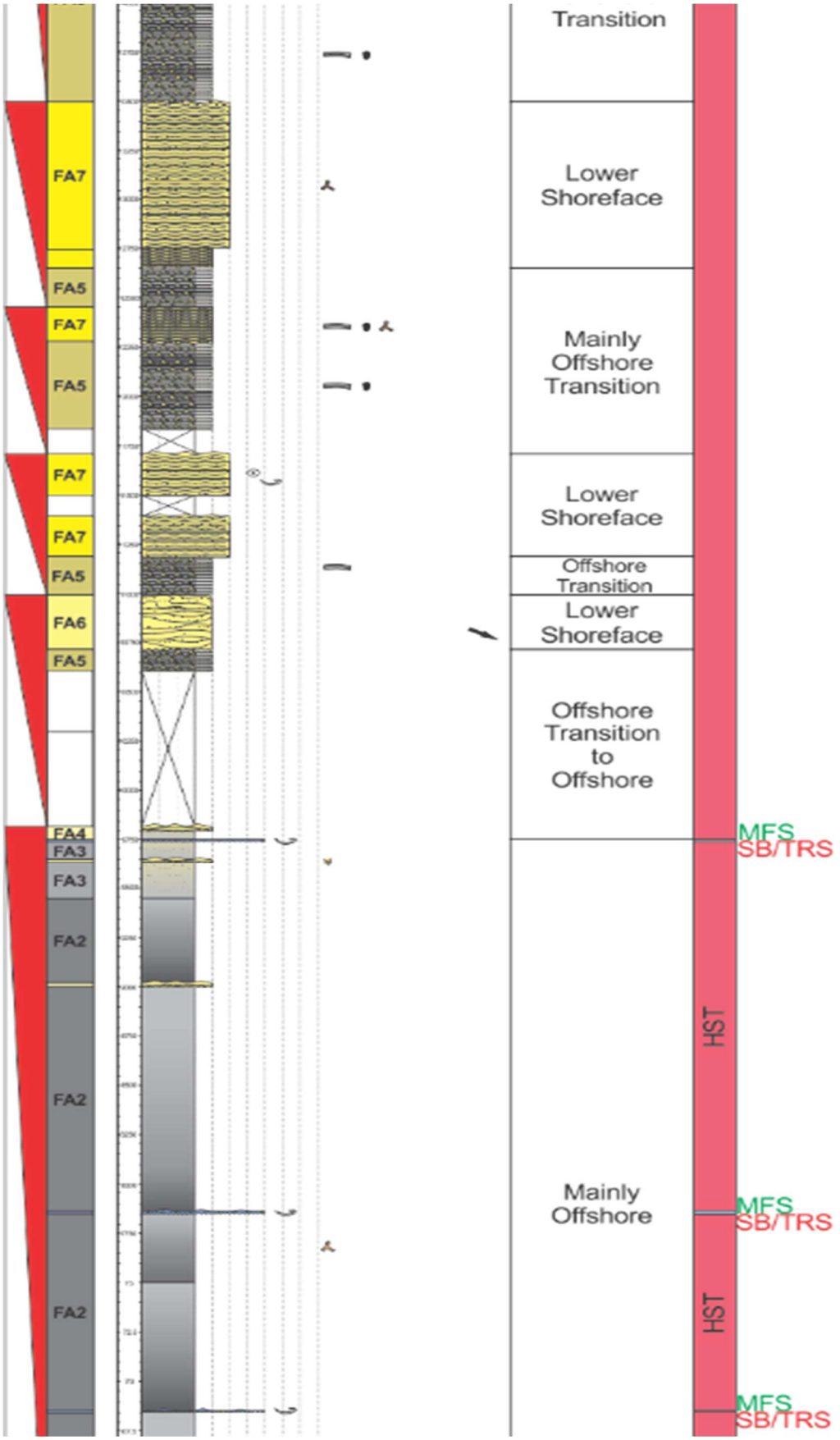
FA7
FA5
FA7
FA5
FA7
FA7
FA5
FA6
FA5
FA4
FA3
FA3
FA2
FA2
FA2
Transition
Lower Shoreface
Mainly Offshore Transition
Lower Shoreface
Offshore Transition
Lower Shoreface
Offshore Transition to Offshore
Mainly Offshore
MFS
SB/TRS
MFS
SB/TRS
MFS
SB/TRS
HST
HST

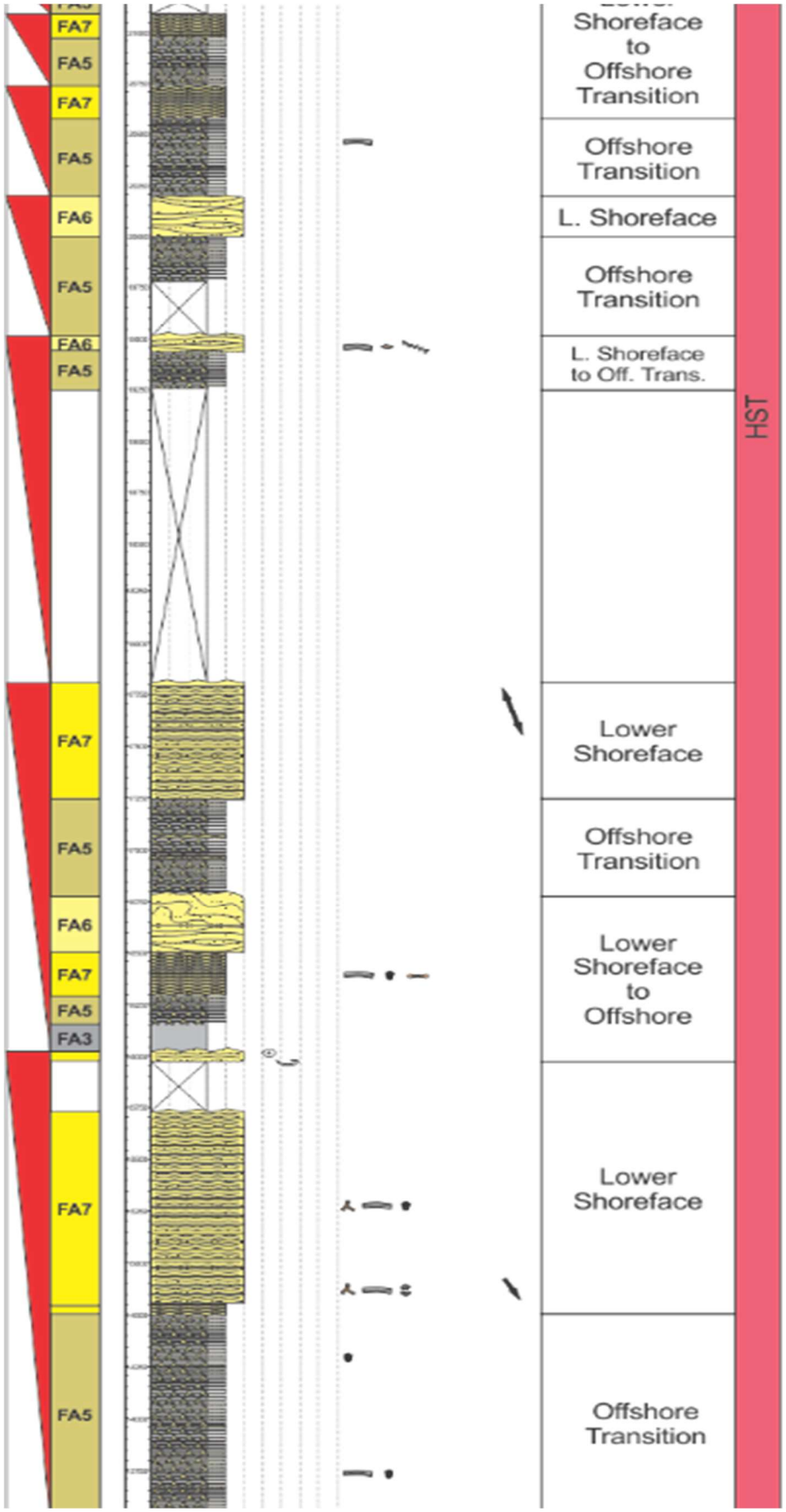
FA7
FA5
FA7
FA5
FA6
FA5
FA6
FA5
FA7
FA5
FA6
FA7
FA5
FA3
FA7
FA5
Shoreface to Offshore Transition
Offshore Transition
L. Shoreface
Offshore Transition
L. Shoreface to Off. Trans.
Lower Shoreface
Offshore Transition
Lower Shoreface to Offshore
Lower Shoreface
Offshore Transition
HST

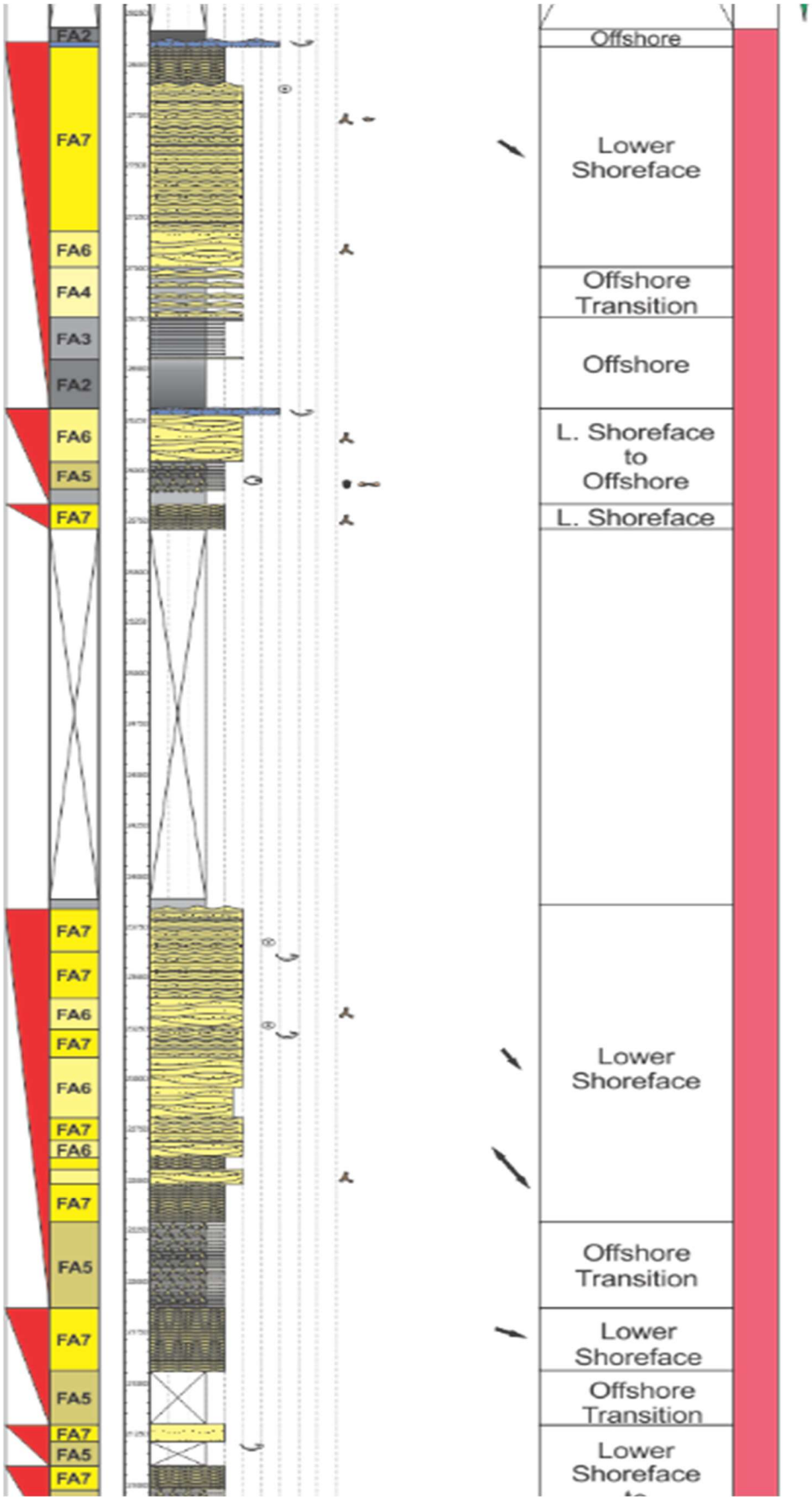
FA2
FA7
FA6
FA4
FA3
FA2
FA6
FA5
FA7
FA7
FA7
FA6
FA7
FA6
FA7
FA6
FA7
FA7
FA5
FA7
FA5
FA7
FA5
FA7
Offshore
Lower Shoreface
Offshore Transition
Offshore
L. Shoreface to Offshore
L. Shoreface
Lower Shoreface
Offshore Transition
Lower Shoreface
Offshore Transition
Lower Shoreface

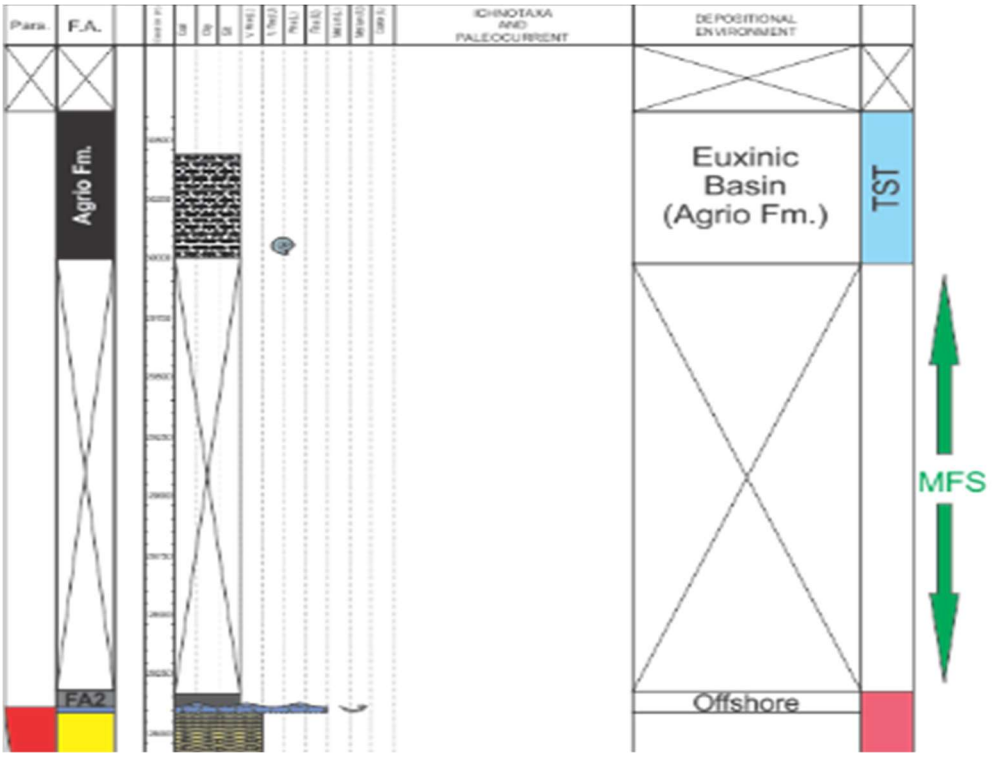
Para.
F.A.
ICHNOTAXA AND PALEOCURRENT
DEPOSITIONAL ENVIRONMENT
Agrio Fm.
FA2
Euxinic Basin (Agrio Fm.)
TST
MFS
Offshore